

AD-A141 100

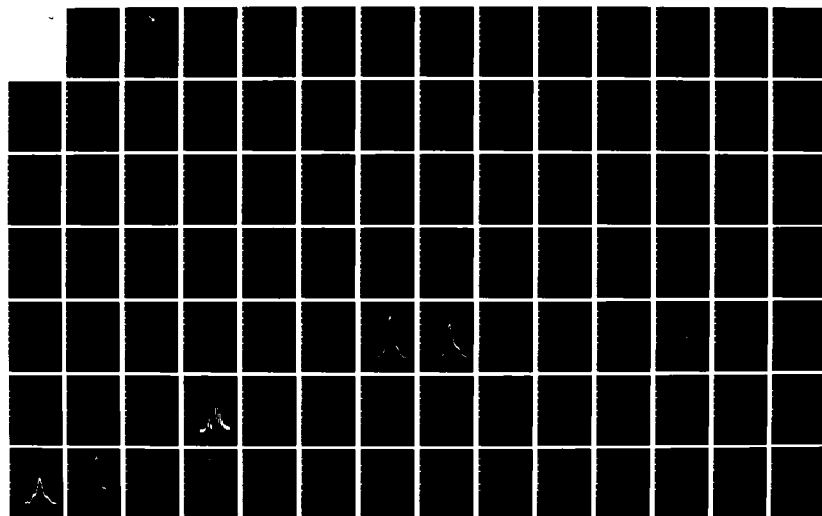
HIGH RESOLUTION CATHODOLUMINESCENCE OF YELLOW AND
WATERCLEAR CVD POLYCRYSTALLINE ZNS(U) AIR FORCE INST OF
TECH WRIGHT-PATTERSON AFB OH SCHOOL OF ENGI.
D BLESSINGER DEC 83 AFIT/GEP/ENP/83D-2

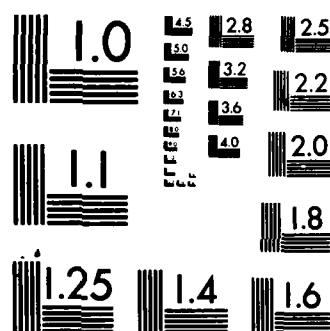
1/2

UNCLASSIFIED

F/G 20/2

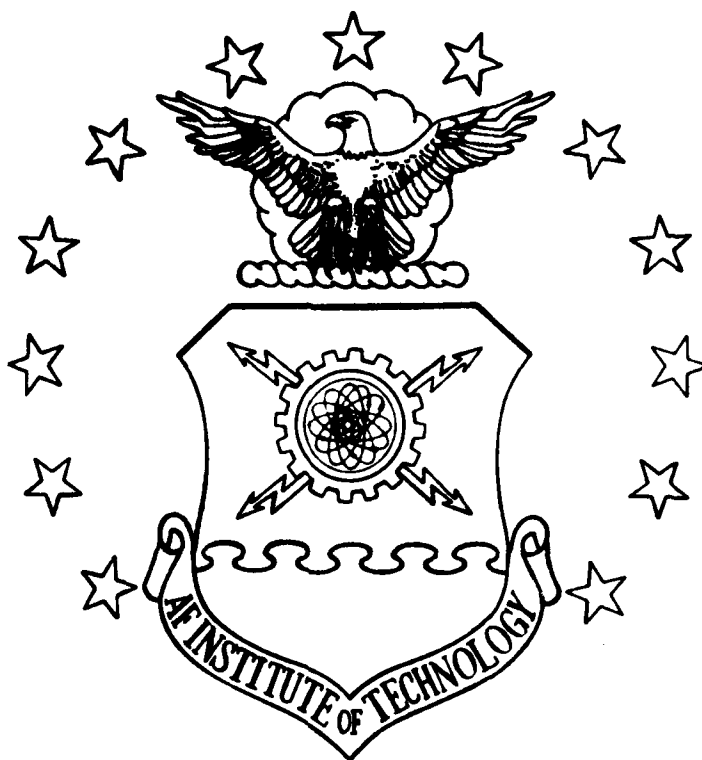
NL





MICROCOPY RESOLUTION TEST CHART
NATIONAL BUREAU OF STANDARDS-1963-A

AD-A141 100



HIGH RESOLUTION CATHODOLUMINESCENCE
OF YELLOW AND WATERCLEAR
CVD POLYCRYSTALLINE ZnS

THESIS

David Blessinger
Captain, USAF

AFIT/GEP/ENP/83D-2

This document has been approved
for public release and
distribution in unlimited quantities

DEPARTMENT OF THE AIR FORCE
AIR UNIVERSITY (ATC)

AIR FORCE INSTITUTE OF TECHNOLOGY

Wright-Patterson Air Force Base, Ohio

DTIC

MAY 16 1984

A

DTIC FILE COPY

84 05 15 012

AFIT/GEP/PH/83D-2

HIGH RESOLUTION CATHODOLUMINESCENCE
OF YELLOW AND WATERCLEAR
CVD POLYCRYSTALLINE ZnS

THESIS

David Blessinger
Captain, USAF

AFIT/GEP/ENP/83D-2

MAY 16 1984

Approved for public release; LAW AFB 100-17.

LYNN E. WOLAVER
Dean for Research and Professional Development
Air Force Institute of Technology (ATC)
Wright-Patterson AFB OH 45433

AFIT/GEP/ENP/83D-2

HIGH RESOLUTION CATHODOLUMINESCENCE OF YELLOW
AND WATERCLEAR CVD POLYCRYSTALLINE ZnS

THESIS

Presented to the Faculty of the School of Engineering
of the Air Force Institute of Technology
In Partial Fulfillment of the
Requirements for the Degree of
Master of Science in Engineering Physics

David Blessinger, B.S., M.S.
Captain, USAF

December 1983

Approved for public release; distribution unlimited

Accession

NTIS	AD
DTIC	AD
USDA	AD
JR	AD

Dist

A1



Preface

Knowledge of the impurities present in cvd polycrystalline ZnS is necessary if more transmissive ZnS windows for lasers and missile IR window domes are to be made. The results of this study and similar studies can be used to determine the impurities in the ZnS crystals so the manufacturing process can be changed to improve the quality of the crystals.

In performing the experimentation assistance was received from a number of individuals whom I would like to acknowledge. I would like to thank Dr. Robert L. Hengehold, my thesis advisor, for his advice and consultation throughout the thesis. Jamie Varni assisted with the initial literature search and provided an occasional consultation. I would also like to thank Ron Gabriel, Curt Atnipp, Don Ellworth, and George Gergal of the AFIT Physics Department Laboratory staff for their valuable technical assistance. Finally I would like to thank my wife, Nora, and two children, Patrick and Christopher, who were so patient and understanding throughout the past 18 months.

David Blessinger

Table of Contents

	Page
Preface	ii
List of Figures	v
List of Tables	vii
List of Symbols	viii
Abstract	ix
I. Introduction	1
Background	1
Problem	2
Scope	3
Assumptions	4
Approach	6
Sequence of Presentation	7
II. Theory and Summary of Previous Research	9
Crystallography	9
Energy Bands	10
Emission Models	10
Spectral Bands	12
Phonons	23
Temperature	24
Electron Flux	25
III. Experimental	26
Sample Information	26
Chemical Vapor Deposition	26
Sample Preparation	27
Color	28
Microscopy and Grain Size	28
Crystal Structure	30
System Overview	34
Vacuum System	36
Cryogenic Transfer System	36
Electron Gun	40
Optical System and Alignment	42
Signal Processing	46
Error Analysis	47

IV.	Results and Discussion	49
	Compiled Spectral Emission List	49
	Near Band Edge Below 3300 Å	54
	UV Range 3300-3399 Å	58
	UV Range 3400-3700 Å	64
	The SAL and SA Peaks	70
	Yellow Polycrystalline	85
	Electron Flux and Temperature Effects	88
	Electron Flux	88
	Temperature Effects	89
	Variation in Emission Spectra	90
	Yellow vs. Waterclear	91
	Sample vs. Sample	93
	Spot vs. Spot	99
V.	Conclusions and Recommendations	101
	Bibliography	108
	Vita	119

List of Figures

Figure	Page
II-1. Transition Models	11
III-1. Comparison of CVD ZnS and Cleartran Visible Transmission	29
III-2. Zincblende Structure	32
III-3. System Setup	35
III-4. Vacuum System	37
III-5. Cryogenic Transfer System	38
III-6. Sample Holder	41
III-7. Major Components of (A) Electron Gun and (B) Faraday Cup	43
III-8. Optical System	44
IV-1. Yellow ZnS #4	50
IV-2. Waterclear #5	51
IV-3. Waterclear #2 FE Shown	55
IV-4. Waterclear #2 FE Shown, 40 K	56
IV-5. Waterclear #2 3267, 3400, 3428 Peaks Absent	59
IV-6. Waterclear #6	61
IV-7. Waterclear #4	72
IV-8. Waterclear #4 Low Flux	73
IV-9. Waterclear #4 Moderate Flux	74
IV-10. Waterclear #4 Very High Flux	75
IV-11. Emission Dependence on Concentration Ratios	82
IV-12. Typical Spectra: Yellow Polycrystalline ZnS	87

IV-13.	Typical Spectra: Waterclear #3	92
IV-14.	Waterclear #3 Typical Spectra	94
IV-15.	Waterclear #4 Typical Spectra	95
IV-16.	Waterclear #6 Typical Spectra	96
IV-17.	Waterclear #4	98
V-1.	Assigned Transitions	103

List of Tables

Table		Page
II-1.	Compiled ZnS Emission Peak Reference List	13
III-1.	Sample Lattice Constants	31
III-2.	Aging of Barium Oxide Cathode Electron Gun	40
IV-1.	Compiled Spectral Emissions of Waterclear and Yellow CVD Polycrystalline ZnS	52

List of Symbols

A	= Angstrom
ABE	= Acceptor Bound Exciton
BE	= Bound Exciton
cm	= Centimeter
cvd	= Chemical-Vapor-Deposition
DAP	= Donor-Acceptor-Pair
DBE	= Donor Bound Exciton
EM	= Electromagnetic
eV	= Electron Volt
FE	= Free Exciton
FTB	= Free to Bound
FWHM	= Full Width Half Maximum
IR	= Infared Radiation
lb	= Pound
K	= Degrees Kelvin
KeV	= Kilo Electron Volt
LHe	= Liquid Helium
LO	= Longitudinal Optical Phonon
MeV	= Milli-Electron Volt
O _S	= Oxygen Substitued at a Sulfur Site
PMT	= Photomultiplier Tube
TO	= Transverse Optical Phonon
UV	= Ultra-violet
V _S	= Sulfur Vacancy

Abstract

This investigation used high resolution cathodoluminescence to determine the spectral emissions and optical properties of the yellow and waterclear forms of undoped cubic chemical-vapor-deposited polycrystals of ZnS. The spectra between 3200 and 9000 Å was investigated at 10 K. The yellow material was determined to have characteristically poor quality with little band edge structure. The partial annealing procedure used to make waterclear ZnS from the yellow ZnS was found to greatly improve the quality of the crystals. Waterclear ZnS was of a quality equivalent to the best single crystals despite the polycrystalline form. It had a complex near band edge structure. Oxygen was found to have migrated to the crystal boundaries.

The spectra of the waterclear ZnS at 10 K agreed with the literature. Additional peaks were detected at 3259, 3270, 3321, and 3380 Å. The 3259 Å peak was determined to be the free exciton peak. The 3321 and 3380 Å peaks were determined to be due to O_S and V_S respectively. The SAL peak was generally not seen in waterclear ZnS below .1 milliamps/cm². Several oxygen and one Mn-related SAL peaks were detected. The blue and green SA peaks appeared to have unresolved substructure which caused the peaks to shift. The blue peak was at 4300-4485 Å instead of 4700 Å for undoped ZnS. No peaks were detected between 5800 and 9000 Å.

I. Introduction

This research is centered on the identification of the spectral peaks in the cathodoluminescent emission from the yellow and waterclear forms of chemical vapor deposition (cvd) grown polycrystalline ZnS. To provide an understanding of the importance of these materials some background information is provided. This will be followed by a discussion of the problem, the scope of the investigation, assumptions, approach to the problem, and the sequence of presentation of this report.

Background

ZnS is a crystalline compound which is widely used in electronic equipment and electro-optical devices. The U.S. Air Force has studied ZnS for a possible laser window material because electromagnetic (EM) radiation of a wide range of frequencies can be transmitted through ZnS with little attenuation. This wide range of frequencies is directly related to the large direct energy gap of ZnS. The energy gap in cubic ZnS is approximately 3.85 electron volts (eV) at 4.2 K compared to 1.1 eV for silicon, one of the most widely used semiconductor materials. ZnS has been made into a very efficient and widely used TV phosphor because the large band gap allows emissions in the blue and green regions of the spectrum (Ref 10:15). Impurities in the ZnS crystal phosphoresce when the crystal is irradiated with EM radiation or electrons with sufficient energy. Because ZnS

phosphorescences and has a large band gap, it is a potential source for blue and white light in discrete diodes and thin film electroluminescent displays (Ref 30:2016; 39:1866). Construction of useable diodes, detectors, and LEDs is not possible at this time because researchers have not yet been able to develop a p-n junction from ZnS. Researchers have been able to create n type crystals, but not p type, with moderately acceptable electrical characteristics (Ref 39:1866).

The primary reason for investigating the spectral properties of ZnS is that the Air Force has studied the use of ZnS as a laser window. Even though ZnS has a large frequency band pass with low absorption, there is still a measurable degree of energy absorption. The absorption causes the laser windows to heat up and distort. This distortion will degrade the laser beam and the effectiveness of the laser. If enough energy is absorbed the windows could be damaged permanently. An important secondary reason for investigating ZnS is that the Air Force has an on-going research program on the possible use of ZnS as an infrared (IR) window dome for missiles.

Problem

The ultimate goal is to make a more transmissive window. Theoretically, ZnS should not absorb any EM radiation in the crystal's band pass frequency range. Therefore, defects and/or impurities must be present in the crystal.

These impurities and defects must be identified and eliminated to improve the transmissive characteristics of the material.

The problem to be solved is to determine what defects and impurities are causing radiation absorption and to identify the processes by which radiation emission takes place. Cathodoluminescent emission spectroscopy was chosen as the method to investigate the material.

ZnS crystals can be grown by many different growth techniques. The crystal's spectral properties have been shown to vary considerably depending on the technique and conditions used to grow the crystal. The purpose of this study is to expand upon the knowledge base of the spectral peaks for yellow and waterclear forms of cvd polycrystalline ZnS. Although numerous articles were found on ZnS the only record found of any examination of the spectral peaks for waterclear ZnS was an unpublished cursory examination by Varni (Ref 115). Only three articles were found concerning yellow cvd polycrystalline ZnS (Ref 78; 91; 115). Most of the literature concerned research on phosphors.

Scope

When irradiated with electrons ZnS phosphoresces. The task was to identify the spectral peaks by determining the wavelengths of each peak, the types of impurities and defects involved in the emission, and the type of transition involved in the emission. The identification of

impurities, defects, and transitions was made, when possible, by comparing the spectral peaks with data in the literature. Trace impurity analysis studies were performed using spark mass spectrometry. No attempt was made to identify peaks by incorporation of impurities.

The effect of varying the temperature from 9.5 to 40 K and varying the incident electron flux from .88 microamps/2.5 mm radius spot to 130 microamps/.3-.4 mm radius spot (0.004 to 26 milliamps / cm²) on the emission.

Assumptions

The pressure effects on the wavelength shift of a peak was considered negligible because of the size of the samples. The induced strain and pressure caused by the low strain sample holder mask are extremely small compared to one bar (2.248 lb) of pressure. One bar of pressure results in a shift of approximately 6/1000 of a milli-electron volt (MeV) (Ref 95:3).

The sample temperature was assumed to be close to the reading of the thermocouple monitor and any differences in data caused by the temperature variation were negligible. The shift of the spectral peaks' wavelength and change of relative peak heights caused by the high flux should be considerably larger than for a few degrees change in the surface temperature of the sample. Although the sample temperature was measured in the center of the copper sample holder, approximately 2 cm from the sample, the error would

not be very large. The copper block is a very good thermal conductor and the temperature of the back side of the sample would be nearly the same as the thermocouple reading. The temperature, in the area of phosphorescence, would be slightly higher due to the excitation beam. When relatively low excitation currents are used the net heating of the sample would be no more than one or two degrees. Higher excitation currents would raise the temperature somewhat more but the effect is considered to be insignificant compared to the effect caused by the higher excitation currents.

Cubic ZnS has a band gap energy of 3.84 eV which decreases at a rate of .46 MeV / K (Ref 74:54). The bound exciton and free to bound peaks do not shift in energy for temperature changes at temperatures below about 40 K while the donor-acceptor pair peaks have been reported to shift about .17 MeV / K. A shift in peak position due to an increase in electron flux is expected only for donor-acceptor pair peaks. This shift could be as high as 10-12 Å or 11-13 MeV in the region of 3300 Å.

When the observed spectral peaks were compared to the literature, the difference between the wavelengths reported at 4 K and the wavelength expected at 10 K was assumed to be negligible for identification purposes.

Although the samples used in the various reports were prepared by different methods and tested under slightly

different conditions, the reported peaks should be caused by the same luminescent center if the peaks detected in this study were at the same energies and reacted in a similar manner. The peaks obtained by photoluminescence should be nearly identical to those obtained by the cathodoluminescence method.

Approach.

Cathodoluminescence was selected as the method to induce phosphorescence in the samples. The large energy band gap of ZnS excludes most excitation sources if the near band edge spectra is to be examined. No lasers were available with a wavelength less than 3200 Å. Cathodoluminescence, however, uses an inexpensive electron gun which was already available. The acceleration voltage on the electron gun was approximately 2000 volts. Therefore the electrons had 2000 electron volts (eV) of energy which could be transferred to the crystal by collisions to induce phosphorescence.

Polished samples were placed in a high vacuum chamber and cooled to 10 K. The samples were irradiated by the electron beam and the emitted radiation was collected by a lens system and passed through a monochromator to a photomultiplier (PMT). The output signal of the PMT was processed by an amplifier/discriminator and stored on a multichannel analyzer. The emitted spectrum for 3200 to 9000 Å was

examined while various temperature and excitation intensities were used.

Sequence of Presentation.

No single model can describe how ZnS or any semiconductor material phosphoresces. Therefore in the "Theory and Summary of Previous Research" chapter the various models are developed for ZnS and the important solid state physics concepts needed to understand this study are presented. Intertwined in this presentation is a review of literature on ZnS.

Chapter III, "Experimental", explains how the samples were examined by describing the procedures, equipment, and samples used in the experiments.

The experimental results are presented in Chapter IV, "Results and Discussion". The data will be analyzed by comparing it with spectral data reported in the literature and by using the known properties of ZnS and those of various impurities in ZnS. The results are tabulated showing the emissions detected, the impurities, and/or emission mechanisms. The consistency of the sample spectra will also be discussed.

The results of the experiments will then be summarized, and general conclusions about the cvd polycrystalline ZnS material will be presented. Because there is little literature on high resolution spectral studies of waterclear and yellow forms of cvd polycrystalline ZnS, some speculations

had to be made concerning the processes involved. Additional experiments are needed to verify some of the conclusions in this report. Recommendations will be presented to accomplish this and to provide ideas of some areas where further investigation is needed.

II. Theory and Summary of Previous Research

A brief description of ZnS crystallography and energy structure is followed by a discussion of the cvd crystal growth technique. A discussion of the spectral bands and phonons in ZnS is followed by a summary of the effects of temperature and intensity variation on the wavelengths of the spectral peaks. The review of literature spans the period from 1957 to May 1983.

Crystallography.

ZnS can crystallize into either a hexagonal (Wurtzite) or cubic (Zincblende or Sphalerite) structure. The Wurtzite structure is formed by interweaving two simple hexagonal structures with the same C-Axis direction. The plane containing a hexagonal net of one hexagonal structure is midway between those of the other structure. One structure is composed of zinc atoms and the other is composed of sulfur atoms. This pattern is then repeated after two double layers. The Zincblende structure is like the diamond structure. In ZnS, one of the two interwoven face-centered cubic lattices is composed of zinc and the other of sulfur. One cubic lattice is displaced $1/4$ the distance along the body diagonal of the other cube. This structure is repeated after three double layers (Ref 102:87-90). In addition to these repeating patterns, there can be a larger scale pattern of mixed cubic and hexagonal structure called a "polytype".

Unless special precautions are used during crystal growth, ZnS easily grows as a polycrystalline substance. Instead of a single crystal, the solid is made up of numerous smaller crystals which can be randomly oriented, and which can vary in polytype or size. These polycrystalline solids are the primary type studied by the Air Force for electro-optic applications.

Energy Band.

The crystal structures of cubic and hexagonal ZnS are very similar. An atom's environment is essentially the same out to the second nearest neighbors in the two structures (Ref 5:123). Therefore, there is only a third order perturbation difference between cubic and hexagonal potential field calculations (Ref 83:875). The result is an energy gap of 3.91 eV for hexagonal crystals and 3.833 eV for cubic crystals (Ref 83:876; 74:54).

Emission Models.

For many years, researchers have known that the presence of impurities and defects causes crystals to phosphoresce. However, the precise mechanisms for the emissions in ZnS are still uncertain. Over the years three primary models have been developed. The Schön-Klasens model explains one type of emission as the radiative recombination of a photon-generated electron in the conduction band with a hole trapped at an acceptor site just above the valence band (See Figure II-1). This is a free-to-bound transition. The

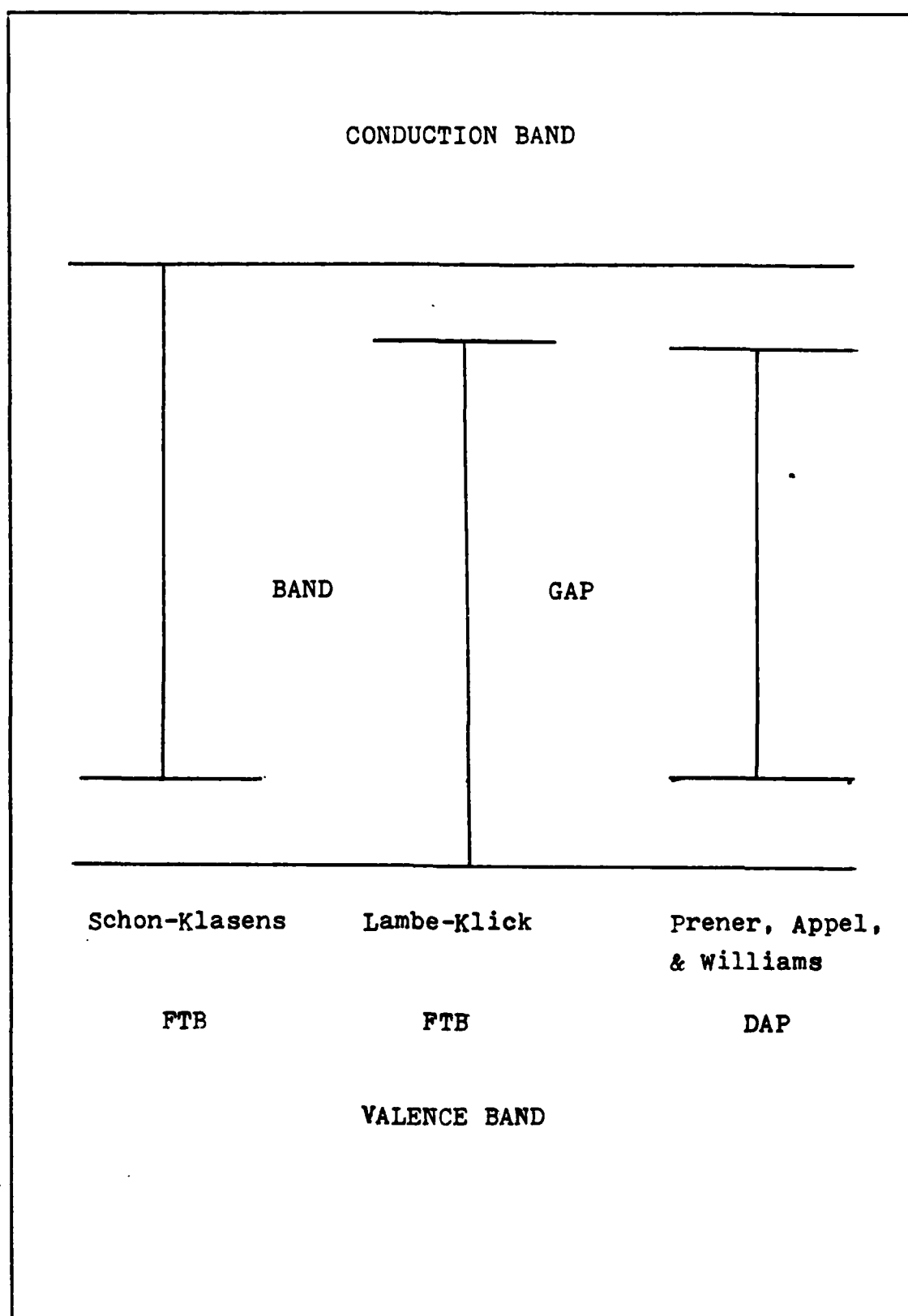


Figure II-1 Transition Models

second model is the Lambe-Klick model. It proposes possible radiative recombination by an electron trapped at a donor site just below the conduction band, in the band gap, with a hole in the valence band. This also is a free-to-bound transition (See Figure II-1). The third model, by Prener, Appel, and Williams, is a donor-acceptor recombination. The radiative recombination is between an electron bound to a donor site below the conduction band and a hole bound to an acceptor site above the valence band (Ref 5:444) (See Figure II-1).

Spectral Bands.

Most of the research conducted so far has been concentrated on the spectral region between 3200 and 3950 Å. A few articles which discussed spectral lines between 3950 and 6400 Å were found. One extensive study identified 75 peaks between 8100 and 9200 Å (Ref 17). Table II-1 is a compilation of the spectral peaks reported in the articles reviewed by the author.

The prominent features in the 3200 to 5200 Å range are the free exciton (FE), bound excitons (BE), donor-acceptor pair (DAP) bands, self-activated-low-temperature luminescence (SAL) band, and the self-activated (SA) bands. The SA and SAL bands are bands which occur in the spectra of undoped samples and hence the name self-activated is given to them.

TABLE II-1

Compiled ZnS Emission Peak Reference List

Temp K	Wavelength Å	Symbol	Mechanism	Reference
4	3224		Packing Defect	94
4	3240		Packing Defect	94
	3258.7	FE	(Calculated)	36
5	3263	X7	BE	36
5	3266	X6	BE	36
80	3266		BE	70
80	3267		BE	94
80	3269		BE	94
80	3270		BE	94
8	3270	FE	FE	39
4.2	3272	X5	BE	36
10	3272	A1	BE	85
5	3275	X4	BE	36
4-5	3275-6	X3	ABE	36
4.2	3276.7		BE	8
80	3275			91
4.2	3282	X2	BE	36
78	3280			27
10	3279		Phonon	70
80	3280			91
4.2	3288	X1	BE	36
80	3290			91
80	3295			91
4.2	3297	FE-LO	Phonon	36
10	3299		Phonon	70
	3300	V -2 + Br -1 or Al or Ga Zn S		79
8	3300	I1	BE + Neutral Accep.	39
10	3302	A2	BE + LO	85
5	3304	X6-LO	Phonon	36
80	3303		BE	70
4.2	3305	X5-TO	Phonon	36
4.2	3312	X5-LO	Phonon	36
5	3313	X4-LO	Phonon	36
4.2	3314-5	X3-LO	Phonon	36
10	3317		Phonon	70
4.2	3320	X2-LO	Phonon	36
4.2	3326	X1-LO	Phonon	36
8	3330	I1	BE	39
4.2	3333-5	FE-2LO	Phonon	36
4.2	3336	FE-LO-TO	Phonon	36
4.2	3340	X5-2TO	Phonon	36
10	3341	A3	Phonon	85

TABLE II-1 CONTINUED

Compiled ZnS Emission Peak Reference List

Temp K	Wavelength λ	Symbol	Mechanism	Reference
4.2	3342.5	X3-2TO	Phonon	36
4.2	3343	X5-TO-LO	Phonon	36
8	3342	I1-LO	Phonon	39
4.2	3345	X2-2TO	Phonon	36
4.2	3348	X5-2TO	Phonon	36
4.2	3353	X3-2LO	Phonon	36
8	3360	Qo	DAP	39
80	3370			91
10	3378	A4	Phonon	85
80	3380			91
4.2	3392	X3-3LO	Phonon	36
84	3400			92
8	3395	Po	DAP	39
80	3400			91
10	3400	Bo	S Vacancy FTB	85
80	3405			91
5	3407-8	K2	DAP	36
77	3405		C1	38
8	3408	Q1	Phonon	39
80	3410			91
80	3415			91
84	3415			92
4.2	3422	K1	DAP	36
80	3415		BE	70
80	3435			91
84	3440			91
10	3442	B1	C1 at S site FTB	85
5	3446-7	K2-LO	Phonon	36
8	3450	Q2	Phonon	39
84	3460			92
4.2	3462	K1-LO	Phonon	36
10	3485	B2	Phonon	85
5	3485-6	K2-2LO	Phonon	36
8	3494	Q3	Phonon	39
4.2	3503	K1-2LO	Phonon	36
84	3500			92
84	3515			91
5	3527	K2-3LO	Phonon	36
10	3529	B3	Phonon	85
4.2	3545	K1-3LO	Phonon	36
	3550	V -2 + Br -1 or Al or Ga Zn S		79

TABLE II-1 CONTINUED

Compiled ZnS Emission Peak Reference List

Temp K	Wavelength Å	Symbol	Mechanism	Reference
84	3560			91
4.2	3568			36
4.2	3588	K1-4LO	Phonon	36
77	3646			38
10	3619	B5	Phonon	36
77	3700		ZnO	94
77	3850-4000	V to V O Zn	in ZnSO	67-8
78	3900		Ag II	27
4	3953		Mn	59
300	3906		Mn++ Zn++	9
300	4000			69
4.2	4064		DAP	57
77	4050-4150		Sulfur Vacancy	113
77	4150-4260		Cl at S site	113
10	4150		Cl + V DAP S Zn	85
4	4150		Ag FTB	107
4	4280		ZnS:I,P	107
78	4220		Cu	27
300	4270			69
300	4292			9
78	4300-4500	Ag + Group III or VII		27
4	4417		Mn	59
300	4400		Cu	69
	4486		ZnS:Ag,Al	57
300	4460		Au	80
300	4520		Cu	69
	4525		ZnS:Ag,Al	57
85	4508		Ag + Accep. DAP	89
300	4500		ZnS:Cu,Cl,Nd	55
300	4580		ZnS:Cl	47
4	4580		ZnS:I,P DAP	107
300	4600		Al	80
78	4610		Ag	27
77	4630		Li	31
	4650			27
300	4651		Mn	9
77	4660		Zn ion	113
	4700		ZnS:Al	57

TABLE II-1 CONTINUED

Compiled ZnS Emission Peak Reference List

Temp K	Wavelength Å	Symbol	Mechanism	Reference
	4700		(V -Cl) + donor Zn	44
300	4670		Cu	69
4.2	4680		B + V Zn Zn	46
4.2	4695		DAP	57
4	4709		Mn	59
4	4710		Mn (estimated)	80
10	4730		Zn" vacancy FTB	85
300	4713		ZnS:Cl faulted	47
300	4750		ZnS:Cu,Cl	55
300	4800		ZnS:Mn,Cl	47
300	4830		Cu	69
4.2	4853		Al	80
77	4960		V + Cl Zn S	113
300	4975			9
300	5050		ZnS:Cu,Cl	55
4	5080		Mn	59
77	5050		Cu + Al	67
77	5100		Cu	67
4	5165		Cu + Cl	98
4.2	5200		Cu + Al	2
77	5220		Cu + Al	67
77	5250		Cu + co-activator	67
	5225		ZnS:Cu,Al	57
300	5348			9
	5250		Cu,Tb or Ag,Tb	112
77	5460		Oxygen	67
4	5494		Stack Faults	58
4	5558		Stack Faults	58
4	5587		Phonon	58
4	5589		Mn	59
4	5682		5587 + LO Phonon	58
	5775		ZnS:Mn	57
4	5781		5587 + 2 LO	58
300	5850			72
4	5860		ZnS:Mn ²⁺	58
4	5883		5587 + 3 LO	58
4.2	5894		ZnS:Mn,Cl	47
300	5900		ZnS:Mn,C,	47
6	5900		ZnS:Mn	43
77	6324		Zns:Pb	66

TABLE II-1 CONTINUED

Compiled ZnS Emission Peak Reference List

Temp K	Wavelength Å	Symbol	Mechanism	Reference
300	6700-6800		Cu	28
300	6800		Sn	28
77	6900		Cu + V Zn S	101
80	7000		Cu + Ag	99
77	7206.9		ZnS:Sn	66
77	7334.9		ZnS:Si	66
77	8791.4		ZnS:Ge	66

When ZnS is irradiated with electrons or EM radiation an electron can be raised from the valence band to the conduction band. A direct recombination of the free electron with a hole is unlikely, due to conservation of momentum. Transitions involving defect states or impurities are needed to conserve momentum during the recombination of a free electron and a hole.

A mechanism which can assist in conserving momentum is the free exciton. As a free electron and a hole pass close to each other, they can interact and the electron drops into a hydrogenic orbit around the hole instead of directly recombining. This complex is called a free exciton. The free exciton is unstable and the electron will eventually recombine with the hole and give off a photon of energy. The emission line will have a very weak intensity because of the low probability of the free exciton forming due to conservation of momentum. The emission line will also be broad for the free exciton because of the random difference of kinetic energy between the free electron and free hole associated with exciton (Ref 104:2; 74:50; and 102:261). In cubic ZnS the 3270 Å peak was tentatively identified by Gezci and Woods to be the FE. Other researchers have identified the 3270 Å line as a BE.

A more likely transition than the eventual recombination of the FE is the recombination of electrons and holes bound by localized impurities or defect sites. The bound

exciton (BE) is an exciton in which the electron is associated with an impurity donor atom and the hole is from the valence band, or the electron is from the conduction band and the hole is associated with an acceptor impurity atom.

Three types of BE have been seen in various materials. The "I" BE is a neutral acceptor plus an exciton. The "I"₁ BE consists of a neutral donor impurity plus an exciton₂. The "I"₃ BE is an ionized donor impurity plus an exciton (Ref 85:1954). Because the massive defect or impurity can absorb the momentum of the exciton, momentum conservation is easily satisfied. Because the sites are localized there is no kinetic broadening of the emission line. Some lifetime broadening is caused by the short lifetime (Ref 104:2-3). The particular symmetries and energies of emission of the BE will be characteristic of the impurity or defect involved. The emission peaks are relatively sharp and intense.

If there is a sufficient concentration of both donor and acceptor impurities or defects, a donor-acceptor pair recombination emission is possible. The excitation radiation ionizes the donors and acceptors. An electron is then trapped by the donor site and a hole is trapped by the acceptor site. The electron then recombines with the hole and emits radiation. The energy of the emission is determined by the following equation.

$$E_G = E_G - (E_A + E_D) + e^2 / Kr - nE_P \quad (1)$$

where

E = The energy of the emitted radiation.

E_G = The band gap energy.

E_A = Energy depth of the acceptor in the band.

E_D = Energy depth of the donor in the band.

K = Low frequency dielectric constant.

r = Separation of the donor and acceptor.

n = Small integer.

E_P = Energy of the assisting phonon, if applicable.

For small separations, the distance r can vary by discrete multiples of the lattice constant, resulting in discrete lines. As r gets larger the discrete emission lines merge into what are called the low temperature emission bands (Ref 104:3-4). These lines are normally seen below 30 K (Ref 114:1124). The DAP lines have been detected in the UV, Blue, Green, Red, and IR parts of the spectrum.

If there are insufficient concentrations of either donors or acceptors or if the temperature is high enough so that the shallow donors are ionized, the acceptors can recombine with free electrons or ionized donors, and the donors can recombine with holes in the valence band. These emissions appear as broad bands and are known as the high temperature or high energy bands (Ref 104:4). They are normally seen above 40 K. The high temperature emission has

also been seen at temperatures as low as 4 K when the donor concentration is very low (Ref 114:1129).

The SAL band has been attributed through the years to Na ions, S vacancies, Cl substituted at sulfur sites, and most recently O vacancies in ZnS-O impurity crystals within the main ZnS crystal (Ref 67:933). Because the wavelength of the peak studied differed with each report and the conditions under which the samples were studied and prepared differed, the source of the SAL peak has not been conclusively determined. The oxygen vacancy, however, does seem to be the best explanation at this time for emissions in the 3700 to 3900 Å spectral region.

There are two Self-Activated (SA) bands. One is in the blue region at about 4200-4800 Å and the other is in the green region near 5200 Å. Confusing terminology exists in the literature because some authors have called peaks in doped samples which are in these areas the SA peak. The literature discusses what apparently are three distinctly different emission sources. The Blue-SA peak of the undoped ZnS and the Blue-Ag peak in Ag doped ZnS both shift to higher energy as the temperature increases while the Blue-Cu peak in Cu doped ZnS shifts to lower energy as the temperature is increased. However a time-resolved peak shift to lower energy of Blue-Ag is reported while the Blue-SA shifts only slightly and the Blue-Cu does not shift (Ref 94:964).

The following history was extracted from James et al. (Ref 44). Prener and Williams suggested the SA center as a zinc vacancy paired with a substitutional halogen ion on an adjacent sulfur site. Kasai and Otomo showed the site was a paramagnetic center, called an A center. Dischler et al. and later Schneider et al. showed the center consisted of a hole trapped on a sulfur ion adjacent to the $V_{Zn}-Cl$ pair." Koda and Shionoya confirmed the Blue-SA emission was due to the A center. Era et al. observed a spectral shift to lower energy during luminescent decay. This was inconsistent with these previous theories so Era suggested the emission was related to the donor state of an isolated co-activator ion and the acceptor state of a (V_{Zn} -- co-activator) center. Blount et al. suggested isolated Cl donors on substitutional sulfur sites are essential to the SA emission (Ref 44:969). James et al. used optical electron-paramagnetic resonance (EPR) to confirm the donor-acceptor nature of the SA emission (Ref 44:970). The emission mechanism is as follows. The self activated center is ionized by radiation which results in an electron in the conduction band and a hole at the A-center. The donor state is filled by electrons from the conduction band and the electron-hole recombination produces the Blue-SA emission (Ref 44:971).

The Green-SA peak is typically found around 5200 Å with a half-width of about .3 eV. Riehl and Siman (Ref 76:80) and van Gool (Ref 11:921) concluded that the Green-SA

emission is caused by an isolated substitutional copper ion replacing a zinc ion at a lattice site with an undistorted neighborhood. This could possibly explain why Hoogenstraaten and van Gool (Ref 11:922) both found the location and half-width of the peak to be independent of the coactivator. Therefore the peaks would appear the same if the coactivator was either Al or Cl. Shionoya, Era, and Washizawa and others agree that there is no fine structure in the Green-Cu emission (Ref 98:1167; 11:922). Work by Nemchenko indicates there is a fine structure in both the blue and green SA peaks (Ref 69). Work by Curie and Grillot, separately, shows Cu in a FTB is responsible for a 5080 Å peak and a $(\text{Cu}_S + \text{a coactivator})$ is responsible for a 5250 Å peak (Ref 69:932).

Phonons.

Phonons are quantized amounts of energy associated with lattice vibrations (Ref 102:326). If radiation is emitted due to transitions through defects or impurities states in the crystal, there may be additional peaks associated with each of the parent peaks. These additional peaks are caused by a resonance interaction between the phonons and the processes which cause the parent peaks. The intensity of a phonon-assisted peak generally is less than the parent peak and any preceding phonon-assisted peak. The energy difference between peaks in the series will be equal to an integral multiple of the energy of the phonon.

Although a substantial number of research articles were found concerning ZnS, most of the research concerned single crystals and platelets. Few articles dealt with undoped materials. Even fewer articles discussed cathodoluminescent emissions of undoped ZnS. Only three articles reported studies on polycrystalline ZnS and only one reported a cursory examination of waterclear ZnS.

These articles generally reported spectral peaks associated with the doped materials. In the undoped materials only the SAL, SA-Blue, and the SA-Green peaks have been tentatively associated with a particular type of defect and/or impurities as well as identifying the emission mechanism. The rest of the peaks have only been tentatively identified as an exciton-related, donor-acceptor pair, or phonon-assisted emission peaks.

Temperature.

The characteristic dependence of a peak's wavelength on temperature is different for each type of emission peak. Samelson and Lempicki found one group of UV peaks, called the A series, to have no temperature dependence up to 45 K but a linear decrease in energy as the temperature was increased (Ref 85:Fig 11). The B series UV peaks exhibited a linear decrease in energy as the temperature increased (Ref 85:Fig 12). Shalimova examined both cubic and hexagonal crystals in powder, single crystal, thin film, and polycrystalline forms at 4.2 K and from 80 to 400 K.

Shalimova primarily examined the UV lines and found the higher energy peaks shifted faster than the lower energy peaks as the temperature increased. The peak's shift was linear (Ref 91:1601). The spectral shift associated with the hexagonal crystals was slightly larger than for cubic crystals. The shift was the same for powder, single crystals, and thin films but depended upon how the samples were grown (Ref 91:1599).

The SA peak energy decreased nearly linearly as the temperature increased (Ref 85:Fig. 6). No literature was found which discussed how the SAL peak varied with temperature.

In the near IR region from .815 to .92 microns, as the temperature increased from 1.5 to 30 K the peaks shifted toward higher energies and the shift was proportional to the temperature cubed (Ref 17:103).

Electron Flux.

A dependence of the wavelength for UV peaks on the electron flux was determined to be quadratic for low flux levels and linear for high flux levels (Ref 70: 144). The SA peaks have been shown to shift to shorter wavelengths as the excitation photon flux increased (Ref 2; and 95). Shionoya found a logarithmic relation between the energy of the emitted radiation and the excitation flux (Ref 95: 3). Kuboniwa et al. (Ref 56) investigated saturation effects of cathodoluminescence in doped ZnS.

III. Experimental

This section describes the procedures and equipment used in the research. The order of presentation is: Sample Information, System Overview, Vacuum System, Cryogenic Transfer System, Electron Gun, Optical System and Alignment, and Signal Processing.

Sample Information

The sample characteristics will be discussed in the following sequence: Chemical Vapor Deposition, Sample Preparation, Color, Microscopy and Grain Size, and Crystal Structure.

Chemical Vapor Deposition. The crystals used in the research were yellow chemical-vapor-deposition (cvd) polycrystalline ZnS and waterclear ZnS, which is a specially heat and pressure treated cvd polycrystal. The starting material, yellow cvd polycrystalline ZnS, is an opaque yellow while the waterclear ZnS is transparent.

Chemical-vapor-deposition uses organometallic precursors as a zinc source to grow the crystals. One typical reaction process for cvd crystal growth is $\text{ZnS} + \text{I}_2 \rightleftharpoons \text{ZnI}_2 + \frac{1}{2} \text{S}_2$. The $\text{ZnS} + \text{I}_2$ mixture is injected in the high temperature (1000 C) end of a silica tube. The ZnI_2 and S_2 compounds are formed and then thermally transported to the cool end (750 C) of the tube. At the cool end of the tube the reverse process takes place and the ZnS crystals grow

(74:34). The particular reactions and conditions for making the waterclear samples of ZnS are still proprietary. Crystals produced by the cvd method are the best available in perfection and purity due to low growth temperature. Typically, these crystals are of a polycrystalline form.

Sample Preparation. The samples used were from CVD Inc. and the Raytheon Corp. One sample of "waterclear" ZnS was made by CVD Inc. about one year ago and obtained from the Air Force Materials Lab. It will be called waterclear #7 in this report. It was a donut shaped ring 15 mm in diameter and 2.5 mm thick. The front and back surfaces were moderately well polished. The rest of the waterclear samples were recently acquired from CVD Inc. From three pieces with one moderately well polished surface, several 5 by 5 by 1.6 mm samples were cut. Waterclear sample #1 was cut from a piece by the Materials Lab. Samples #2 through #6 were cut from two different pieces and were polished by the University of Dayton (U of D). Waterclear samples #2 through #6 had a better surface preparation than #1.

Yellow polycrystalline sample #1 was cut from a piece of CVD Inc. yellow ZnS by the Materials Lab. One piece of Raytheon Corp. yellow ZnS was obtained from the Materials Lab. It was cut and polished, along with samples from two pieces of CVD Inc. yellow ZnS, in 5 by 5 by 1.6 mm pieces by the U of D.

Color. The waterclear samples were transparent to the eye. The yellow ZnS from CVD Inc. had an opaque light yellow color. The polycrystalline ZnS from Raytheon Corp. was a very opaque dark brownish yellow.

The difference between the colors of the CVD Inc. waterclear and yellow ZnS is consistent with the transmission curves of the two materials (See Figure III-1) (Ref 109:4). There is little transmission in the blue and green regions for the yellow cvd polycrystalline materials. A theory is proposed in this report as to why the transmission is increased when the polycrystalline ZnS is heat and pressure treated.

Microscopy and Grain Size. The five pieces of ZnS from which the University of Dayton cut samples were each microphotographed. The samples were prepared by etching with H_2SO_4 . Etch time for CVD Inc. waterclear pieces #1 and #2 and yellow piece #1 was 7 to 8 minutes. Etch time for CVD Inc. yellow #2 and the Raytheon yellow sample was 15 minutes. All samples were micro-photographed with white light at 250 X.

Waterclear piece #1 appeared to have more defects than #2. What appeared to be cracks or holes were more prevalent in #1. The shapes and sizes of the crystals in #1 also were more irregular than #2. The size of the individual crystals in the waterclear samples was about ten times that of the individual crystals in the yellow base material. This is

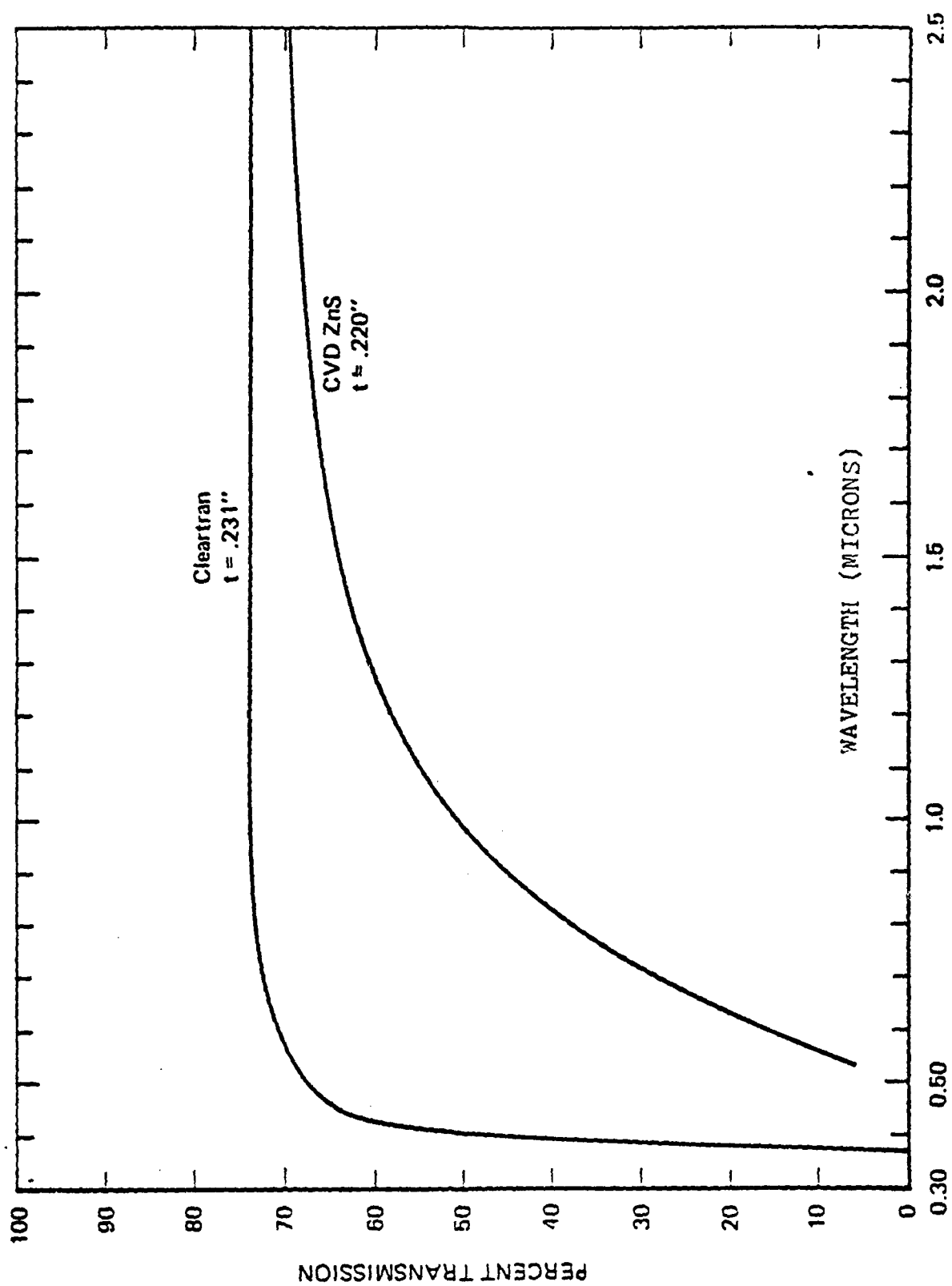


Figure III-1 Comparison of CVD ZnS and Cleartran Visible Transmission

consistent with commercial literature by CVD Inc. and a report by Taylor and Lefebvre (Ref 109). Taylor and Lefebvre found the yellow ZnS material to have 2-6 micron crystals while the individual crystals were about 20-30 microns large in the waterclear. This is consistent with the current micro-photographs.

The crystals in photographs of the CVD Inc. yellow #1 and the Raytheon yellow sample appeared as long irregular needles. The CVD Inc. crystals were more irregular in shape and wider than those in the Raytheon sample. The needles appeared to be about the same length in the two samples.

The photograph of CVD Inc. yellow ZnS piece #2 appears to be an end view of the needles. Proof of this assertion will be provided in the Crystal Structure section. If this is the case, then the material has numerous crevices or holes between the crystal needles (like the stacking of pipe). A few cracks were observed between crystal needles in the end view micro-photographs.

Crystal Structure. X-ray diffraction studies were done by Doug Wolf at U of D on these five sample pieces. The samples were studied in both the flat surface and powdered forms. The d-spacing and relative intensities corresponded to the cubic B form for all samples. There was no indication of any polytype or hexagonal structure. Therefore the possible percentage of hexagonal form was less than 5%. The precision lattice constants are shown in Table III- 1.

TABLE III-1

Sample Lattice Constants

Sample	Piece	a o	Error
1	CVD Inc. Waterclear #1	5.410	.001
2	CVD Inc. Waterclear #1	5.4120	.0006
3	CVD Inc. Yellow #1	5.408	.001
4	CVD Inc. Yellow #2	5.4138	.0007
5	Raytheon Yellow #1	5.4128	.0004

Samples #2 and #3 showed a preferred orientation in the (220) plane with a d-spacing of 1.905. Sample #1 showed preference for the (311) plane with a d-spacing of 1.625. Sample #4 tended to have both orientations.

Piece #1, as examined by the micro-photographs and the x-ray diffraction studies, appears to correspond to what was originally the end view of the crystal needles before the pressure and heat process converted the yellow cvd polycrystalline ZnS into waterclear ZnS. Because of the larger size of the crystals in waterclear ZnS there were some, but fewer, crevices present and the end-view planar orientation (311) of the cubic B form was seen. Pieces #2 and #3 appeared to be of the side view of long slender crystal needles in the microphotographs. The x-ray diffraction studies showed these pieces to have the (220) planar orientation.

The end and side views of the crystal structure are indicated in Figure III-2. The coordinate system of the lattice is chosen as indicated in Figure III-2. The lattice structure is such that the zinc face-centered cube has its

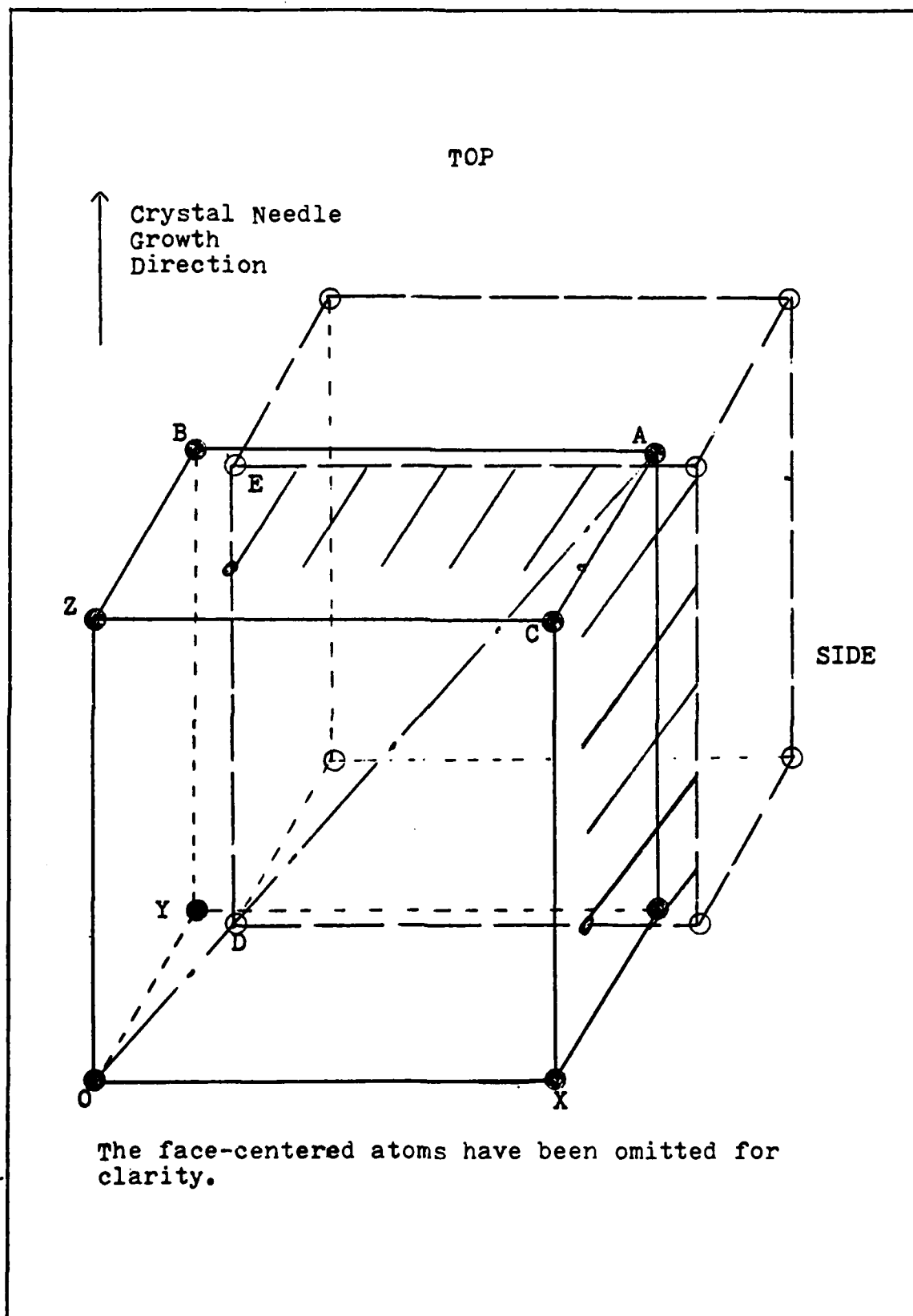


Figure III-2 Zincblende Structure

origin at the lattice origin designated O. The sulfur face-centered cube would then be displaced $1/4$ the body diagonal length from point O to point A in the zinc cube. The crystals grow primarily in the OZ direction and the OZ axis is the long axis of the crystal needles observed in the photographs. The side of the needles corresponds to planes incorporating the points O, X, Z or O, Y, Z. The end view would be of the plane of points O, X, Y. The (220) plane seen in the X-ray diffraction studies would be the plane formed by the points X, Y, B, and C. The (311) plane would include the points Z, Y, and D. An equivalent plane would include points B, C, and E where the origin is at point Z and the basis vectors are \overline{ZO} , \overline{ZC} , and \overline{ZB} . This equivalent plane would provide a plane nearly perpendicular to the (220) plane detected for the side view of the crystal needles.

Sample #4, whose picture looks like an end view, had a mixture of both the (220) and (311) planes. The small size of the crystals and some random orientation could be why both planar orientations were detected. The side planar orientation (220) was present in a 30% concentration and the end view orientation (311) was present in a 70% concentration. The pressure and heat treatment which cause the crystal needles to grow considerably also appears to reorient the crystal structure so that only the end-view planar orientation is detected when the end of the crystals

are examined. The larger size of the individual crystals and the realignment of the crystal structure, so that only one orientation is present, are proposed as the reason why the waterclear ZnS transmits very well in the 3500 to 5200 Å range while untreated cvd polycrystalline ZnS is yellow and does not transmit in this range.

Trace impurity studies were performed by the University of Dayton. Spark mass spectrometry studies, capable of detecting impurities as low as 5 parts per million, revealed no impurities.

System Overview

Figure III-3 is a schematic of the system used to obtain data. The samples were mounted on a Heli-Tran coldfinger in the vacuum chamber and pumped down to about 4×10^{-9} torr using sorption pumps and a vac-ion pump. An electron gun was used as the excitation source for the cathodoluminescence. A HeNe laser and a mechanical iris on a bi-directional traversing mount were used to align the optics. The luminescence was collected by a two lens system and focused on the entrance slit of the spectrometer. A cooled photomultiplier tube (PMT) converted the luminescence into an electrical signal. The signal was processed by an amplifier/discriminator unit and recorded by a multichannel analyser. The data was permanently recorded with both an X-Y plotter and on a cassette tape with the Techtran Datacassette recorder.

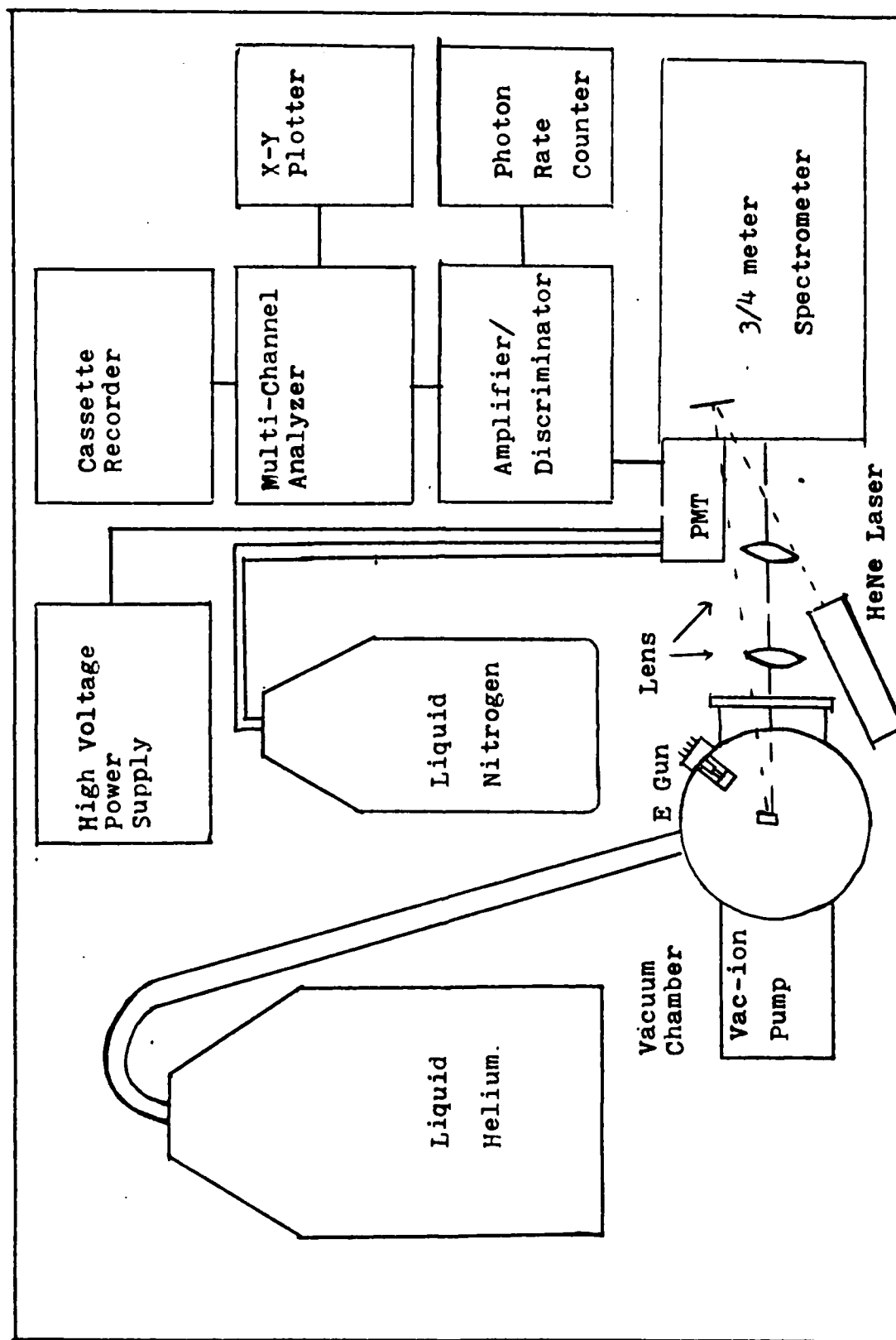


Figure III-3 System Setup

Vacuum System

The vacuum chamber was 12 inches in diameter and 2 feet tall (See Figure III-4). It had four 8 inch ports at 90° around the chamber with four 2 and 3/4 inch ports spaced between the 8 inch ports. A quartz window used for the experiments was in one of the eight inch ports. The electron gun used was located in the 2 and 3/4 inch port to the right of the window. A Faraday cup on a retractible arm was in the port to the left of the window and the leads were routed through the 2 and 3/4 inch port to the left of the Faraday cup. The Heli-Tran was mounted in a 2 and 3/4 inch port in the top of the chamber.

The vacuum system was rough pumped to below 1 micron with two Vacsorb sorption pumps. A 110 liter per second, Varian model 92/0041 vac-ion pump was then used to reduce the pressure to an operating pressure of around 4×10^{-9} torr.

Cryogenic Transfer System

The cryogenic transfer system consisted of the liquid helium (LHe) dewar and an Air Products and Chemicals model LT 3-110 Liquid Heli-Tran (Figure III-5). The Heli-Tran consisted of a central cryo-tip line to transfer LHe to cool the sample holder. This tube was surrounded by two interconnected concentric lines to insulate the cryo-tip line. The LHe flowed through the inner sheathing tube toward the sample holder and then flowed in the outer sheathing tube

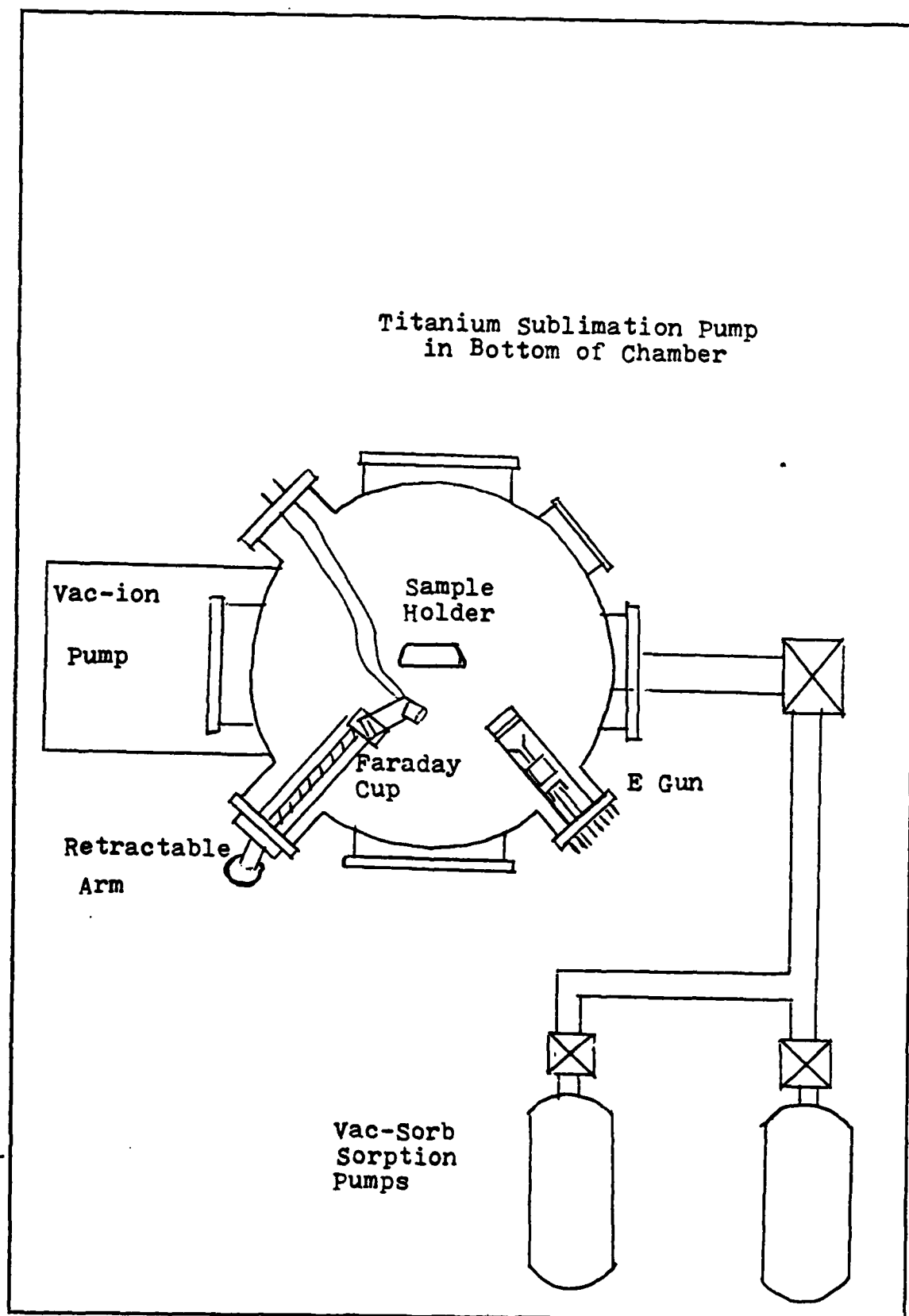
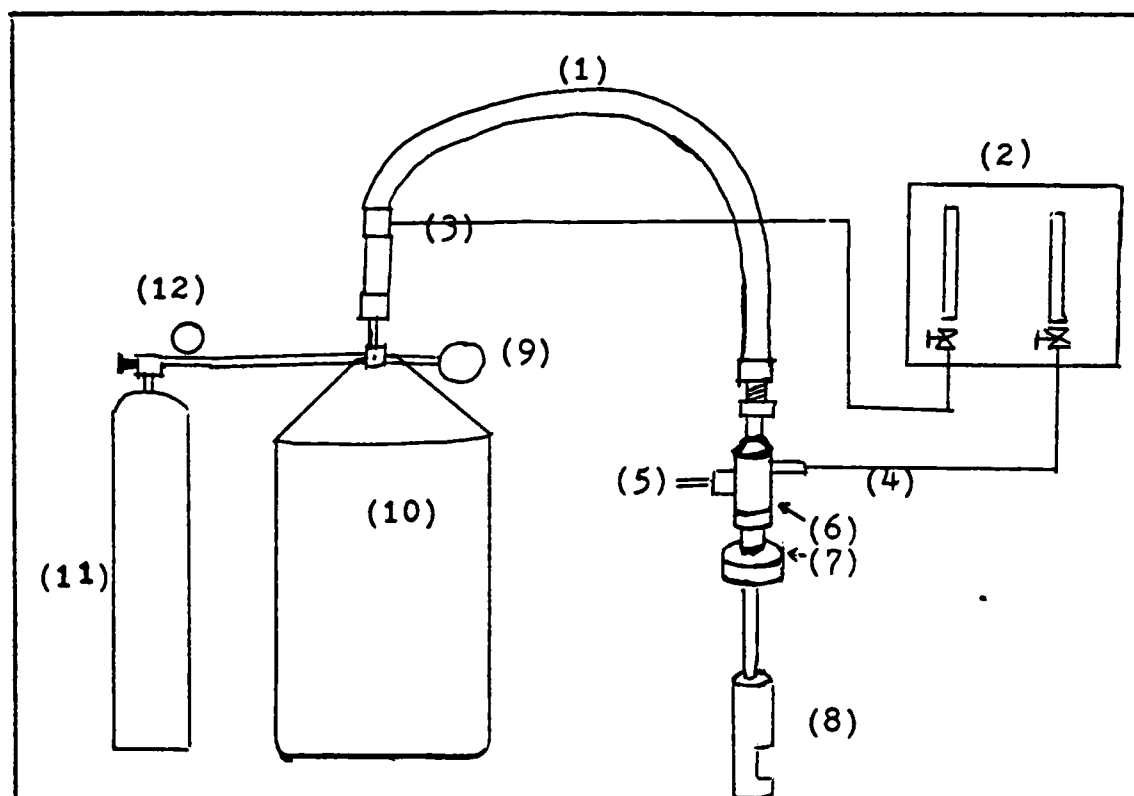


Figure III-4 Vacuum System



1. LHe Transfer Hose
2. LHe Flow Control Valves
3. Shield Flow Vent
4. Tip Flow Vent
5. Thermocouple Output Leads
6. Heli-Tran Cold End
7. Chamber Port
8. Sample Holder
9. Dewar Pressure Gauge
10. LHe Dewar
11. Gaseous Helium Tank
12. Gaseous Helium Tank Pressure Gauge

Figure III-5 Cryogenic Transfer System

back toward the dewar. The sheathing tubes were surrounded by a vacuum tube. The exhaust gases from the cryo-tip flow and the sheathing were routed to two cryo-control valves. The temperature of the sample was maintained by adjusting the outflow of the cryo-tip control valve when a temperature above the maximum cooling rate, approximately 9.5 K, was desired.

The samples were cooled down by the following procedure. The transfer line was purged of air and moisture to avoid line freeze up by flowing oil-free gaseous helium through the transfer line for a few minutes. The transfer line probe was inserted into the LHe dewar a short distance with the cryo-control valves open and the pressure built up to about 5 psi in the dewar. The dewar was pressurized by gaseous helium from a K-bottle. After allowing the gas to flow a short time the probe was slowly lowered into the LHe to avoid excessive pressure buildup and LHe loss. Cool down time to 9.5 K was about 45 minutes. When the temperature approached 200 K the heater jacket was plugged in to prevent freeze-up of the cryo-tip exhaust line.

The sample holder was on the end of the cryotip cold-finger and level with the electron gun and the center of the quartz window. The sample holder was made of a solid copper cylinder with the front and back sides cut flat to hold the samples (See Figure III-6). The samples were held in place with a thin, flexible copper mask. The mask was held

in place with four screws at the corners. Four 5 mm diameter holes were cut as shown in Figure III-6 for access to the samples. In the sample mount was a gold chromel thermocouple which was connected to a digital Instrulab 5000 temperature indicator to monitor the temperature of the samples. The sample holder was covered with an chrome plated brass cylinder to prevent extraneous radiation from hitting the samples. A rectangular hole was cut in the cylinder to provide access to the samples for the electron beam and to permit collection of the emission.

Electron Gun

A standard RCA electron gun with a barium oxide cathode was used as the excitation source (See Figure III-7). The cathode was replaced and was aged and activated using the procedure in Table III-2.

Table III-2
Aging of Barium Oxide Cathode Electron Gun

Time	Filament Voltage (DC)	Grid Voltage (DC)	Anode Voltage (DC)
1 min	6.3	0	0
1.5 min	12.5	0	0
10 min	9.0	5	150
10 min	9.0	0	0
5 min	6.3	0	0

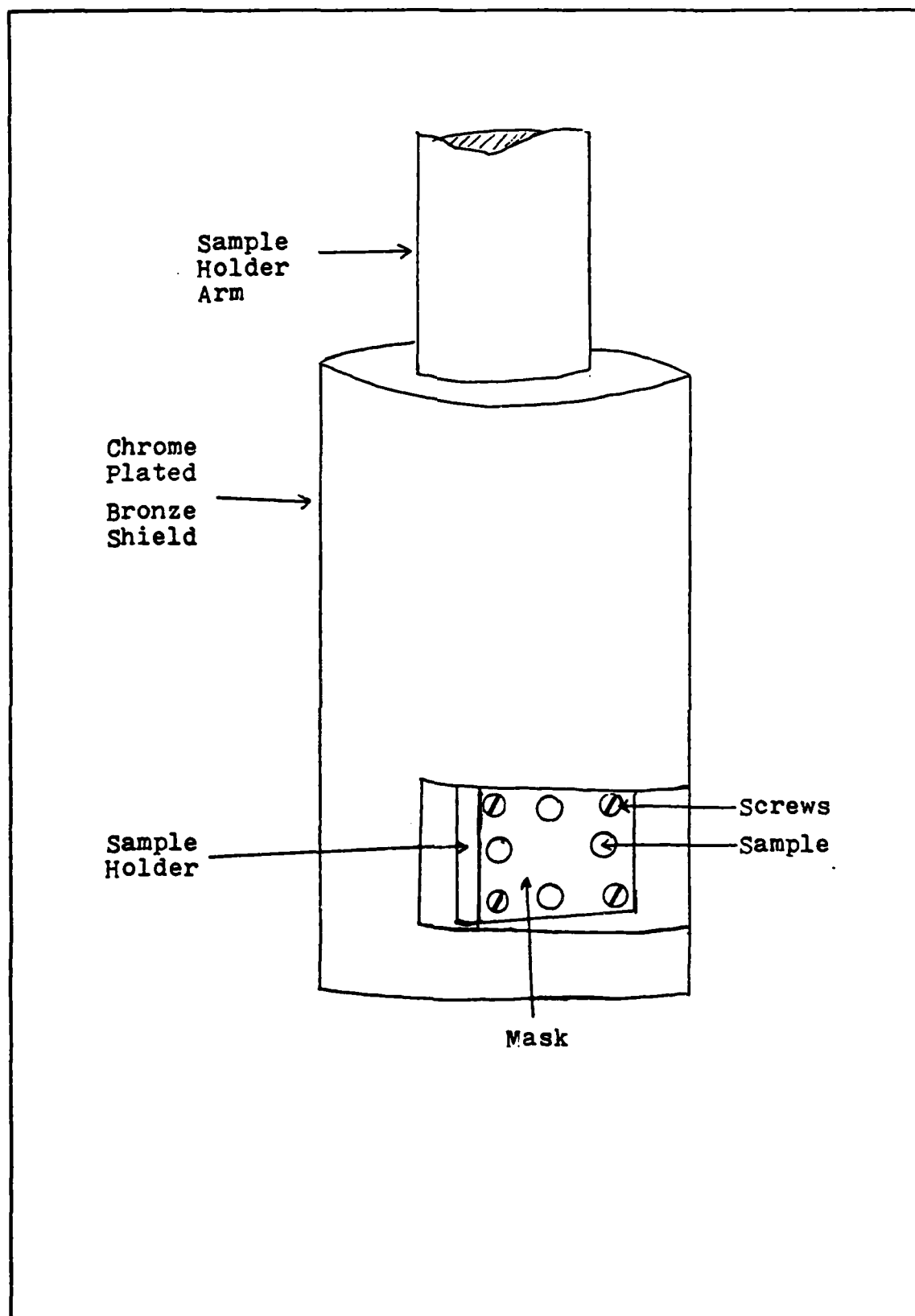


Figure III-6 Sample Holder

During most measurements, the grid, cathode, and filament were floated at -2000 V potential by a Keithley 246 High Voltage power supply. The voltage for the deflector plates was provided by seven 45-volt dc batteries. Five were below ground potential and two above ground to provide the required beam control. The current was measured by a Faraday cup made of mickel and boron nitride (See Figure III-7). A 45-volt dc battery was used to keep the entrance screen at -45 volts to reduce the loss of secondary electrons. Measured currents varied from 1 to 130 microamps. The particular amperage desired for a run was set by adjusting the grid voltage. The output current was monitored with a Keithley 410 Micro-microammeter.

Optical System and Alignment

The optical system utilized two quartz lenses for collection of the sample emission. Both lenses were 33 mm in diameter. The first lens had a focal length of 250 mm and the second was 100 mm initially. Toward the end of the research, an 150 mm lens was located to replace the 100 mm lens. The 250 mm lens was used as the collection lens because the other two lenses could not be positioned at their focal length from the sample to achieve a collimated output beam. The second lens was positioned to focus the collimated beam on the entrance slit (See Figure III-8). A second lens close to but not exceeding 250 mm, with the 33 mm diameter, would have been of the ideal focal length.

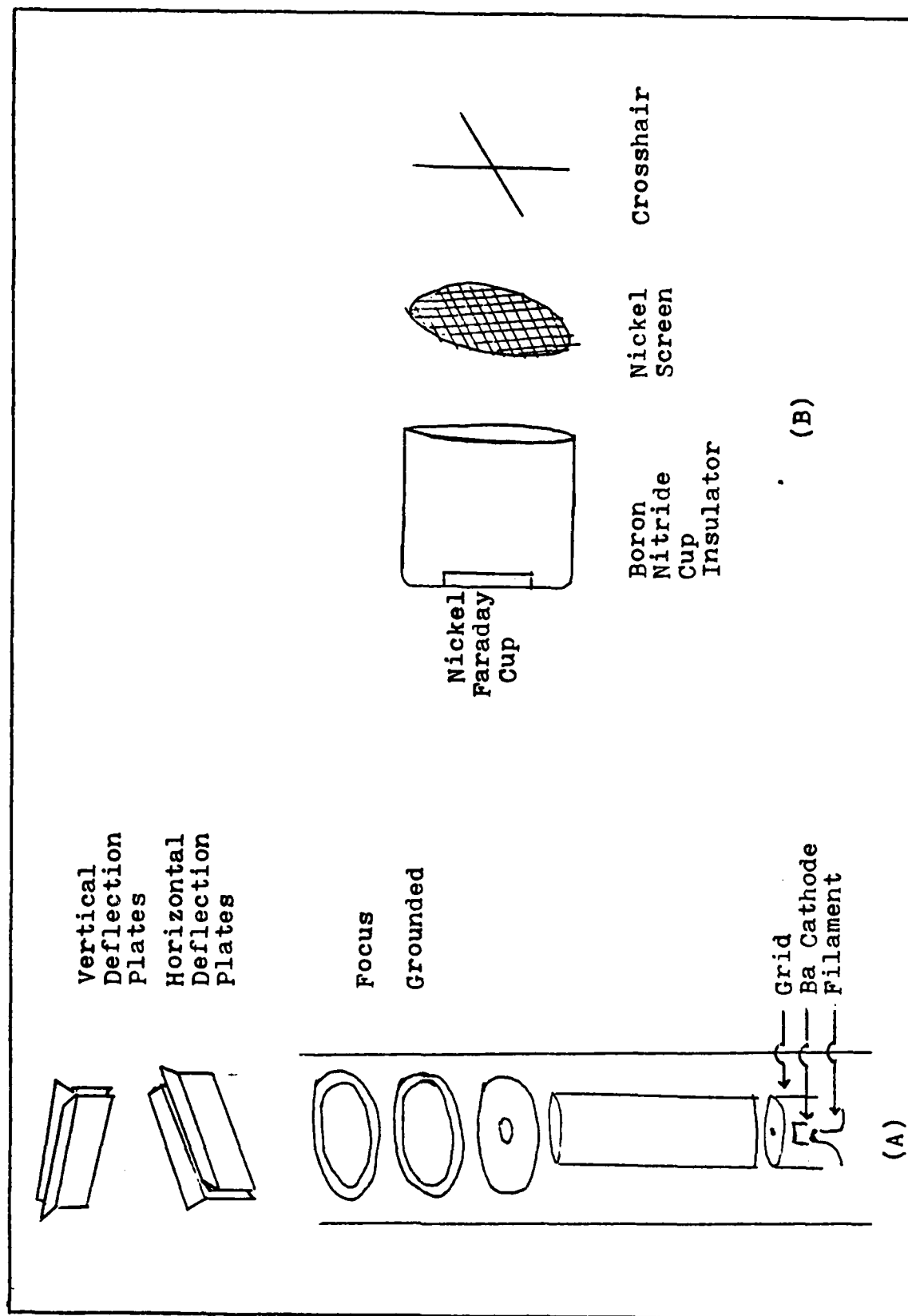


Figure III-7 Major Components of (A) Electron Gun and (B) Faraday Cup

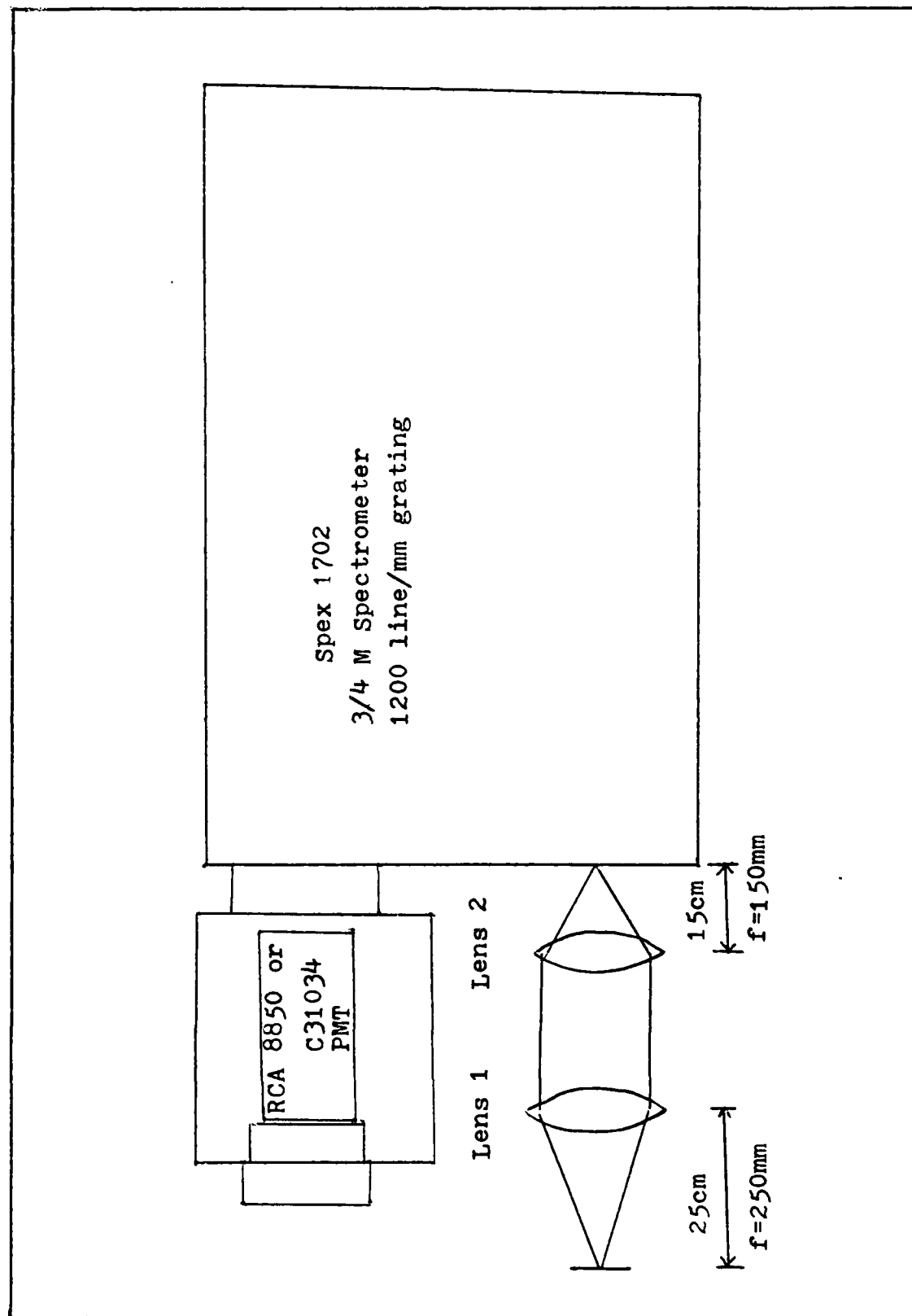


Figure III-8 Optical System

This is based on equation (2).

$$\frac{f_L}{D_L} = \frac{f_S}{D_G} \quad (2)$$

where

f_L = Focal length of lens 2.

D_L = Diameter of lens 2.

f_S = Focal length of spectrometer.

D_G = Width of the grating.

Maximum resolution is achieved by choosing the second lens so equation (2) is satisfied and the diffraction grating is just filled. Alignment and stability considerations make it desirable to slightly overfill the grating with a lens with a focal length slightly shorter than the optimum length.

The low level of sample phosphorescence and the large distance between the sample and the spectrometer necessitated using a two lens system.

The following procedure was used to align the optical system. The voltage was adjusted on the horizontal and vertical deflection plates of the electron gun to position the cathodoluminescent spot on the sample. The voltage of the focus plate was used to adjust the size of the spot. A 2.5 mW HeNe laser, a mirror, and a mechanical iris were used to place a small laser spot over the cathodoluminescent spot. The scattered laser light was then collected by the first lens and collimated. The collimated output of the 250 mm lens was then focused by the second lens onto the entrance slit of the spectrometer. The laser light was thus

focused on the entrance slit. With the laser turned off, the second lens, on a bi-directional traversing mount, was fine adjusted while monitoring a photon rate counter.

Signal Processing

Two different photomultiplier tubes (PMT) were used. The RCA model 8850 was used from 3200 to 6000 Å and the RCA model C31034 was used from 6000 to 9000 Å. The 8850 PMT was cooled in a Products for Research TE-114 PMT housing with liquid nitrogen to -50° C. The C31034 PMT was cooled in a Products for Research thermoelectric cooling housing, model TE 104 TS^oRF, to -20° C.

The output of the PMT was preamplified and then processed by a Princeton Applied Research Model 1121 Amplifier/Discriminator. This unit also supplied the high voltage for the PMT. The discriminator, set in the single mode, acts as a high pass filter. This eliminates most of the low frequency noise and thus increases the signal-to-noise ratio. The discriminator was set by taking photon rate counts with the slit open and closed for various discriminator and PMT voltage levels. The voltage and discriminator setting which gave the best signal to noise ratio for the 8850 PMT were 1500 volts and a .2 discriminator setting. For the C31034 PMT, 1300 volts and .15 were used.

The output of the discriminator is a series of 5 nanosecond pulses each of which corresponds to an individual photon. One output of the discriminator was fed to a

Princeton Applied Research model 1112 Photon Counter/Processor, which was used for alignment purposes. The other output was processed by a homemade interface to adjust the output voltage to match the input required for the Canberra Multichannel Analyser, model 8100. The MCA had 4096 storage channels. The stored data could be read off the oscilloscope, sent to a Hewlett-Packard X-Y Plotter model 7045, or stored on an audio cassette tape with a Techtran Datacassette recorder. The information on the tapes could then be fed into the CDC Cyber computer to punch out data cards. These cards would then be fed back into the computer with a MC PLOT program, which the author revised, to produce a finished point plot product.

Error Analysis

No corrections were made to the plots to adjust for the spectral response of the particular PMT used. Also no correction was made for the influence of nearby peaks such as the influence the large blue SA peak has on the green SA peak.

The spectrometer was calibrated using Argon, Krypton, Mercury, Neon, and Xenon low pressure calibration sources. The linear dispersion was determined. The uncertainty in calculating the actual peak of the calibration line was ± 0.6 angstrom.

The wavelengths of peaks detected in the spectra were determined by equation (3).

$$W_p = (C_p - C_c) \times \frac{\Delta}{c} + W_c \quad (3)$$

where

W_p = Wavelength of the peak.

C_p = Channel of peak center.

C_c = Channel of calibration peak.

$\frac{\Delta}{c}$ = Angstroms per channel.

W_c = Wavelength of calibration peak.

The uncertainty of an actual peak, for a 355.56 Å spectral run with an uncertainty of the calibration channel of $\pm .6$ Å and an uncertainty of the signal peak channel of 1 is $((1 \times .0868)^2 + .6^2)^{\frac{1}{2}}$ Å = .61 Å. If the uncertainty in the peak channel was 5 then the uncertainty would be .74 Å. On a 3555.56 Å run with an uncertainty in the sample peak of 10 channels yields an uncertainty of 8.7 Å. This last case is used in the broad SAL and SA peaks. The wavelengths were converted to eV by dividing 12395.912 by the wavelength in angstroms.

IV. Results and Discussion

A general picture of what spectral peaks are seen in cubic yellow and waterclear forms of cvd polycrystalline ZnS in the 3200 to 9000 Å range is provided first. This is done by examining a compiled list of all the peaks detected. The effect of varying the electron beam current density will then be discussed along with the effect of varying the temperature. Next the spectra of the individual samples will be examined to show how the spectra varied from sample to sample and even from spot to spot on a single sample.

Compiled Spectral Emission List

The diversity of the emission spectra of the individual samples was quite large. Figures IV-1 and IV-2 are typical emission spectra of yellow and waterclear ZnS samples using electron beam current densities of .336 milliamps/cm² and .061 milliamps/cm² respectively. Before looking at how the spectra of samples differ, a compiled list of all the spectral emissions detected during this investigation will be discussed.

The compiled list will be examined by discussing the peaks seen in the four main wavelength regions: the near band edge below 3300 Å, the UV region between 3300 and 3400 Å, the UV region between 3400 and 3700 Å, and the region from 3700 to 9000 Å where the SAL and SA emissions occur. The waterclear samples will be discussed first with a short

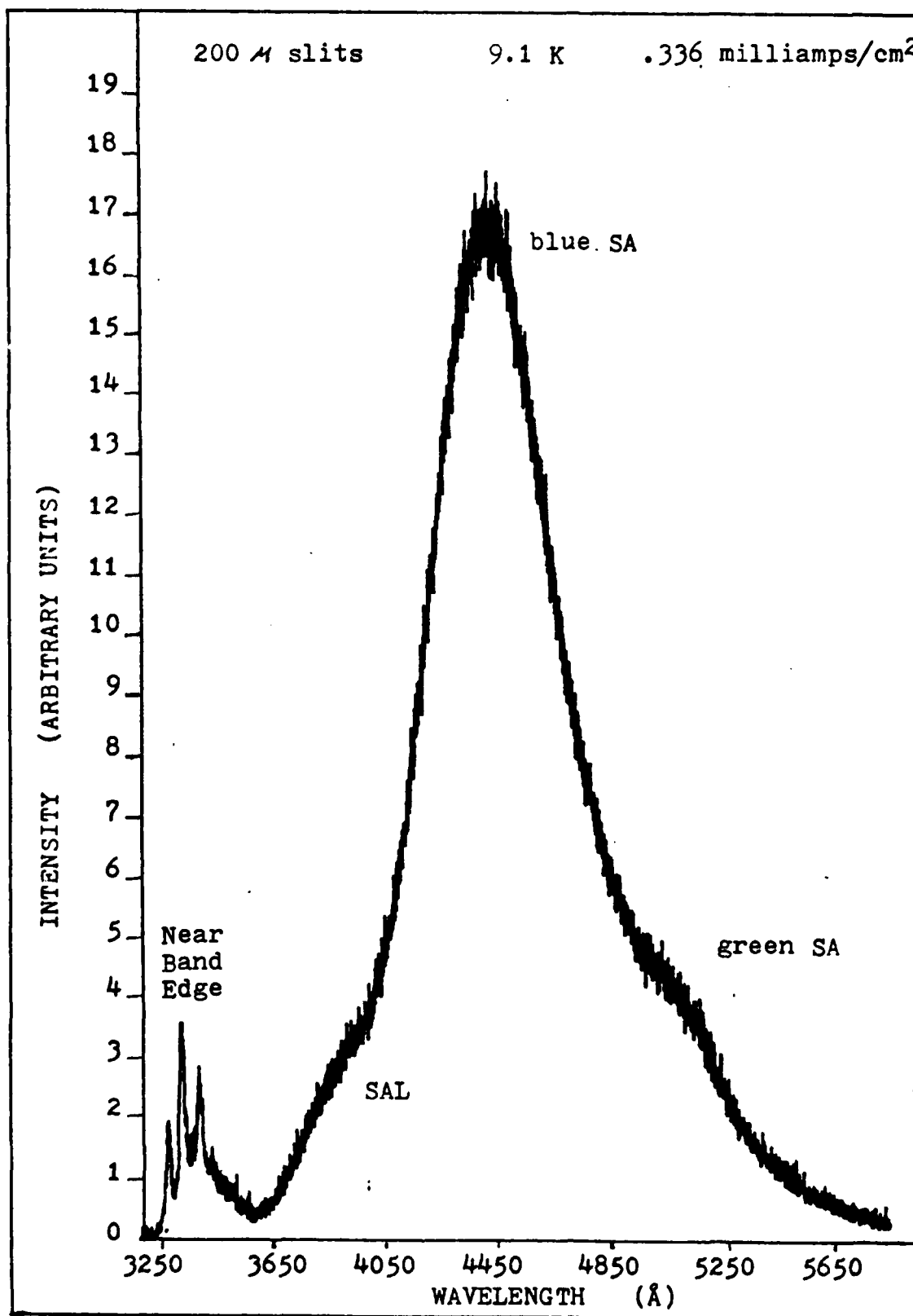


Figure IV-1 Yellow ZnS #4

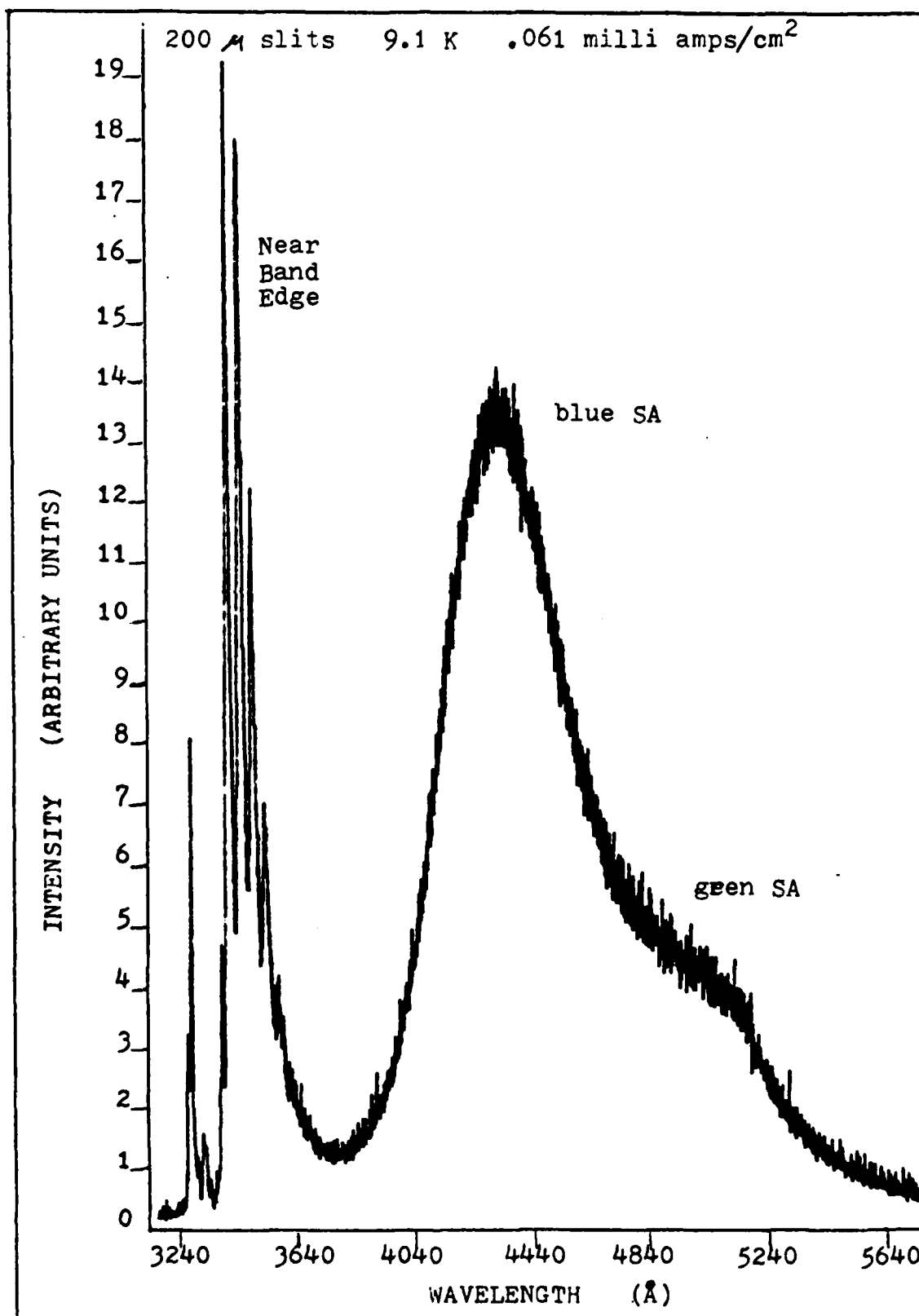


Figure IV-2 waterclear #5

TABLE IV-1

Compiled Spectral Emissions of Waterclear and Yellow

CVD Polycrystalline ZnS

Wavelength (Å)	eV	Symbol	Site/Type	Ref
3226-3229	3.843-39		Packing Defects	92
3238-3240	3.826		Packing Defects	92
3259	3.804	FE	Free Exciton	36
3262	3.800	X7	(A1)/DBE	36
3266-3267	3.794	X6	(C1)/DBE	36
3269-3270	3.791		DBE	39
3272	3.788	X5	BE	36
3275.5	3.784	X3	BE	36
3282	3.777	X2	BE	36
3291	3.767	FE-T02	Phonon	
3297	3.760	FE-LO	Phonon	36
3304	3.752	X6-LO	Phonon	36
3310.5	3.744	X5-LO	Phonon	36
3314	3.740	X3-LO	Phonon	36
3317	3.737	X2-LO	Phonon	
3321	3.733	X0	(0)/DBE S	
3336.5	3.715	FE-2LO	Phonon	
3345	3.706	X6-2LO	Phonon	
3349.5	3.701	X5-2LO	Phonon	36
3354	3.696	X3-2LO	Phonon	36
3363	3.686	X0-LO	Phonon	
3374.5	3.673	FE-3LO	Phonon	
3380	3.667	F1	(V)/FTB S	
3383.7	3.663	X6-3LO	Phonon	
3390	3.700	X5-3LO	Phonon	
3400	3.646	F2	(C1)/FTB S	
3420	3.625	F1-LO	Phonon	
3428	3.616	K1	(C1 to (0 -V) S S Zn") /DAP	36
3442	3.601	F2-LO	Phonon	
3468	3.574	K1-LO		36
3484	3.558	F2-2LO	Phonon	
3506	3.536	K1-2LO	Phonon	36
3527	3.515	F2-3LO	Phonon	
3571	3.471	F2-4LO	Phonon	
3616	3.428	F2-5LO	Phonon	

TABLE IV-1 CONTINUED

Compiled Spectral Emissions of Waterclear and Yellow

CVD Polycrystalline ZnS

Wavelength (Å)	eV	Symbol	Site/Type	Ref
3675	3.373		(ZnO)	94
3720-3729	3.332-24		(ZnO)	94
3789	3.272		(ZnO)	94
3840-3890	3.228-187		(V _O to V _{Zn}) in ZnSO solids/DAP	67-8
3920-3960	3.162-30		Mn	59
4300-4485	Range		(Due to Cu + coactiva- tor such as Al, Cl, Br, and I for all peaks in 4300-4485 range except 4417)	
4300	2.883			
4320	2.869			
4340	2.856			
4370	2.837			
4390	2.824			
4417	2.806		Mn + Cu	59
4486	2.763			
5080-5175	Range			
5090-5108	2.435-27		Cu _S /FTB	67
5130	2.416		Cu _S + Coactivator (Al)	67
5150	2.407		Cu _S + Coactivator	67
5175	2.395		Cu _S + Coactivator	67
5741-5775	2.160-47		Mn	59

eV = 12395.912 / Wavelength (Å)

The () indicates tentative assignments by author.

discussion following on the additional peaks seen in the Raytheon yellow polycrystalline sample.

Near Band Edge Below 3300 Å. In the 3200 - 3299 Å region, peaks which can be attributed to packing defects, donor bound excitons (DBE), acceptor bound excitons (ABE), phonons, and the free exciton (FE) were detected. A couple very weak peaks were detected at 3226 and 3240 Å which Shalimova et al. (Ref 94) have attributed to packing defects. These peaks were seen only in waterclear samples #1, #2, #6, #3 (in one isolated spot), and in yellow polycrystalline #3. X-ray diffraction and microphotography indicate that waterclear samples #2 and #6 and yellow polycrystalline samples #3 and #4 were cut so the end of the crystalline needles formed the surface examined. Waterclear samples #3, #4, and #5 and yellow sample #2 were cut showing the long side of the needles. The other samples were not studied by x-ray diffraction and micro-photography. These results indicate that packing defects were present and the concentration of isolated locations of packing defects can reasonably be expected to be higher when the end view of the crystal is examined.

The peak at 3259.4 Å is identified as the Free Exciton (FE). This peak was detected several times as a very weak peak on the side of a peak at 3263.3 Å in waterclear sample #2 (See Figures IV-3 and IV-4). Flesch et al. identified a peak at 3297 Å (3.760 eV) is the first longitudinal optical

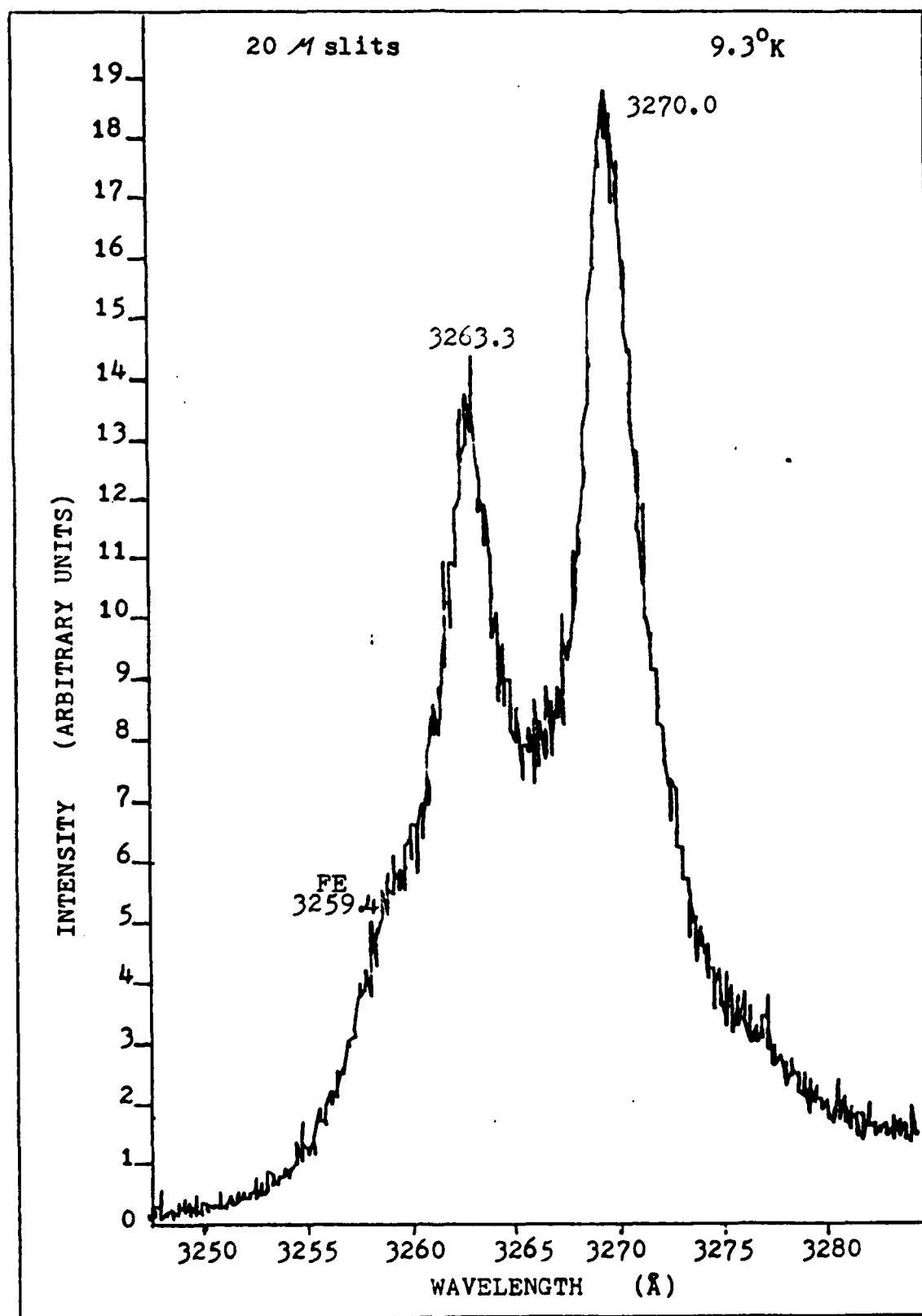


Figure IV-3 Waterclear #2 FE Shown

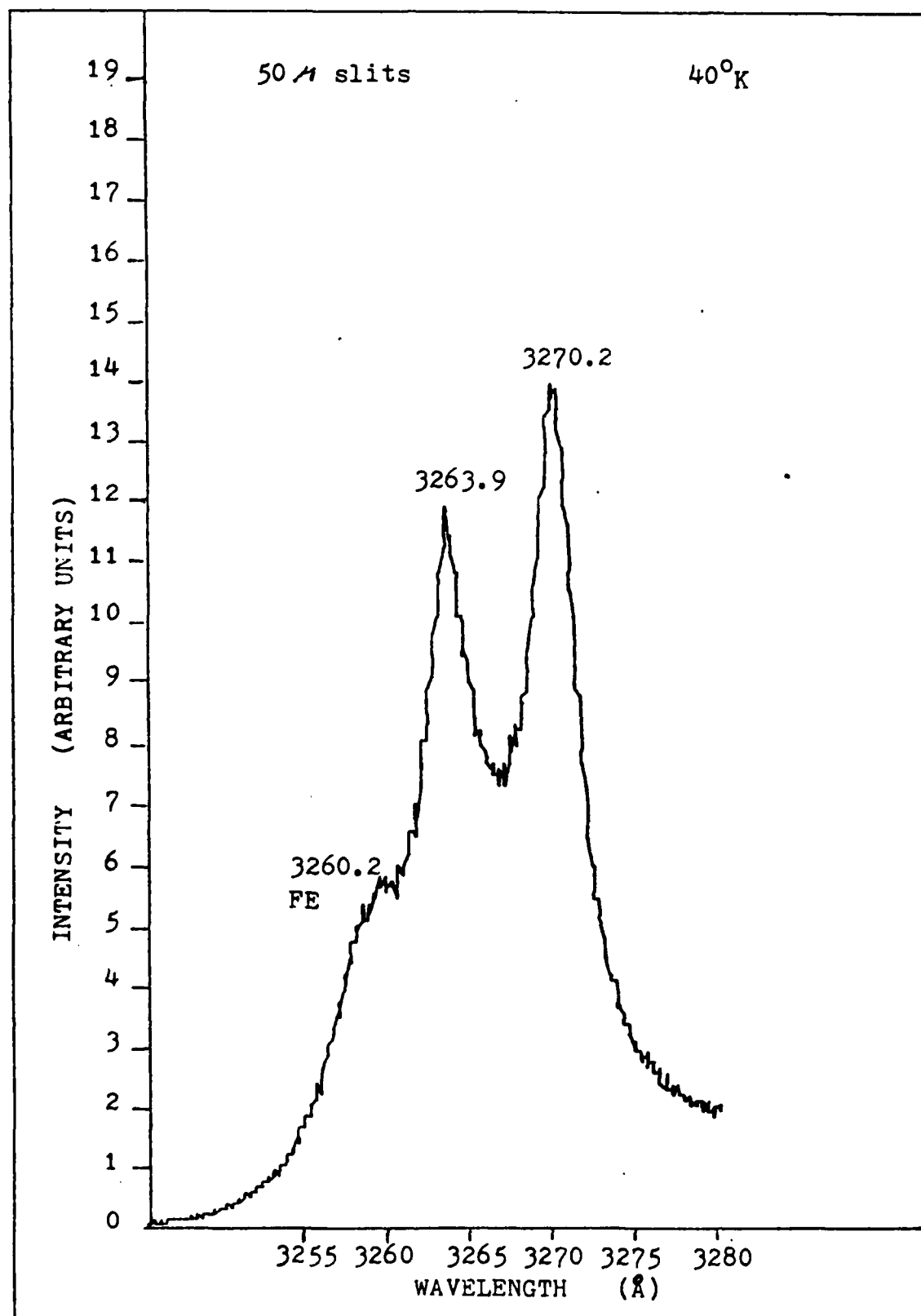


Figure IV-4 waterclear #2 FE Shown, 40°K

(LO) phonon replica of the FE, based on reflection measurements of the FE (Ref 36). If the energy of the LO phonon (44 MeV) is added to the energy of the first phonon replica of the FE then the FE would be at 3258.7 Å. Shionoya stated that the FE emission peak should become more prominent with increasing temperature (Ref 97:17). That is exactly what is seen in Figures IV-3 and IV-4. Therefore, the 3259 Å peak detected in these experiments is concluded to be the FE transition.

Peaks at 3262, 3267, 3272, 3275.5, and 3282 Å were observed. These correspond to the X7, X6, X5, X3, and X2 peaks reported by Flesch et al. (Ref 36). One additional peak was observed at 3270 Å in this study. Flesch suggested these peaks are due to bound excitons. Furthermore they suggested that the shape of the X3 peak was comparable to that of the ABE reported by Thomas and Hopfield for CdS (Ref 111; and 36:138). The position of the X7, X6, 3270 Å, and X5 peaks in relation to the X3 and the FE indicates these are probably due to DBE transitions while the X3 and X2 are probably due to ABE transitions.

Assignment of the BE peaks to specific impurity states is difficult because little is known of the trap depths. Based upon the relative depths of Al, Cl, Na, Li, N, and Cu reported in the literature for ZnSe and CdS, the 3262 Å peak can be associated with Al and the 3267 Å peak with Cl (Ref 97:19).

Another reason why Cl_S is being assigned to the 3267 Å peak is the peak appears to be related to the series of peaks between 3400 and 3650 Å. The amplitude of the 3267 Å peak ranged from low to strong relative to other peaks in the near band edge spectra while the 3400 and 3468 Å peaks were strong. In Figures IV-3, IV-4, and IV-5 the 3267 Å peak is absent. This peak was not seen in sample #2 spectra. This is the only case when the entire 3400 to 3650 Å series was absent or weak. Therefore, all of these peaks were concluded to be related to the 3267 Å peak. The assignment of Cl_S to these peaks will be discussed later. The remaining BE peaks at 3270, 3272, 3275.5, and 3282 Å were not assigned to specific impurities due to insufficient data.

Nearly always, there was a low intensity peak at 3297 Å. Based upon reflection measurements, this peak was identified by Flesch as the first LO phonon replica of the FE (Ref 36:141). On a few experimental runs the shape of this peak indicated another peak was probably present at 3291 Å. There is a possibility that the 3291 Å peak is due to a BE but it is more likely to be a transverse optical (TO) phonon (37 MeV) replica of the FE transition (Ref 36:141).

UV Range 3300 - 3399 Å. This region is characterized by primarily phonon replicas with a few possible BE and FTB parent peaks.

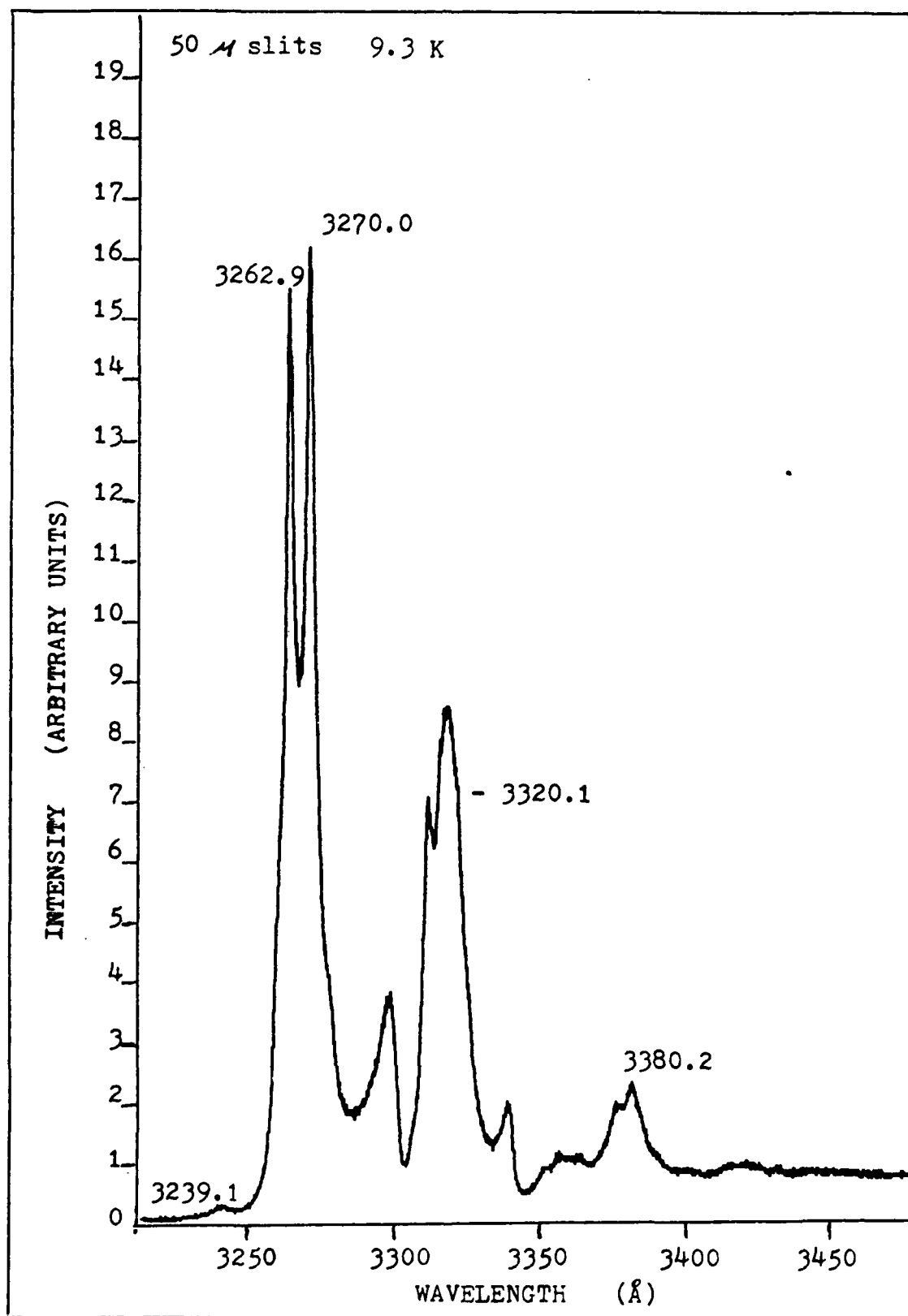


Figure IV-5 Waterclear #2 3267, 3400, 3428 Peaks Absent
59

A compound of peaks at 3310.5, 3314, and 3317 Å can generally be attributed to the first phonon replicas X5-L0, X3-L0, and X2-L0. The peaks were generally poorly resolved or unresolved and these values are the best estimates of the peak positions. There were some experimental runs on which the intensity of the compound peak was too large to be attributed just to phonon replicas of the BE peaks between 3262 and 3282 Å (See Figure IV-6). Part of the high peak intensity can be attributed to a peak detected at 3321 Å.

The 3321 Å peak has no identifiable parent peak if it is indeed a phonon replica. The FWHM of the 3321 Å peak, in most waterclear samples, indicates it might be a deep ABE or DBE. The FWHM was 3.8 Å, the same width as the BE in these studies. A deep Cu trap might seem a logical choice but the relative intensity of the 3321 Å peak did not change when an inclusion shown to be related to Cu was examined. This was in contrast to the Cu related 5175 Å green SA peak which increased in intensity considerably. Because the 5175 Å peak is assumed to be related to Cu the 3321 Å peak probably is not.

The 3321 Å peak was concluded to be related to a deep O_S trap. Ray reported work done by Hoogenstraaten in 1958 which showed that the O_S trap was 590 MeV deep (Ref 74:124). The 3321 Å peak appeared to be related to the SAL peak at 3850 Å. The 3850 Å peak has been attributed to the V_O to V_{Zn} transition in ZnSO solids within the ZnS crystal (Ref 67

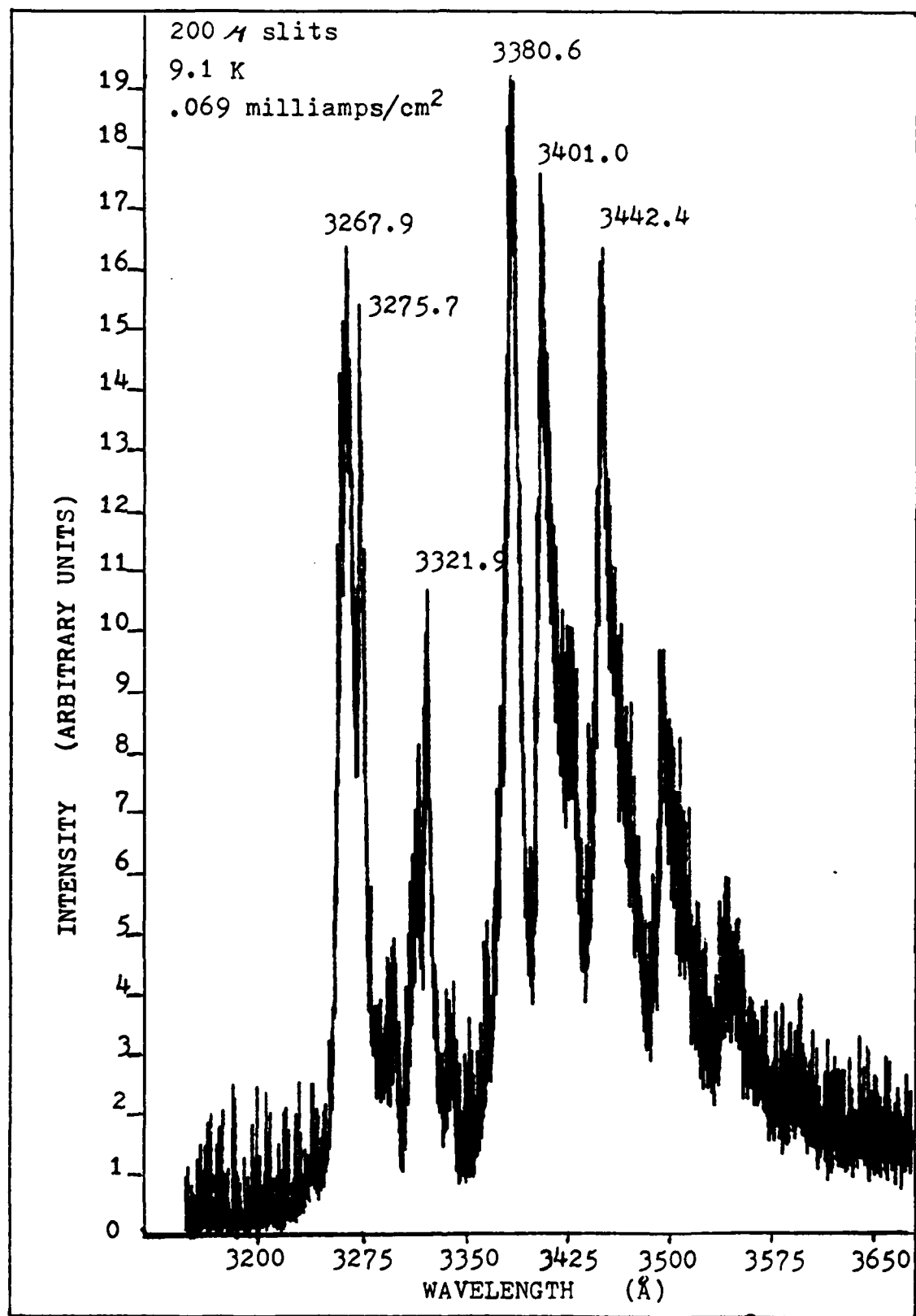


Figure IV-6 waterclear #6

and 68). This indicates a possible presence of oxygen, a common contaminant. The 3321 Å peak is also apparently related to the 3380 Å peak. In a given sample, the ratio of the amplitudes of the two peaks remains constant. This relationship could be explained by the fact that the relative concentration of V_S should be nearly constant over the small area of the crystal pieces examined. If the oxygen contaminant is located at a V_S site forming O_S , the distribution or concentration of O_S sites would then be nearly a constant. In a given sample, the ratio of the amplitudes of the 3321 to the 3380 Å peak should be a constant. (The reason for assigning the V_S site to the 3380 Å peak will be discussed shortly.) The difference in relative amplitude of the 3321 Å peak could then be attributed to the amount of the oxygen impurity present in the crystal and the number of V_S defect sites which are in the crystal. Therefore the 3321 Å peak is concluded to be due to an O_S DBE. The first phonon replica of the 3321 Å peak was seen at 3363 Å.

The yellow ZnS energy band gap was tentatively concluded to be 3-7 MeV larger than the waterclear ZnS energy band gap. In the yellow ZnS samples a broad peak was centered between 3313 and 3317 Å. In several samples this peak was the most intense peak in the near band edge spectra. The intensity of the 3313-3317 Å peak was far too large to be explained as the first LO phonon replica of a BE peak in the 3262-3270 Å region. The 3313-3317 Å peak was theorized

to be the 3321 Å peak seen in the waterclear samples' spectra. Assuming that the 3313-3317 Å peak is the same as the 3321 Å peak then the yellow ZnS energy band gap must be 3 to 7 MeV larger than the waterclear ZnS energy band gap. This theory was supported by the fact that all the yellow ZnS near band edge spectral peaks could be matched with peaks in the waterclear ZnS near band edge spectra when a correction factor of 3 to 7 MeV was subtracted from the energy of the yellow ZnS spectral peaks. The theory proposed here that the yellow ZnS material has a larger energy band gap than the waterclear ZnS material can account for the apparent shift 3-7 MeV of the 3321 and 3380 Å peaks seen in the waterclear spectra to higher energies in the yellow material and why the 3313-17 Å peak had so large of a relative intensity in the yellow ZnS. This conclusion is considered tentative because there was a large uncertainty in peak position, 2-3 Å, due to the poor signal to noise ratio, resolution, broadness of the peaks, and apparent crystal quality.

The 3380 Å peak exhibited the characteristics of a free to bound transition (FTB) peak. The 3380 Å peak's FWHM generally was about 7.7 Å but was as large as 15 Å. The 7.7 Å value is about twice the FWHM value for the BE peaks detected in this study and about half the value for the donor acceptor pair (DAP) transition peak at 3428 Å detected in this study. (The larger FWHM values were attributed to surface preparation and/or poorer crystal quality.)

The 7.7 Å value is about the value which should be expected for a FTB transition peak. The 3380 Å peak did not shift in wavelength as the temperature was increased from 9.3 to 40 K. Also, the wavelength of the 3380 Å peak did not shift as the electron flux was increased from .05 to 26 milliamps/cm².

The 3380 Å peak is probably due to sulfur vacancies. The trap depth of V_S is 170 MeV as reported by Samelson and Lempicki (Ref 85:908). With a band gap of 3.84 eV, this would yield a FTB transition at 3378 Å. Since the 3380 Å peak is always present, the V_S trap must be a common problem in these crystals.

All of the other peaks detected between 3300 and 3399 Å can explained attributed as LO phonons replicas of the FE and BE peaks.

UV Range 3400-3700 Å. The 3400 to 3700 Å spectral range was characterized by a FTB emission and a DAP emission and their associated phonon replicas. Most of the time only FTB series was seen. Occasionally the DAP series was seen instead of the FTB series, and twice the FTB and DAP series were seen together with the DAP series dominant in both cases.

Initially the 3400 to 3700 Å region was thought to contain parent peaks at 3400, 3428, 3442, and 3468 Å but subsequent data proved only the 3400 and 3428 Å peaks were parent peaks. The 3442 Å peak was concluded to be the first

LO phonon replica of the 3400 Å peak and the 3468 Å peak was concluded to be the first LO phonon replica of the 3428 Å peak despite the fact that most of the time the 3442 and 3468 Å peaks were slightly larger than the 3400 and 3428 Å peaks. The high relative intensity of the 3442 and 3468 Å peaks could be easily explained if the first LO phonon assisted transitions are as probable as the parent transitions at 3400 and 3428 Å. The relative intensity between the parent peaks and the first LO phonon replicas varied from 90 to 110% which gave the impression that the 3442 and 3468 Å peaks were independent parent peaks. This variation was concluded to be due to variations in the crystal quality. The energy separation between the 3400 and 3442 Å peaks and between the 3428 and 3468 Å peaks was equal to the LO phonon energy. Both the 3400 and 3428 Å series were conspicuously absent when the 3267 Å peak was definitely absent. Figures IV-3, IV-4, and IV-5 were taken from runs when all three peaks were absent. The absence of all the peaks provides strong support for the conclusion that the peaks have a common impurity and the 3442 and 3468 Å peaks are LO phonon replicas.

The 3400 Å peak was concluded to be a FTB transition peak. The FWHM was always the same as the 3380 Å peak which was concluded to be a FTB transition peak. The FWHM generally was 7.7 Å and occasionally was as large as 15 Å. The 3400 Å peak did not shift in wavelength when either the

temperature was increased from 9.3 to 40 K or when the electron flux was increased from .05 to 26 milliamps/cm². These facts are all characteristics of a FTB transition peak.

A Cl_S trap is proposed as the donor site for the 3400 Å emission. A trap at 200 ± 20 MeV to 220 ± 20 MeV has been detected by several researchers (Ref 20, 21, 85). Samelson and Lempicki did several thermoluminescent studies in which they determined the trap was Cl_S. If the trap depth is actually 195 MeV then the Cl_S trap in a FTB would emit radiation at 3400 Å.

The 3428 Å peak exhibited the characteristics of a DAP transition peak. The FWHM of the 3428 Å peak was always greater than 15 Å. The DAP peak is expected to have a FWHM around 15 Å. The wavelength of the peak decreased 10 to 12 Å as the electron flux was increased from .05 to 26 milliamps/cm². The wavelength increased approximately 3.7 Å when the temperature was increased from 9.6 to 25 K. The 3428 Å peak matches the K1 DAP reported by Flesch (Ref 36).

Comparison of the 3400 and 3428 Å peak series and their characteristics revealed that the two series of peaks have a common donor impurity trap, Cl_S, involved in the emissions. Comparison of the pattern of the amplitudes of the peaks in the 3400 and 3428 Å series' spectra revealed the patterns were the same. The energy difference between peaks in each series was also the same, the LO phonon energy of 44 MeV.

The similarity in appearance of these two series of peaks and the fact the two series were seen on the same crystal and even simultaneously leads one to suspect the donor impurity traps for the two series are the same. Further support for this theory is the fact that both series were completely absent when the 3267 Å peak was absent, which indicates all the peaks had a common impurity. Since the 3400 Å transition has already been shown to be caused by a Cl donor trap, the 3428 Å transition must also be caused by the Cl_S trap and the 3267 Å transition must be related to Cl.

The conclusion that Cl_S is the donor site for the 3428 Å transition raises the question of what acceptor is shallow enough to provide a difference of only 30 MeV between the 3400 and 3428 Å peaks if the donor centers are indeed the same. One possibility is an excited state of an impurity acceptor near the valence band. However excited state emissions are expected to be only of a low intensity and not the dominant peaks. The excited state is created when the BE complex annihilates during recombination which leaves the donor or acceptor, to which the exciton was bound, in an excited state. Therefore, a peak due to an excited state should be less intense than the associated BE peak.

A complex involving the O_S trap is being proposed as the acceptor for the 3428 Å transition. In the Raytheon yellow ZnS sample and the CVD Inc. yellow #4 sample, samples

in which the 3321 Å O related peak was very strong, the 3428 and 3468 Å peaks were clearly separated. In both the yellow and waterclear ZnS when the 3428 and 3468 Å peaks were not well separated or not present, the 3321 Å peak was weak or almost non-existent. This indicates that some very shallow complex containing oxygen or defect due to ZnSO in the ZnS crystal is acting as an acceptor or creates an acceptor complex. It is likely that a complex like $(O - \overset{S}{V})^-$ is created and acts as the acceptor in 3428 Å Zn emission. The presence of such an acceptor in sufficient quantities, as might exist in the yellow ZnS, would make the DAP transition favored. If the number of acceptor sites is approximately half the number of donor sites then both the 3400 Å FTB series and the 3428 Å DAP series may be detected, as it was several times. If the number of acceptors is too low then only the 3400 Å peak series would be seen. This was the case in the waterclear samples #2-#6.

These conclusions are contradictory to the conclusions of Samelson and Lempicki (Ref 85). They also found a series of peaks at 3400 Å, 3442 Å, and the associated phonon series. They called the 3400 Å peak a DAP emission although the model was a sulfur vacancy recombining with a free hole from the valence band. They attributed the recombination of Cl with a free hole from the valence band as the transition mechanism for the 3442 Å peak. These two models are FTB transitions, but the 3400 and 3442 Å peaks displayed a

wavelength-temperature dependence and varied in position. These are indications of a DAP not a FTB. They concluded that the hole was from the valence band because no traps corresponding to an acceptor were seen in the thermoluminescent curves.

The behavior of the peaks at 3400 and 3442 Å reported here varied considerably from that reported by Samelson and Lempicki. These peaks showed no wavelength-temperature dependence when the temperature was increased from 9.3 to 40 K. The peaks did not shift with electron flux was increased from .05 to 26 milliamps/cm² and the peak values were always within a few tenths of an angstrom of the reported values. Samelson and Lempicki showed their peaks varied by several angstroms. No reason was given for the variation of their peaks. The 3400 Å peak also was large even at 9 K instead of disappearing like the peak did in their report. The FWHM of the 3400 and 3442 Å peaks was generally 7.7 Å instead of over 15 Å for the 3428 and 3468 Å peaks and the 15 Å expected for DAP peaks. Samelson and Lempicki did not report the FWHM of their peaks.

The logical conclusion is that the radiative processes, for the 3400 and 3442 Å peaks, and possibly the centers involved in this report are different from Samelson and Lempicki's report.

Although the 3428 Å peak series reacted similar to the 3400 Å series in Samelson and Lempicki's report, the peaks

can not be concluded to be the same. The 3428 Å peak did not change its relative amplitude with respect to the 3468 Å peak as the temperature changed. The 3428 Å peak was large even at 9 K. The 3400 Å peak varied considerably with respect to the 3442 Å peak and was not seen below 25 K in their report. The 3428 Å peak could possibly be equivalent to the 3442 Å peak in Samelson and Lempicki's report. Because their figures indicate the peak was measured as low as 3433 Å in certain samples it is possible their crystals had a smaller energy band gap. The displacement of the V_S peak from 3400 to 3380 Å would be consistent with this proposal. No conclusive evidence was found in their report to prove a difference exists in the size of the energy band gap between their samples and the samples used in this study.

The 3420 Å peak appeared to be the LO phonon replica of the 3380 Å peak.

The SAL and SA Peaks. The spectrum between 3700 and 9000 Å will now be discussed. The spectrum of the water-clear samples in this range is characterized as having one or more peaks in the SAL range 3675 to 3960 Å, a peak in the blue SA range 4300 to 4485 Å, a peak in the SA green range 5100 to 5175 Å, and sometimes a peak between 5740 and 5775 Å. No peaks were seen between 5775 and 9000 Å.

The SAL peak was generally not seen at low electron flux rates (below .15 milliamps / cm²) (See Figure IV-8).

Once, however, the SAL peak was very evident, in a localized sample spot, in a run with an electron flux near .0045 milliamp / cm² (See Figure IV-7). Generally the SAL peak appeared as a poorly resolved peak on the side of the blue SA peak when .15 to .2 milliamps / cm² electron flux was used. In several cases the SAL peak dominated the spectrum when excitation intensities over 26 milliamps / cm² were used (See Figures IV-9 and IV-10).

When the SAL peak was present one or more of the following peaks were also detected: 3675, 3720-30, 3790, 3840-90, and 3920-60 Å. In the Theory and Review of Literature section, the SAL peak between 3850 and 4000 Å was discussed. The most probable mechanism discussed was the recombination of an electron trapped at an oxygen vacancy with a hole trapped at a zinc vacancy in ZnSO solid within the ZnS crystal (Ref 67, 68). Datta (Ref 26:68) claims the peak he observed at 3900 Å was due to the second Ag band. Since he made his measurement at 80 K, 10 to 15 Å must be added to the 3900 Å to adjust for the difference between 80 and 10 K. This would make it closer to the 3920-60 Å peak but not as good a match as the 3950 Å peak Langer reported for Mn (Ref 59).

On a few runs there were multiple peaks in the SAL region. Peaks at 3675, 3729, and 3789 Å appeared together, and peaks at 3717 and 3861 Å appeared together. Peaks at 3790 and/or 3958 Å occasionally appeared along with a strong

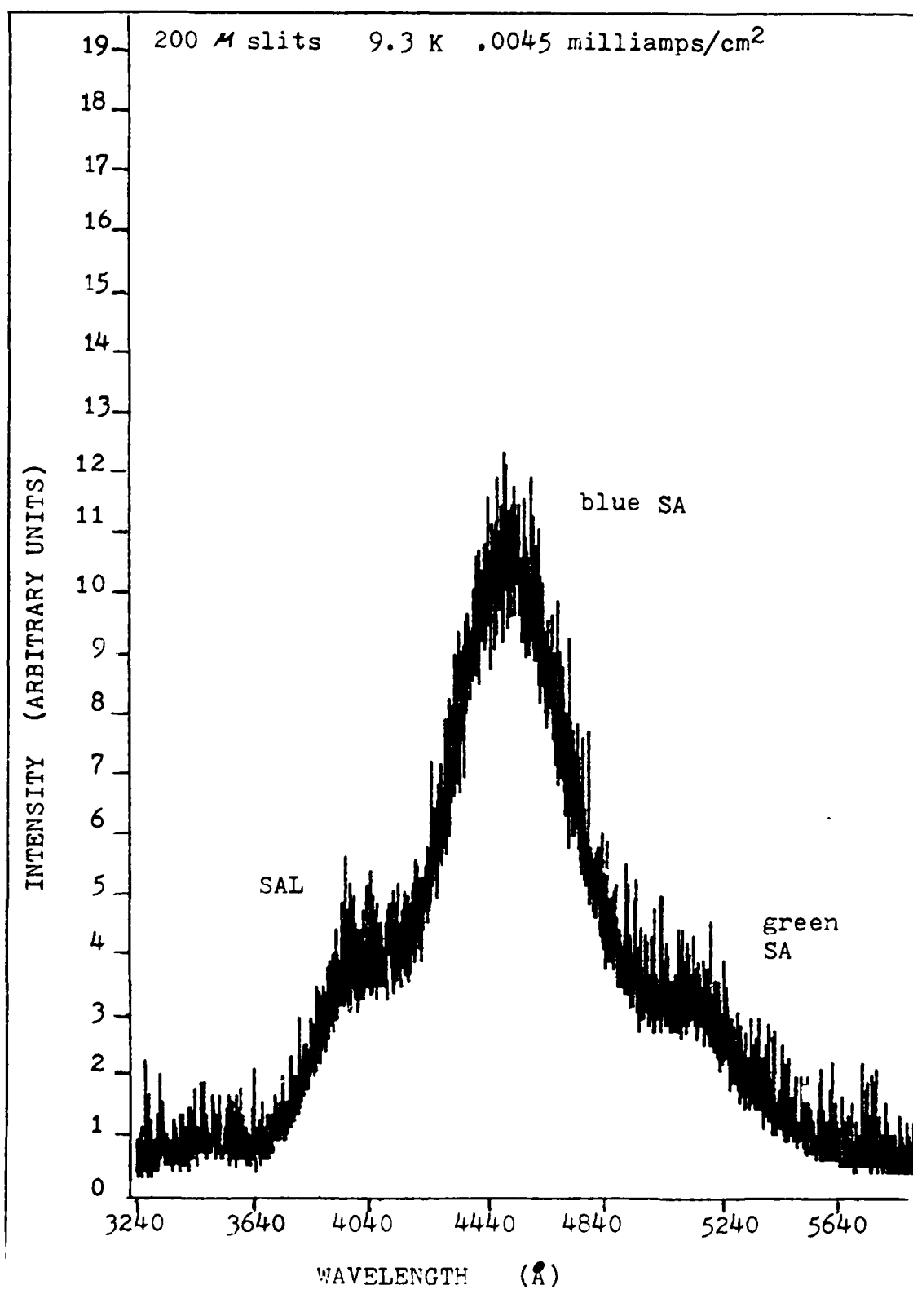


Figure IV-7 waterclear #4

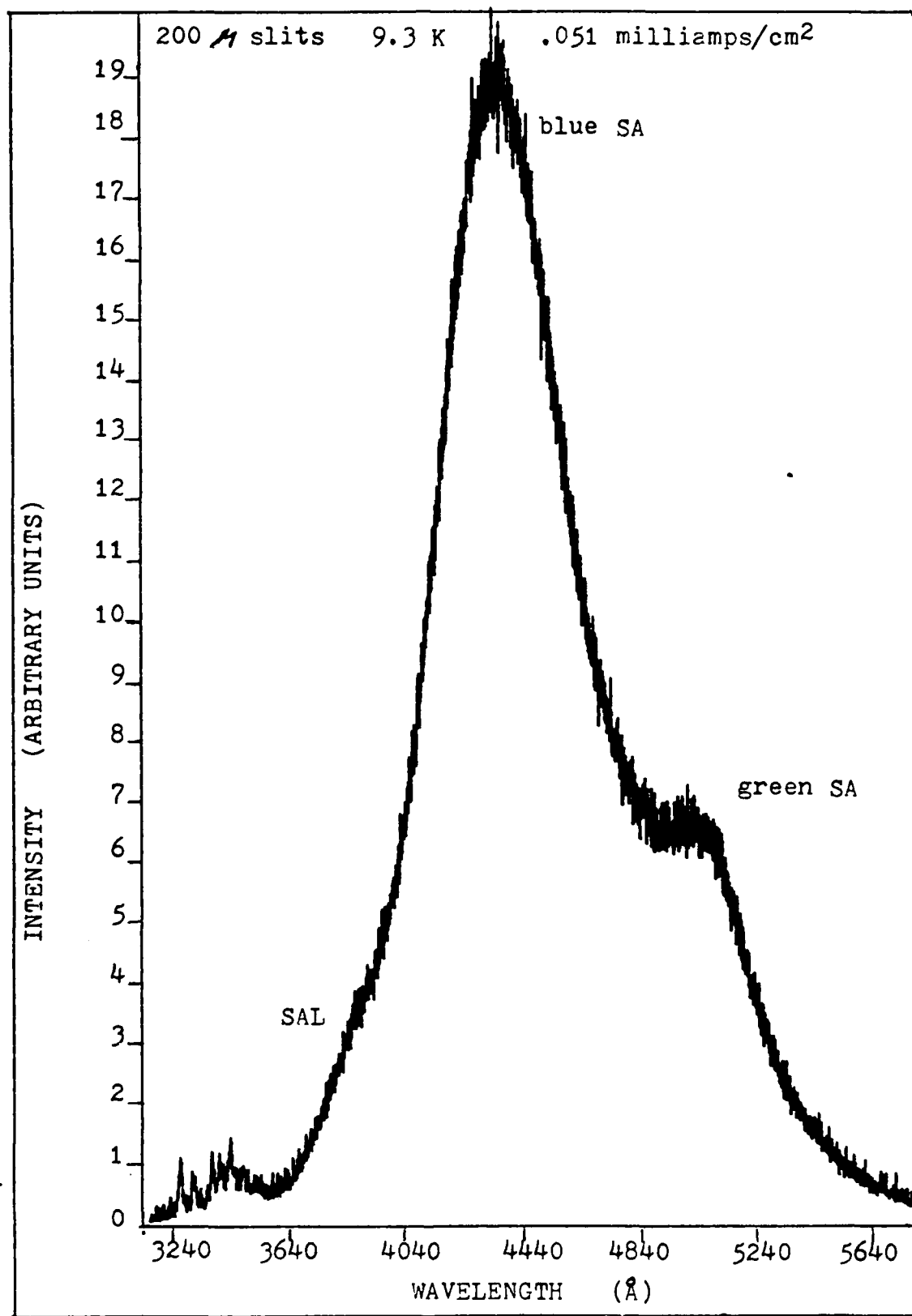


Figure IV-8 Waterclear #4 Low Flux
73

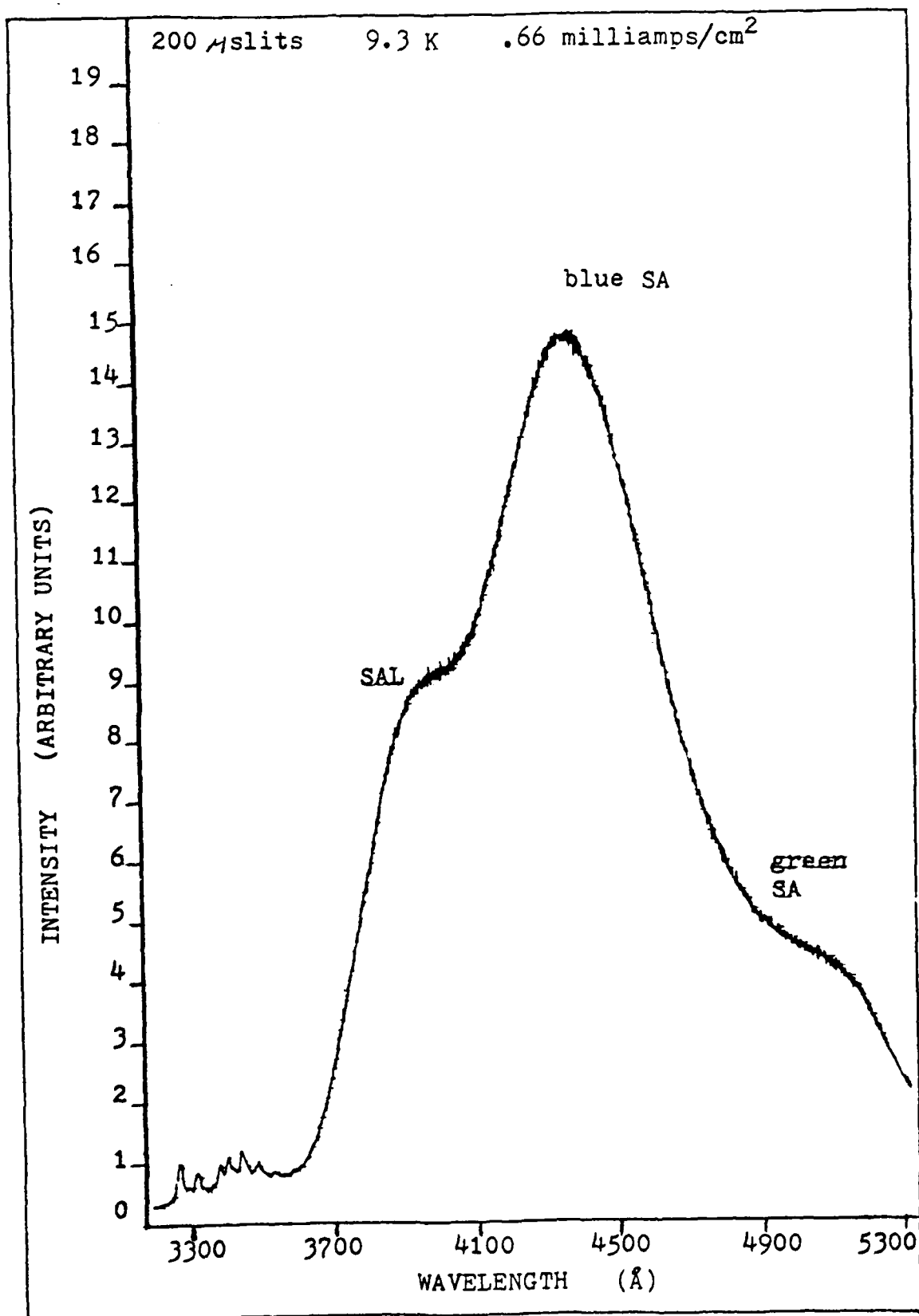


Figure IV-9 Waterclear #4 Moderate Flux

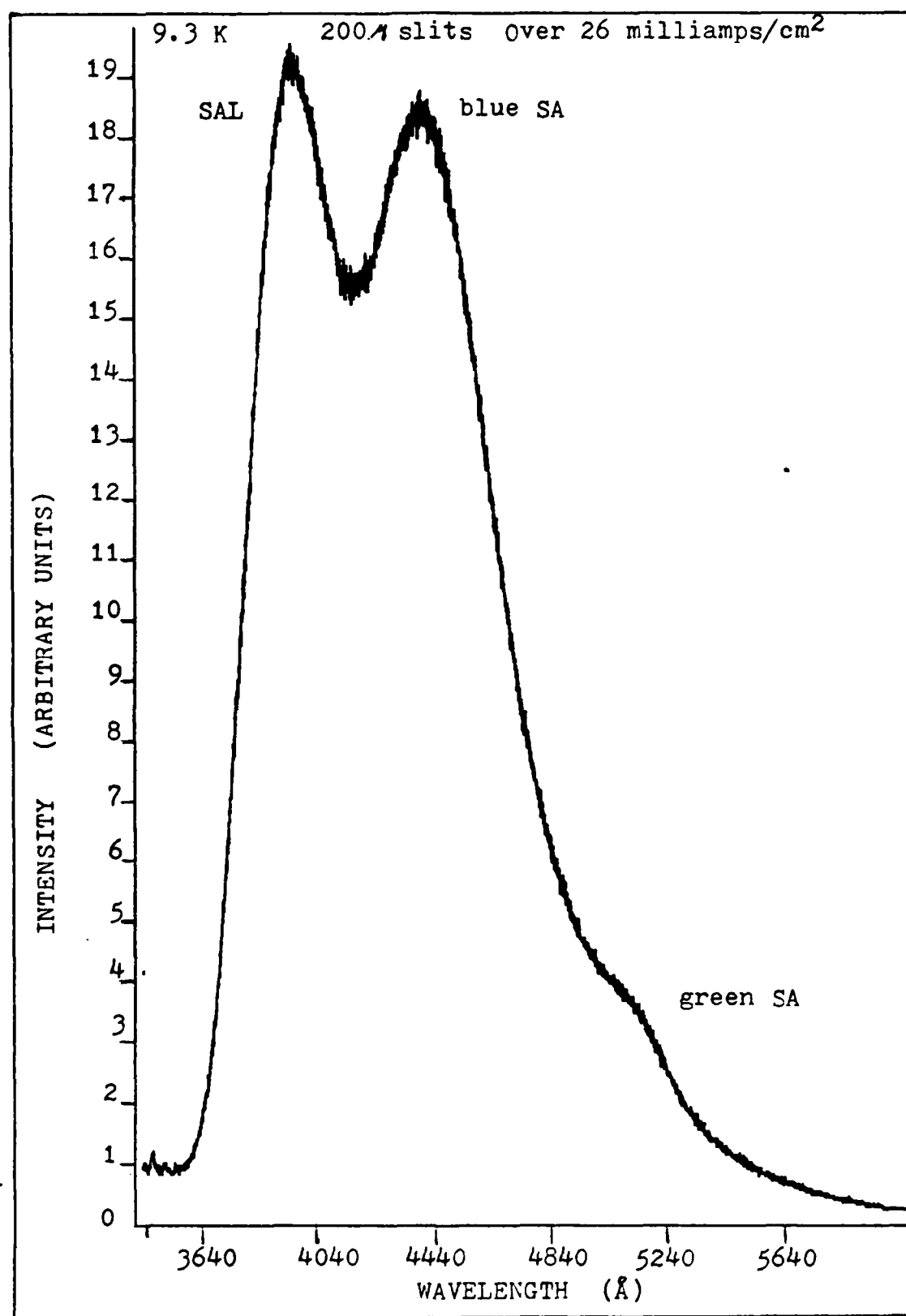


Figure IV-10 waterclear #4 Very High Flux

3848 Å peak. The 3920-60 Å peak was the peak normally seen in the spectra and was often the only SAL peak present. The peaks other than the 3920-60 Å peak generally had a higher intensity and were more often detected in the yellow ZnS and waterclear #7 samples than in the waterclear samples #1-#6. The 3675 and 3729 Å peaks were concluded to be due to ZnO (Ref 94). The 3790 Å peak is probably associated with the ZnO since it was detected several times in association with the peaks between 3700 and 3730 Å. The 3848-3890 peaks are probably the V_{O} to V_{Zn} transition discussed in the Theory and Review of Literature section (Ref 94). The 3920-60 Å peaks were concluded to be due to Mn, in agreement with Langer, since several other peaks related to Mn were also seen along with the 3920-60 Å peak. This will be discussed more with the blue SA and the 5775 Å peaks (Ref 69).

The blue SA peak's wavelength varied from 4300 to 4500 Å. Nemchenko found the blue SA peak in doped samples to vary also in a same manner between 4400 and 4500 Å (Ref 69:931). Johnson found the peak to vary from 4400 to 4600 Å (Ref 48). The wavelengths of peaks seen the region from 4300 to 4500 Å, in the current research, were compensated for shifts caused by different electron flux levels and the resulting values were grouped around seven wavelengths. These wavelengths were 4300, 4320, 4340, 4370, 4390, 4417, and 4486 Å. In general, the further the detected peak was from one of these values the larger the FWHM of the peak.

The wider peaks exhibited a faint structure in which two or more of these peaks were present. Nemchenko also observed that the blue SA peak had a poorly resolved substructure. He attributed the apparent shifting of the peak and the substructure to the presence of different centers (Ref 69: 931).

Several general trends were noted. The 4300 Å peak was seen on only one small target spot, approximately .4 mm in radius, and only on the waterclear #1 sample. The 4300 Å peak was also broad; being about 566 Å wide. The 4340 Å peak was seen when either the whole sample, 2.5 mm radius spot, or just a tiny spot, .4mm radius spot, was targeted with the electron beam. The 4340 Å peak was the narrowest of the seven peaks with a FWHM of 515 Å. The 4370, 4390, and 4417 Å peaks were seen during whole sample and spot illumination and had a FWHM between 550 and 600 Å. The 4486 Å peak was observed primarily when a small spot was targeted with the electron beam. It was also detected when a very low beam intensity, 4.5 microamps / cm², was used to target the whole sample.

The assignment of emission sites or impurities is particularly difficult for these peaks because most of the blue SA peaks in doped and undoped have been reported at 4700 to 4800 Å. Several reports of doped samples have been reported with emission peaks between 4200 and 4600 Å but most of these studies were conducted at room temperature. The position of a peak reported at 300 K can not be determined for

10 K without knowing which way it will shift as the temperature is decreased. The direction and amount of shift is peculiar to each impurity and transition class. For most reported impurities the blue SA peak either increased or decreased by about 170 Å as the temperature was decreased from 300 to 10 K.

Three sets of temperature runs were conducted. In two cases the blue SA peak shifted to a higher energy as the temperature was increased. The results are not conclusive because in one case the dominant center jumped from 4375 to 4340 Å when the temperature was raised from 9.3 to 40 K. (Data was taken at only 9.3 and 40 K.) In the second case there was a definite shift from about 4321 to 4313 Å. The third temperature run was made with yellow ZnS and there was a definite shift from 4378 to 4390 Å when the temperature was raised from 11.5 to 75 K. The shift of 12 Å to longer wavelengths is what would be expected for a copper-related site. The other two sets of data indicate the center involved may not be copper. Nemchenko's arguments, which will be given shortly, show this does not necessarily exclude Cu. These results indicate that copper could be one of several sites responsible for the blue SA peak.

The temperature related wavelength shift detected is due to the dominant site at the position on the crystal being examined at the time. In the case of the wavelength jumping from 4375 to 4340 Å, the 4375 Å peak center probably

saturated at a temperature lower than 40 K. Instead of shifting a few angstroms in a direction characteristic of the center involved, the blue SA peak appeared to jump 35 Å.

Nemchenko was able to explain the apparent shifting of the blue SA peak at a constant temperature. He found that the ZnS:Cu,Al blue SA peak shifted to shorter wavelengths as the temperature was decreased. He mathematically modeled the energy structure using the Alentsev-Fok method to test whether the ZnS crystal would produce several luminescent centers of a similar nature (Ref 69). His analysis showed that several centers can be produced and that each would have its own individual emission band. The relative intensities of these bands would be dependent upon the growth conditions which might produce the two crystallographic forms, polytypes, dislocations, and other packing defects.

Nemchenko also found that some of the subband peaks are more localized than others (Ref 69). If this is the case, then individual bands may not shift much and any detected shift, associated with a temperature change, may actually be a shift in the relative peak heights. This could well be the case when the wavelength shifted from 4375 to 4340 Å as the temperature was raised from 9.3 to 40 K.

The three common activators for the blue SA emission in doped ZnS are Ag, Au, and Cu but in this study of undoped ZnS it was concluded that Ag and Au were not involved in the blue SA emission.

Datta reported the 4300-4500 Å peaks as normally being attributed to Ag coactivated with either a group III or VII element. These wavelength values are for 300 K and the Ag blue SA peak shifts to longer wavelengths as the temperature decreases (Ref 27: 66-8). Kukimoto reported a 4486 Å peak in ZnS:Ag,Al but no sample temperature was reported (Ref 56). However it is reasonable to assume the experiments were done at room temperature. Since Datta reported Ag peaks between 4300 Å and 4500 Å at 300 K (Ref 27), it was concluded that Ag is not likely to be one of the traps involved in the blue SA peak seen during this study.

Rodine reported a Au-related peak at 4460 Å at 300 K. No report was located which discusses the temperature shift of Au peaks. Since Au is an unlikely contaminant in our case, Au was dropped from consideration as a center responsible for the strong blue SA peak.

Cu was concluded to be the activator responsible for the blue SA peak. Nemchenko reported a blue Cu peak around 4400 Å at 75 K (Ref 69:931). Datta's findings indicate the Cu-related blue SA peak could have a wavelength as short as 4230 Å (Ref 27). Cu is also a common natural contaminant of ZnS crystals. Because of these arguments and the fact that the temperature dependence data does not preclude Cu as a trap involved in the blue SA emission, Cu was concluded to be associated with the blue SA peak.

The concentration of the co-activator impurities was determined to be greater than the activator (Cu). The appearance of various bands due to Cu was found to be linked to the ratio of the activator (Cu) to the co-activator (See Figure IV-11) (Ref 4:443). Because the green SA peak was weak compared to the blue SA peak and because the orange and red peaks were not present, the concentrations of the activator and the co-activators could not be equal. Therefore the emissions between 4300 and 4500 Å must be either the copper blue emission or the self-activated emission. The copper blue emission occurs when the Cu concentration is greater than the co-activator concentration and the SA emission occurs when the Cu concentration is less than the co-activator concentration.

The 4300 to 4500 Å peak in this study was not the Cu blue emission. This peak did not always shift to higher wavelengths, like the Cu blue peak should, when the temperature was increased and the peaks were not near 4220 Å reported for the Blue-Cu peak by Datta (Ref 27). An increase in the relative size of the Green-SA peak to the blue peak at an inclusion, on one sample, indicated an increase of the Cu concentration at the inclusion. Because the intensity of the green SA peak increased when the Cu concentration increased, the Cu concentration must be less than the co-activator concentration. Therefore the peaks

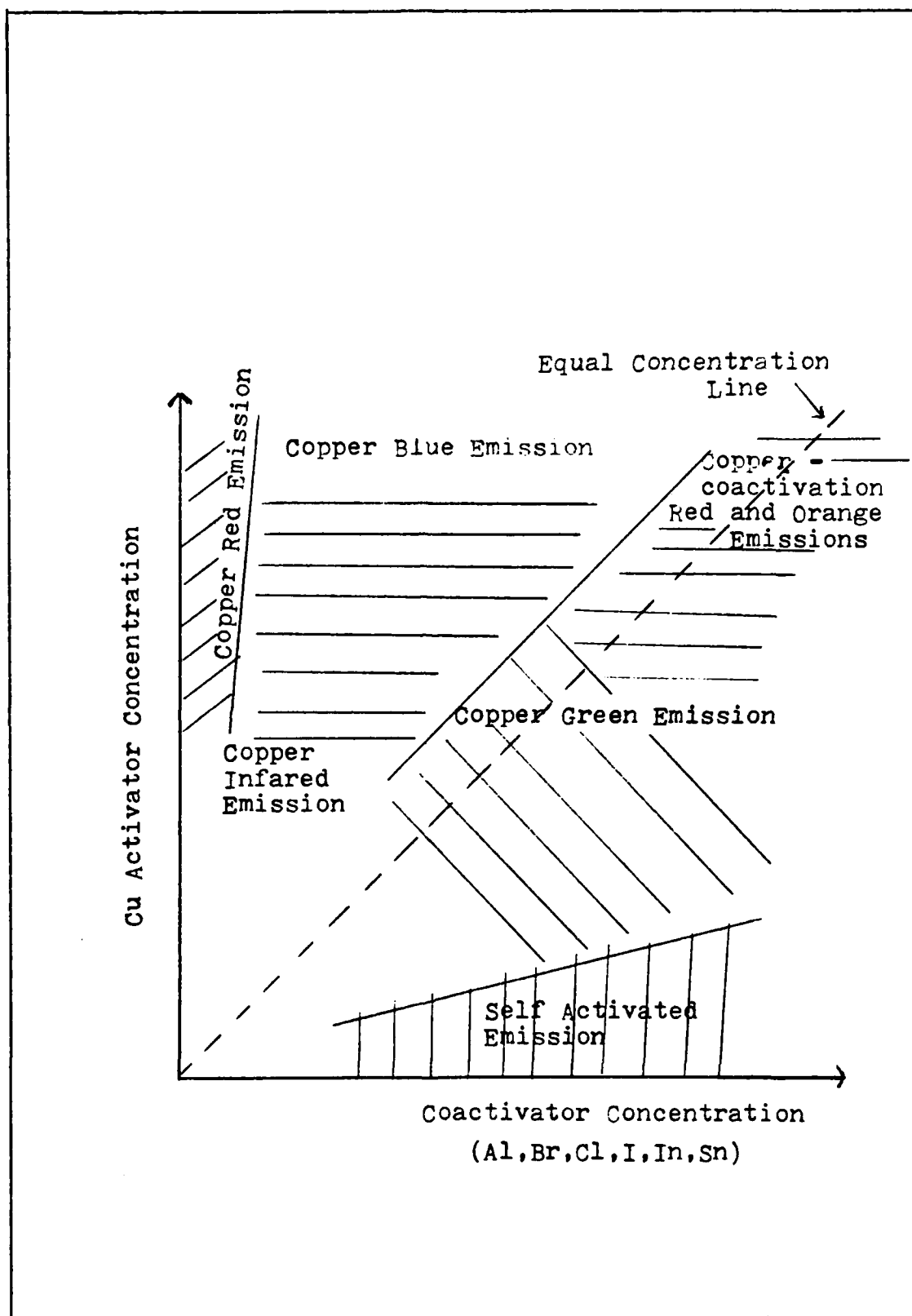


Figure IV-11 Emission Dependence on Concentration Ratios

must be in the blue SA region where the Cu to co-activator ratio is low.

When the co-activator predominates it is reasonable to expect the peak to be more characteristic of the co-activator than the activator Cu. This could explain why the peak appeared at so many wavelengths and why the temperature dependence runs appeared contradictory. Possible co-activators include Cl, Al, Mn, Br, and I. The 4300 Å peak is close to the peak reported by Taguchi for ZnS:I,P (Ref 107). The 4320, 4340, 4370, 4390, and 4485 Å peaks are probably due to co-activators such as Cl, Al, and Br. The 4417 Å peak is probably due to Cu + Mn because Langer reported ZnS:Mn produced a peak at 4417 Å as well as at 3950, 5080, and in the 5700 Å range (Ref 59). The arguments for the presence of Mn will be presented when the 5740-75 Å peak is discussed.

Several restrictions on the wavelengths reported for the green SA peak must be kept in mind. The green SA peak always appeared as a side peak of the blue peak and was never well resolved. The uncertainty in the peak position was comparatively large. In some individual experimental runs the uncertainty was as high as ± 30 Å. The effect of the large blue peak on the green SA peak's wavelength was not taken into account. The blue peak would cause the reported values to be shifted slightly to shorter wavelengths than the true emission wavelengths.

The green SA peak observed in the present samples is probably due to a combination of the subbands of the Cu_S site in a FTB transition and the Cu_S with an Al donor site as a DAP. The peak appears to have subbands around 5093, 5108, 5130, 5150, and 5175 Å. Nemchenko also discussed the subbands of the green SA peak. He stated the subbands in the green region were mathematically possible just as they were in the blue SA emission. He mentioned work done by Curie who proposed a Cu atom substituted at a sulfur site (Cu_S) was responsible for an emission peak at 5100 Å. Curie's work was supported by Grillot who observed a peak at 5080 Å with a 280 MeV FWHM instead of the 330 MeV FWHM observed for a 5250 Å peak. The 5080 Å peak was seen in ZnS:Cu with a low co-activator content; therefore, Curie proposed the 5250 Å peak was due to the Cu_S associated with a co-activator. Nemchenko stated a peak at 5220 Å is always associated with ZnS:Cu,Al (Ref 69:932). Shionoya (Ref 98) ascribed a peak at 5165 Å to $\text{Cu} + \text{Al}$.

In three experimental runs on the waterclear #1 sample, on small sample spots of .4mm radius, a low intensity peak was observed between 5740 and 5775 Å. The literature reported only ZnS:Mn and ZnS:Mn,Cl with peaks within 300 Å of this peak (See Table II-1). If Mn was the emission site, one might expect to see peaks also at 3953, 4417, 4700, 5080, or 5589 Å (all of which have been linked to the presence of Mn) as well as the 5740 Å peak (Ref 59). Peaks

were indeed observed in the 3950, 4417, 5080, and 5740 Å regions. The 5740-75 Å peak was seen only when a peak at 5090-5110 Å was detected. On the three runs when the 5740-75 Å peak was seen the blue SA peak was at 4417, 4391, and 4300 Å. The SAL peak was not seen because only a low electron flux was used on these runs and the SAL peak normally was not seen when a low electron flux was used. No peaks were detected at 4700 and 5589 Å.

If the 5080 Å peak is due to the Cu_S FTB as concluded by Curie and Grillo^t, the depth of Cu would be about 1.4 eV. Bhargava has reported the depth of the Cu trap as 1.25 eV (Ref 10:20). Considering the uncertainty of the thermoluminescence technique, the 1.4 and 1.25 eV trap depths are relatively close and the Cu trap could actually be equal to the 1.4 eV value.

With a band gap of 3.84 eV, the 5740-75 Å peak would require a trap with an energy depth of 280 to 294 MeV. Allen calculated depths of various impurities and his value for Mn was about 300 MeV. He found close agreement with this value in his experiments with ZnS:Mn (Ref 1:784). This value supports the hypothesis that the 5080 Å peak is a Cu_S FTB and the 5740-75 Å peak is a Cu_S + Mn DAP. This data indicates that Mn could be the emission center responsible for the 3920-60, 4417, and 5740-75 Å peaks.

Yellow Polycrystalline ZnS. All but two of the peaks observed in the yellow ZnS samples' spectra were also

AD-A141 100

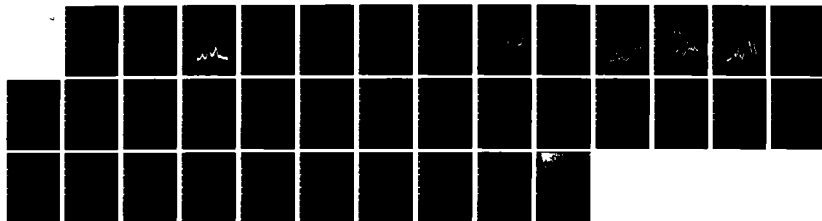
HIGH RESOLUTION CATHODOLUMINESCENCE OF YELLOW AND
WATERCLEAR CVD POLYCRYSTALLINE ZNS(U) AIR FORCE INST OF
TECH WRIGHT-PATTERSON AFB OH SCHOOL OF ENGI.
D BLESSINGER DEC 83 AFIT/GEP/ENP/83D-2

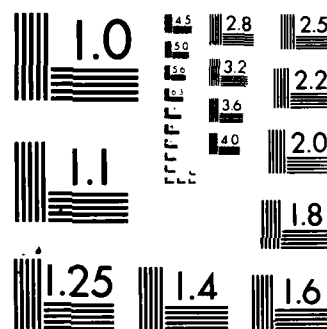
2/2

UNCLASSIFIED

F/G 20/2

NL





MICROCOPY RESOLUTION TEST CHART
NATIONAL BUREAU OF STANDARDS 1963-A

observed in the waterclear samples' spectra. Once the Raytheon yellow ZnS spectra had peaks at 3717 and 3860 Å. (Many of the peaks observed in the waterclear sample spectra were not seen in the yellow sample spectra because of the crystal quality.) The 3717 peak is near the 3700 Å peak for ZnO reported by Shalimova et al. (Ref 94). The 3860 Å peaks falls within the 3850-4000 Å range where Shalimova et al. reported a peak due to the V_O to V_{Zn} transition in ZnSO within the ZnS crystal (Ref 94). Because oxygen is a common contaminant in ZnS these two peaks could be due to these centers.

The signal to noise ratio and resolution of the emission peaks in the yellow ZnS spectra was so low that the wavelengths of peaks in the near band edge region could not be accurately determined. Figure IV-12 is the spectra with the highest signal-to-noise ratio obtained from the yellow ZnS in the near band edge region. It is not clear whether the peaks are composite peaks or a single peak. The intensity of the 3313-17 Å peak is difficult to explain because all the peaks around 3313-17 Å in the waterclear samples were LO phonon replicas. In the yellow ZnS spectra the 3313-17 Å peak was two to three times the amplitude of any possible Parent peak if it indeed was a LO phonon replica. One possibility is that the yellow material has a band gap energy about 3-7 MeV larger than for the waterclear material. This theory has already been discussed.

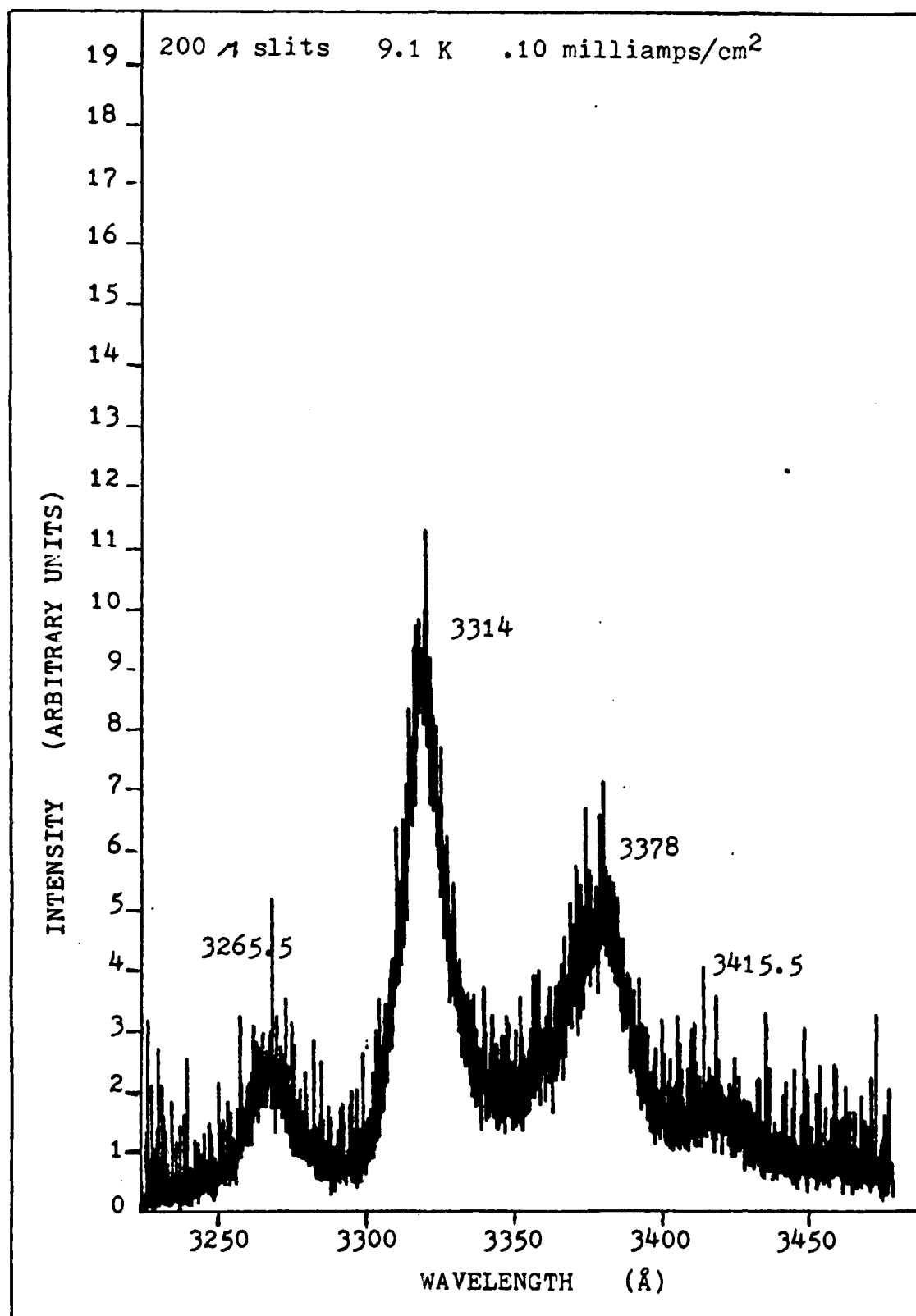


Figure IV-12 Typical Spectra, Yellow Polycrystalline ZnS

Electron Flux and Temperature Effects.

Whenever spectra are compared the excitation photon flux or electron flux and the temperature at which the data was taken must be considered. These two variables can cause shifts in the spectral peaks. The direction and degree of shifting for each emission peak is characteristic of the traps involved for that each individual emission peak. Therefore information about the sites can be gained using these variables. The electron flux will be examined first and followed by the temperature dependence.

Electron Flux. The electron flux was varied from about .0045 to over 26 milliamps / cm². Figures IV-7, IV-8, IV-9, and IV-10 show how varying the excitation intensity can change the appearance of the SAL peak. Figure IV-7 is at a very low intensity of about 4.5 microamps / cm². The SAL peak is prominent here because the SA blue peak at 4485 Å is so weak due to the low excitation rate. As the intensity is increased the SA peak increases more rapidly than the SAL peak. Figure IV-8 shows the spectra for a low excitation intensity of 50 microamps / cm². In this case the SAL peak is present as only a slight bump on the side of the SA peak. The preferred recombination is through the SA sites. As the intensity is increased further to 662 microamps / cm² in Figure IV-9 the SAL peak has increased its relative intensity considerably. This is probably due to saturation of the SA sites; the recombination then being channeled to the

less preferred SAL site. As the intensity is further increased to over 26 milliamps / cm², the SAL peak intensity increases to where it is much greater than the SA peak (See Figure IV-10). The relative intensity of the peaks versus the excitation intensity is heavily dependent upon the site concentrations for the concerned peaks.

The level of excitation can be used as a means of increasing the signal to noise ratio or as a means of separating peaks to identify the wavelength when they are otherwise unseparable. This technique was used occasionally in the current research. Caution must be used because a high excitation flux can simultaneously cause a shift as great as 15 Å in the wavelength of the peak. In these studies a shift of 10 Å for the DAP peaks was detected.

Temperature Effects. A series of temperature effect runs was made using waterclear sample #3. The intensity was moderately low at 102 microamps / cm² across the whole sample. Measurements were made at 9.5, 15, 20, and 25 K. The uncertainty of the peak values was less than ± 0.6 Å. Peaks were measured in the near band edge from 3260 to 3442 Å. The results showed no detectable shift on the 3262.8, 3275.5, 3321.0, 3380.3, 3400.5 and 3442.5 Å peaks.

A series of temperature effect runs on waterclear #1 showed a temperature dependence of the 3428 Å peak. A moderately low intensity was used on a small spot. A shift of approximately 2.1 Å was noted from 9.6 to 15 K and an

additional shift of approximately 1.6 Å was noted between 15.0 and 25.0 K. The uncertainty on these runs was approximately ± 0.8 Å for the peak position. The .17 MeV / K temperature shift between 15 and 25 K is identical to the shift Samelson and Lempicki calculated for their B series peaks (Ref 85:905). The shift of 2.1 Å between 9.3 and 15.0 K indicates a substantially higher rate of shift occurs as the temperature approaches liquid helium temperature. More experiments are needed to confirm this.

The temperature dependence of the blue SA peak has already been discussed but will be summarized here. The temperature dependence of the blue SA peak varied depending on the spot of the sample examined. This was probably due to a difference in the dominant emission center. The peak at about 4321 Å shifted 8 Å to 4313 Å. The 4375 Å peak jumped to 4340 Å when the temperature was increased to 40 K. (Data was taken only at 9.3 and 40 K.) This was probably partially due to a change in centers because the shift of 35 Å is about seven times what would be expected for the change in temperature. The 4378 Å peak moved in the opposite direction to 4390 Å at 75 K. This shift was in the direction and amount expected for a copper impurity.

Variation in Emission Spectra.

The variation of the emission spectra of the samples will be examined in three different comparisons. These are Yellow vs. Waterclear, Sample vs. Sample, and Spot vs. Spot.

Yellow vs. Waterclear. The yellow cvd polycrystalline ZnS is the starting material for waterclear ZnS. The yellow material is subjected to a special heat and pressure treatment which causes the individual crystals to grow and realign the crystal pattern to one direction. This restructuring is probably the reason why the new material is highly transmissive in the UV, blue, and green regions of the spectrum. The result is the "waterclear" appearance of the new material. The special annealing process could also be expected to cause a migration or diffusion of some impurities to grain boundaries or out of the samples entirely.

Therefore it is not surprising to find that the spectra of the yellow and waterclear forms of cvd polycrystalline ZnS differ considerably. Figures IV-1 and IV-2 are of yellow #4 and waterclear #5 respectively. Very little structure is seen in the near band edge of yellow #4.. No additional structure was found while examining narrower regions near the band edge (See Figure IV-12). The SAL peak is noted on the high energy side of the large SA peak in Figure IV-1. The SAL peak is located at about 3850 Å which corresponds to an oxygen impurity. The second and third peaks at 3313-7 and 3375 Å are attributed to O_S and V_S traps. However in the waterclear spectra, shown in Figure IV-2, there is considerable structure in the near band edge. Even greater detail is detected when smaller ranges of wavelength are examined (See Figure IV-13). The 3313-7 Å

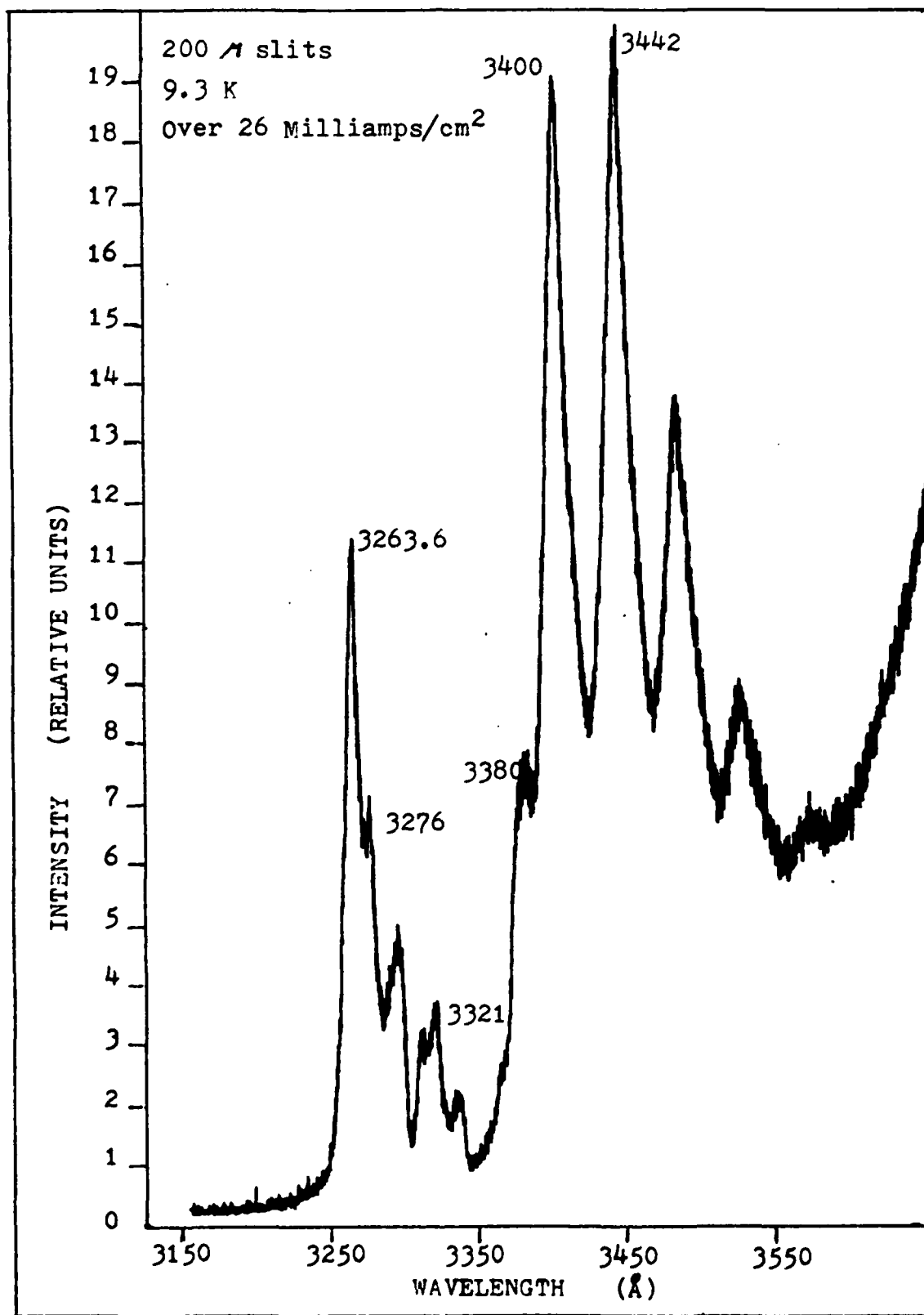


Figure IV-13 Typical Spectra Waterclear #3

peak of the yellow ZnS has shifted to about 3321 Å in the waterclear ZnS. The 3375 Å peak is now at 3380 Å.

All of the yellow ZnS near band edge peaks had a FWHM over 15 Å FWHM while the waterclear ZnS near band edge peaks had a FWHM ranging from 3.8 to over 15 Å depending on the type of transition involved in the emission and the quality of the surface preparation. These differences indicate that there is less oxygen content in the individual crystals of waterclear ZnS and that the quality of the crystals is greatly increased by the special annealing process. In fact, the quality of the waterclear ZnS samples is comparable to the best single crystals although the material is polycrystalline. The great spectral detail also indicates that the waterclear crystals are of very high purity.

Sample vs. Sample. The differences between samples can be nearly as great as between the yellow and waterclear forms. Figures IV-14, IV-15, and IV-16 dramatize the radical differences which can occur. The figures are of waterclear samples #3, #4, and #6 respectively. Samples #2 and #6 were from the same boule. Samples #2 and #6 had strong peaks at 3400 and 3442 Å whereas sample #4 had only weak emissions in this region. Sample #6 had strong BE peaks at 3262, 3267, and 3321 Å and a strong FTB peak at 3380 Å in addition to the strong 3276 Å BE peak seen in sample #2. Sample #4 had strong BE peaks between 3262 and 3276 Å and

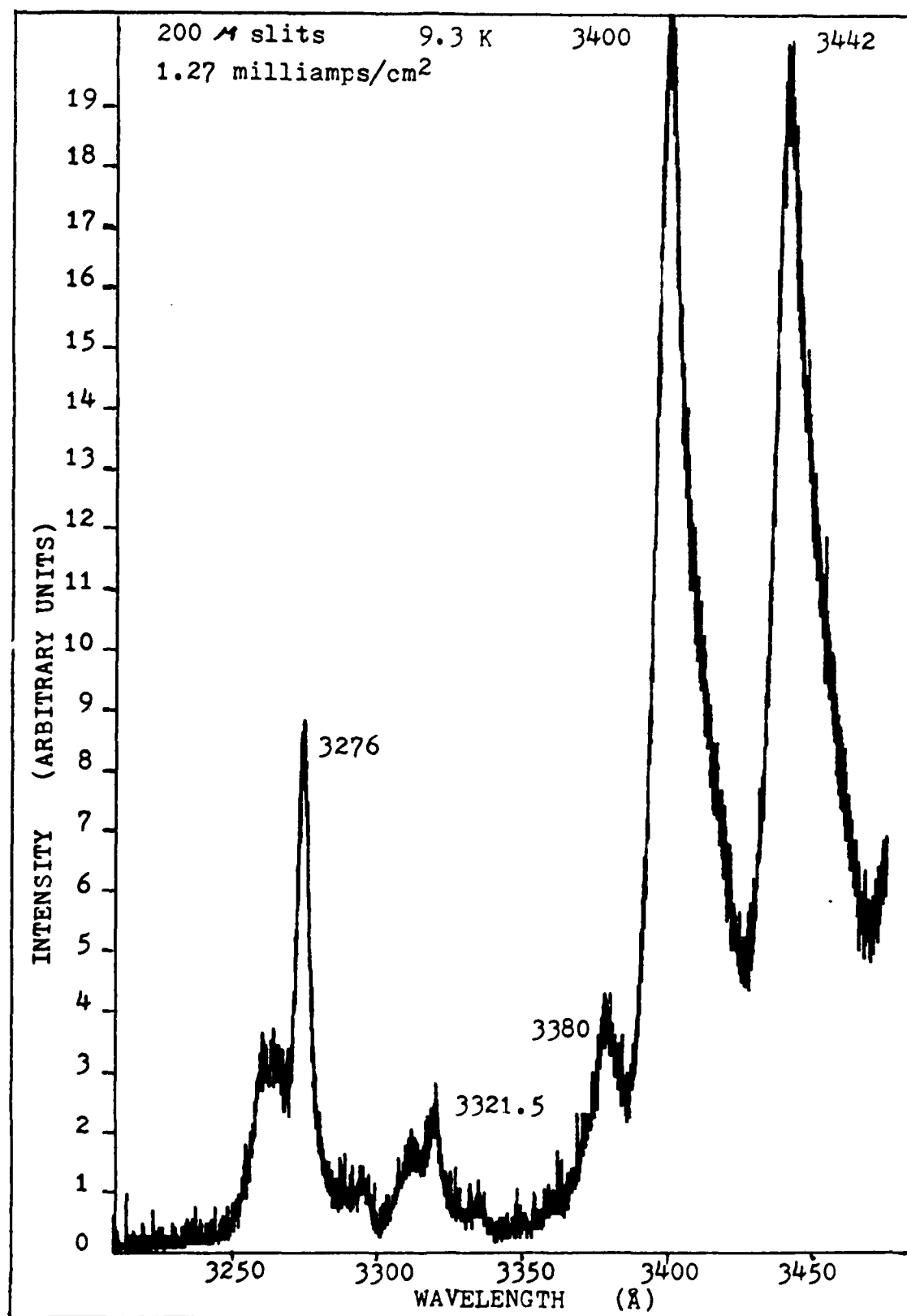


Figure IV-14 Waterclear #3 Typical Spectra

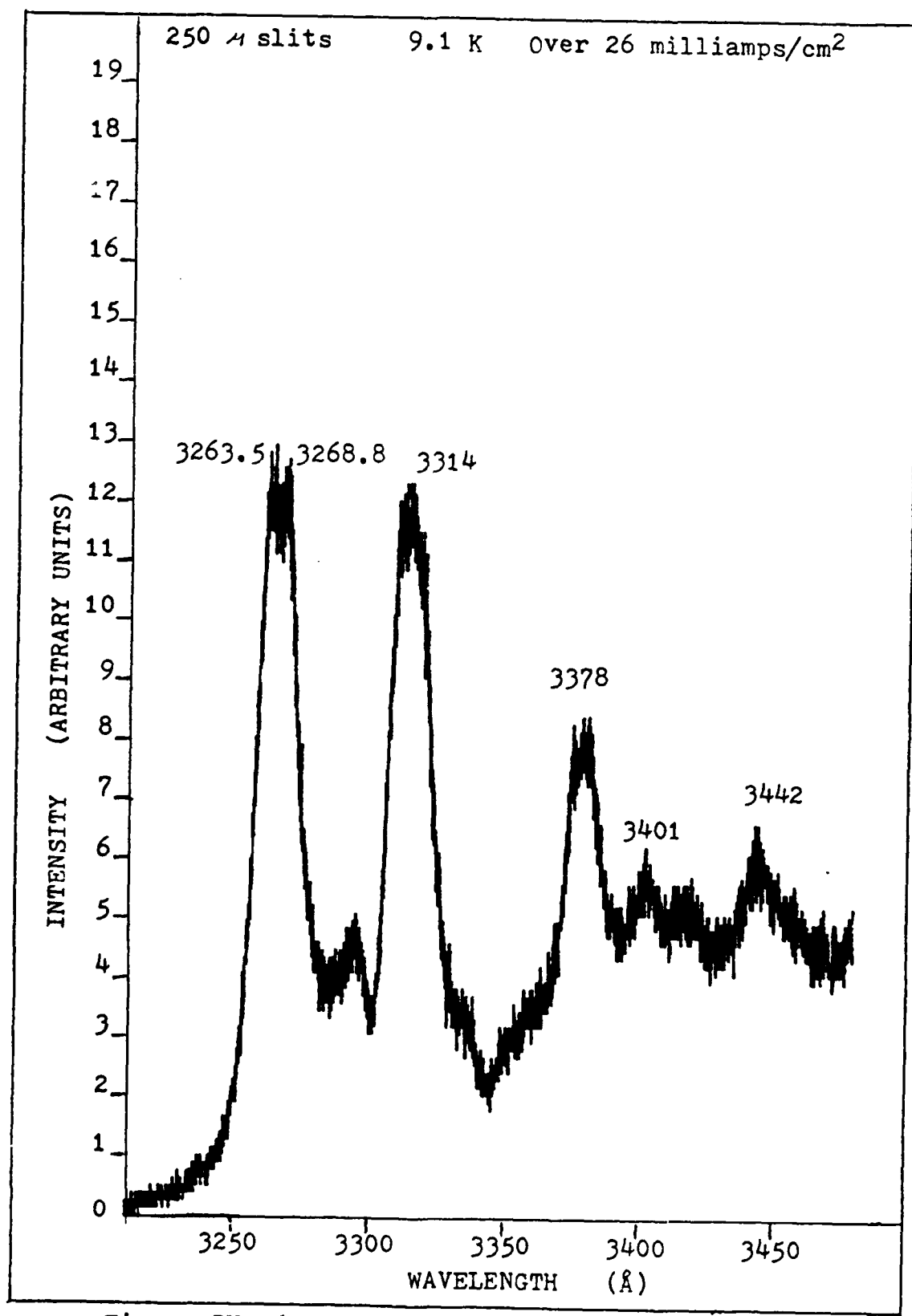


Figure IV-15 Waterclear #4 Typical Spectra

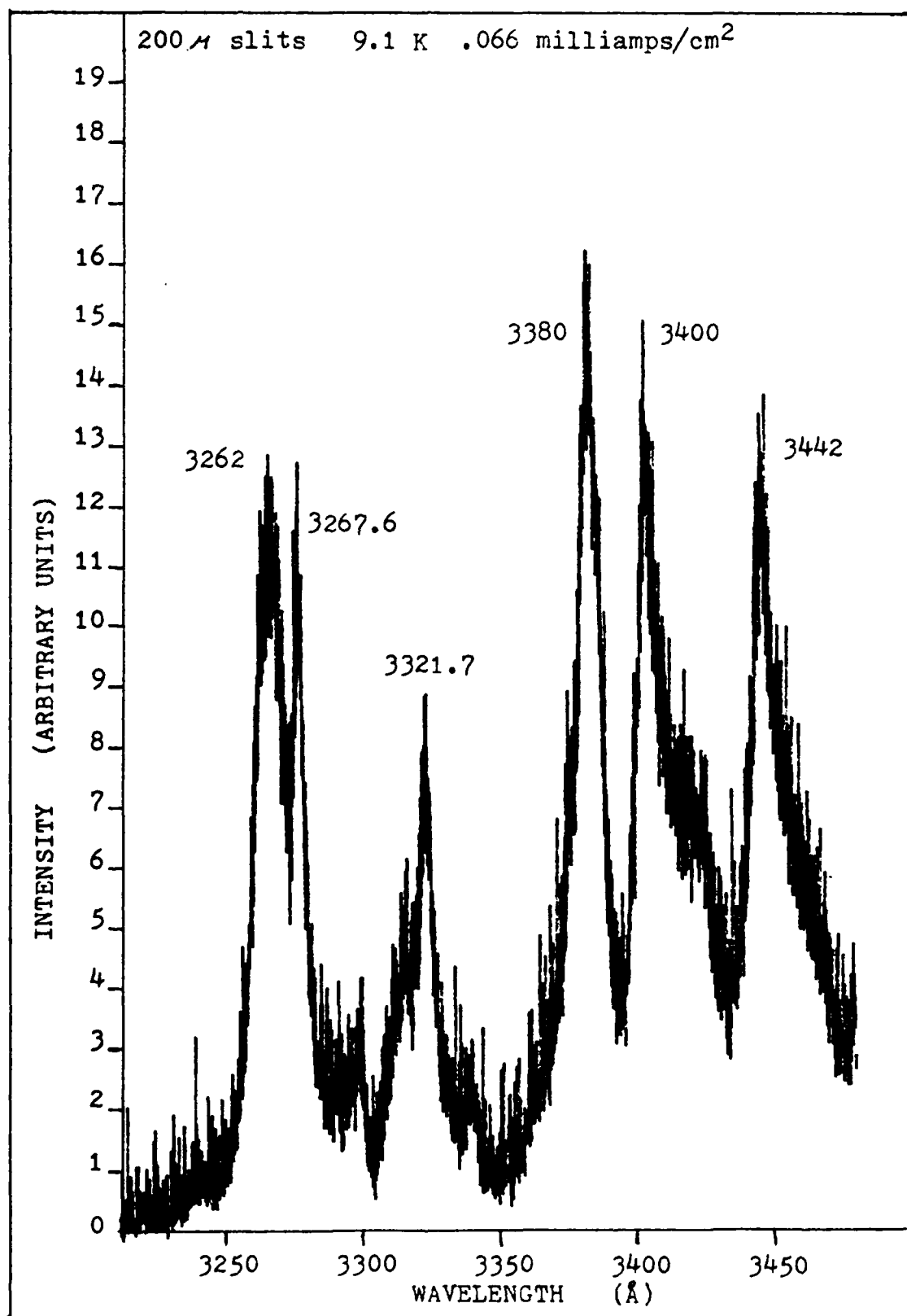


Figure IV-16 waterclear #6 Typical Spectra
96

between 3310 and 3322 Å. The peaks between 3310 and 3321 Å were not resolved.

The detection of packing defect peaks was related to the sample preparation. Defect peaks were seen more frequently in the waterclear samples which were cut perpendicular to the length of the crystal needles so the end view of the crystal needles was seen. This is because more packing defects should be seen on the ends of the needles. The 3240 Å peak can be seen in Figure IV-16.

The peaks reported at 3428 and 3468 Å were intense only in waterclear sample #1 and in the yellow samples.

The appearance of visible inclusions at the surface could not be related to a particular type of sample but some samples had considerably more inclusions than others. The size and shape of the inclusions also varied considerably.

The spectra of waterclear sample #4 indicated that the surface preparation was poorer than the other waterclear samples. Sample #4 was from the same boule as sample #5 which is shown in Figure IV-2. Sample #4 was the only waterclear sample which exhibited such a low intensity near band edge structure shown in Figure IV-17. This could mean two things. Either the quality of sample #4 is low or the impurity concentration responsible for the near band edge emission is very low. Additional experiments indicated considerable near band edge structure with the FWHM values larger than for sample #5, but smaller than for the yellow

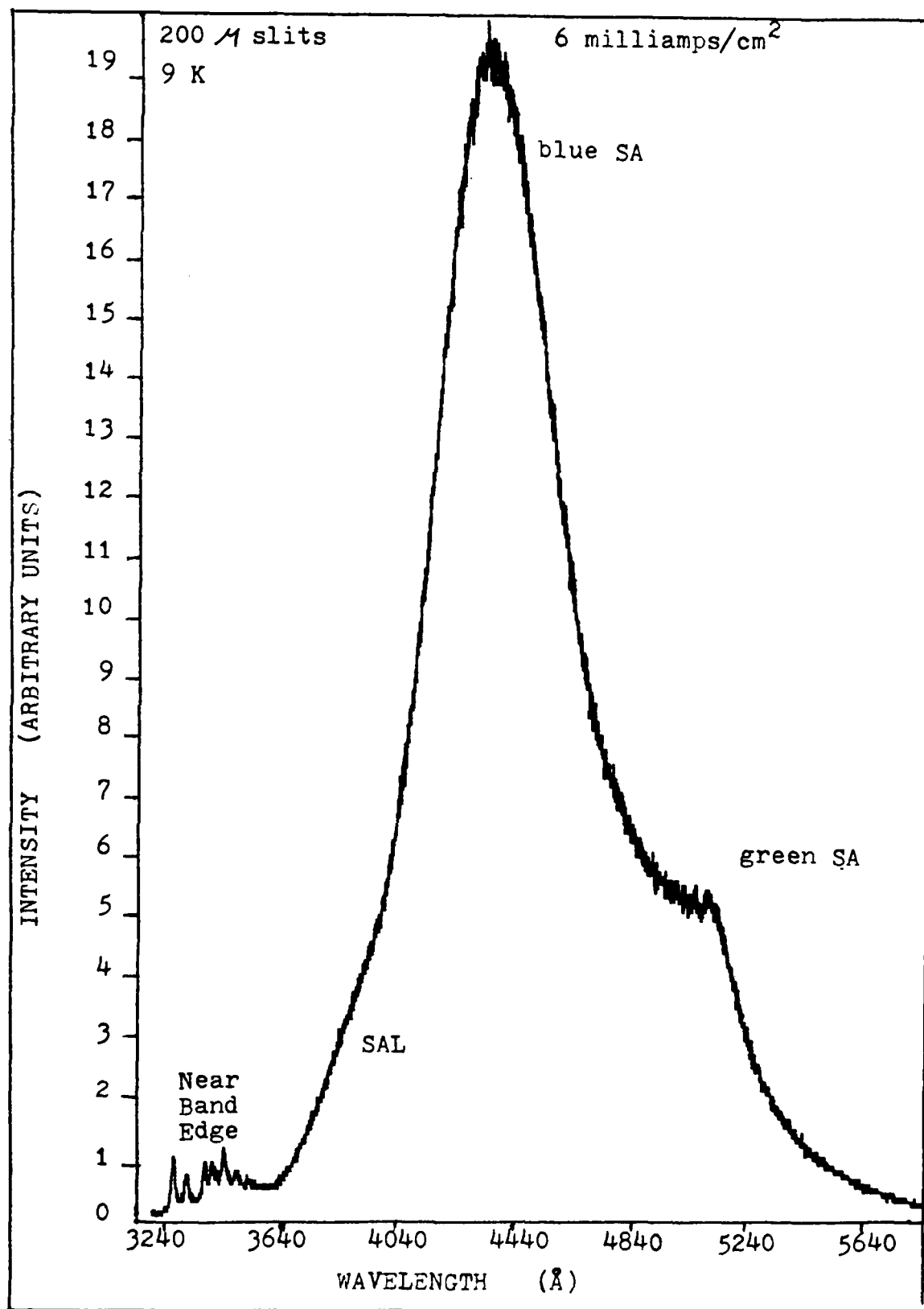


Figure IV-17 waterclear #4

Ans. The intensity of the near band edge spectra can be expected to be highly dependent upon slight changes in the crystal quality. The large SA peak apparently was not so dependent upon the quality of the crystal. It was concluded that the low intensity near band edge emission from water-clear sample #4 was due to a slightly lower sample surface quality caused by the polishing.

The Raytheon sample was a dark brownish yellow color instead of the light yellow of the CVD Inc material. The only differences seen in the spectra of the Raytheon sample vs. the CVD Inc. samples were that the 3313 and 3375 Å peaks were very intense and the SAL peaks around 3700 and 3860 Å were more intense. No additional peaks were seen in the Raytheon ZnS sample spectra although Bryant and Hamid reported that excess sulfur turned their samples brown and quenched phosphorescence (Ref 21:613). The 3375 Å peak corresponded to the V_S emission in the waterclear so it was concluded that excess sulfur did not cause the brownish color of the Raytheon sample. Because the oxygen related peak at 3313 Å is so large the brownish color of the Raytheon sample is probably due to a relatively large concentration of oxygen compared to the CVD Inc. samples.

Spot vs. Spot. The spectra from different spots on a given sample exhibited many of the differences seen in the spectra for different samples. Different peaks and relative intensities are related to definite spots on the crystals.

The green SA peak increased in intensity at inclusion sites. This was attributed to an increase in the local copper concentration. Packing defects appeared with various relative intensities at different spots on the sample. In some spots on waterclear #1 the 3428 and 3468 Å peaks were present, in others the 3400 and 3442 Å peaks were present, and in yet others a combination of all four of these peaks were seen. Generally, in the waterclear samples the 3262, 3267, 3321, 3380, 3400, and 3442 Å peaks were seen. In the yellow samples peaks at 3262, 3313-7, 3375, and 3422 Å were seen. (Note these are shifted in relation to the waterclear peaks because of the larger energy band gap for the yellow material.)

V. Conclusions and Recommendations

Yellow and waterclear forms of cubic chemical-vapor-deposition polycrystalline ZnS were examined using high resolution cathodoluminescence at liquid helium temperatures. The quality of the waterclear material was determined to be comparable to the best quality single crystals available. The waterclear ZnS near band edge spectra exhibited a complex structure of numerous high and low intensity peaks, indicating the high quality and purity of the material. The special annealing process used to transform the base yellow ZnS material into the waterclear ZnS material was found to 1) lower the oxygen impurity content in the individual crystal needles, 2) increase the size of the individual crystal needles by 10 fold in each dimension, 3) realign the crystal structure to one direction, 4) reduce the number of stacking defects, and 5) reduce the energy band gap by 3-7 MeV.

The 40% reduction of hardness of the waterclear material compared to the yellow material was concluded to be due to migration of oxygen to the grain boundaries. A similar effect has been reported for calcium fluoride polycrystals (Ref 12).

The high absorption coefficient for the waterclear material in the UV, blue, and green regions of the spectrum compared to the yellow material was concluded to be due to 1) the realignment of the crystal structure to one

direction, 2) the reduced number of stacking defects, 3) increased crystal needle size, and 4) the reduction of oxygen in the crystal needles (Ref 120).

Spectral emissions of waterclear ZnS agree to within a few tenths of an angstrom with those reported in the literature. The band edge was determined to be below 3226-9 Å and would vary as the energy band gap varied. The LO phonon energy was confirmed to be 44 meV. Figure V-1, "Assigned Transmissions", shows a schematic diagram of the suggested centers for the observed peaks.

Characteristic features included packing defects seen on samples with end views of the crystal needles at 3226-9 and 3240 Å. Donor bound exciton peaks were detected at 3262, 3267, 3270, and 3313-21 Å. The 3262, 3267, and 3321 Å peaks are proposed to be due to Al, Cl, and O respectively. The 3272, 3276, and 3282 Å peaks are bound exciton peaks. Free to bound transitions were observed at 3380, 3400, and 5080 Å. The 3380 and 3400 Å peaks were attributed to V and Cl respectively. The 5080 Å peak has been attributed to Cu_S in the literature (Ref 69).

The donor-acceptor pair (DAP) at 3428 Å was the only near band edge peak which shifted with temperature and electron flux. This peak is proposed to have the same donor site as the 3400 Å peak. A shallow complex such as (O - V_{Zn})⁻ is proposed as a possible acceptor site.

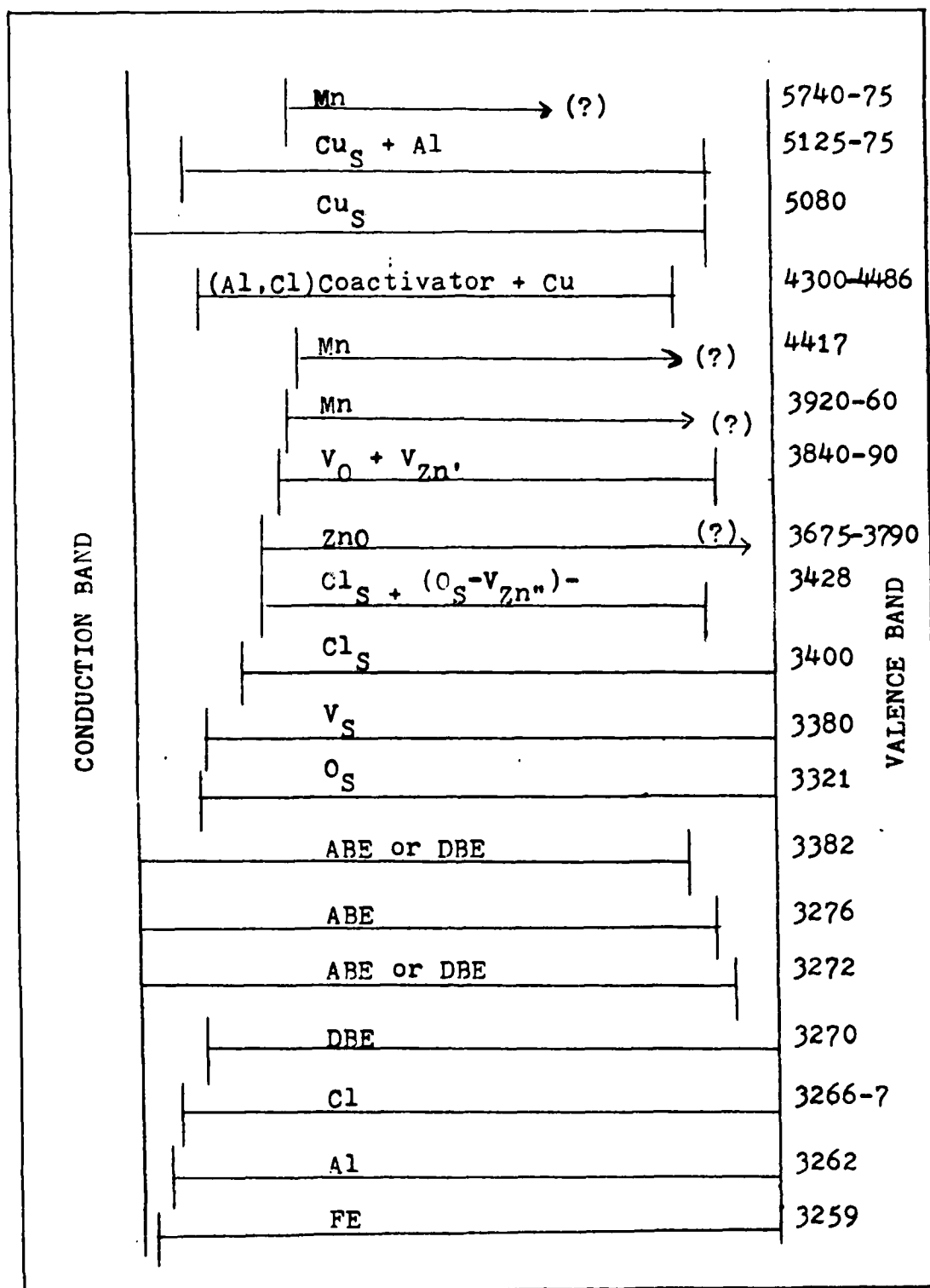


Figure V-1 Assigned Transitions

SAL peaks, normally only seen at moderate to high excitation intensities in these experiments, were found between 3675 and 3960 Å. The peaks at 3675 to 3730 Å were attributed to ZnO, the peak at 3840-90 Å to the (V_O to V_{Zn}) transition, and the peak at 3920-60 Å to Mn. The multiple blue SA peaks between 4300 and 4486 Å were caused by low concentrations of Cu with several co-activators such as Al, Br, Cl, and Mn. The 4417 Å peak has been linked with Mn in the literature. The multiple green SA peak between 5080 and 5175 Å was attributed to Cu in a FTB transition or in a DAP_S transition with a co-activator such as Al. The 5080 Å peak in literature is linked to a Cu free to bound transition. And the 5120-75 Å peak was linked to Cu + Al in a donor-acceptor-pair_S. A peak at 5740-75 Å was attributed to Mn.

This study is the only in-depth examination of the near band edge spectral properties of waterclear cvd polycrystalline ZnS known of by the author. Only three other reports were located discussing yellow cvd polycrystalline ZnS and, as a whole, no impurities or centers were assigned to the near band edge emission peaks. Additional studies are needed to verify the conclusions in this report.

1) To verify that packing defects are more prevalent in the end view of the crystals, three groups of samples should be cut from the same boule in three perpendicular planes. These should be studied with X-ray diffraction to determine the crystal orientation. The sample surface

should be acid etched and microphotographed to determine which direction the crystal needles are orientated. Finally, the samples should be examined using either photo or cathodoluminescence to determine if packing defect peaks are present at 3226 and 3240 Å.

2) To further check the effects of the special annealing process used to create waterclear ZnS, a piece of yellow ZnS should be held as a control sample while another piece from an adjacent spot on the same boule is sent to CVD Inc. to be transformed into waterclear material.

3) The trace impurity analysis, done by spark mass spectrometry with a sensitivity of 5 ppm, was unable to detect any impurities in the waterclear samples. Three other trace impurity analysis techniques which have a better sensitivity are "Solid Mass Spectroscopy", "Secondary Ion Mass Spectroscopy", and "Ion-Probe Microanalysis". These techniques or very minute doping of samples at very low temperatures (below 300 °C) may be used to confirm the relationships of various impurities to the detected emissions.

4) Further testing of temperature and intensity effects are needed near liquid helium temperatures to determine the rate at which peaks will shift. These tests are also needed to help confirm the transition mechanisms of the FTB and DAP peaks. Electron-paramagnetic resonance, time

resolved decay, and selective pair luminescence can also be used to verify the assignments.

5) Thermoluminescent measurements are needed to help verify the depths of various traps to confirm transition assignments.

6) A larger quartz collecting lens is needed to improve the signal to noise ratio and resolution. The larger lens would also permit the reduction of the electron flux which would reduce the wavelength shift caused by a higher temperature and excitation flux.

7) The samples should also be very highly polished to reduce the effects of surface damage. Small surface damage can result in considerable line broadening due to poor crystal quality. This is especially true when the samples are as high in purity as the waterclear samples.

8) Experiments are needed to verify the extent of the energy band gap variation between yellow and waterclear ZnS. Experiments are needed to show how the wavelength of the peaks vary as the excitation spot is moved across the sample surface and between yellow vs. waterclear ZnS. Reflection measurements could also be used to check variation in the energy band gap.

9) Verification of the theory that the oxygen is migrating to the grain boundaries and out of the crystal lattice could be done by checking for absorption or emission lines corresponding to electronic transitions in oxygen

compounds which might form in the grain boundary region.
The most likely compound would be O_2 although ZnO and SO_2
are also possible.

BIBLIOGRAPHY

1. Allen, J.W. "Energy Levels of Transition Metal Impurities in Semiconductors." Physics of Semiconductors, Proceedings of the 7th International Conference, 781-787. New York: Academic Press, 1964.
2. ----- "Kinetics of Long-Wavelength Infrared Stimulation of Donor-Acceptor Pair Luminescence in ZnS." Physical Review B, 9: 1564-1577 (February 1974).
3. Arpiarian, N. "The Centenary of the Discovery of Luminescent Zinc Sulfide." Proceedings of the International Conference on Luminescence, 1966, 903-6. Budapest: Akademiai Kiado, 1968.
4. Aven, M. and J. S. Prener. Physics and Chemistry of II-VI Compounds. New York: John Wiley and Sons, Inc., 1967.
5. Baars, J.W. "The Fundamental Reflectivity of ZnS Single Crystals with 3C, 2H, 4H, 6H, 10H Structures." II-VI Semiconducting Compounds: 1967 International Conference, 631-638. New York: W.A. Benjamin, Inc., 1967.
6. Balkanski, M., R. Beserman, and D. Langer. "Cathodoluminescence of Manganese in Zinc Sulfide." Proceedings of the International Conference on Luminescence, 1966, 1186-90. Budapest: Akademiai Kiado, 1968.
7. Baltrameyunas, R.A. et al. "Luminescence of ZnS Single Crystals Excited by a Laser Beam and an Electric Field." Journal of Applied Spectroscopy, 30 no. 1: 110-112 (January 1979).
8. Baltrameyunas, R.A. and E. Kuokshtis. "Edge Luminescence of ZnS Single Crystals Under Strong Photoexcitation Conditions." Soviet Physics-Solid State Physics, 22: 589-591 (April 1980).
9. Berseman, R. and M. Balkanski. "Photon-Phonon Interaction in Radiative Recombination by the Impurity Center in ZnS:M." Contract # E00AR-68-0016. Paris Univ (France) Laboratoire De Physique Des Solides, June 1971. (AD-725 077).
10. Bhargava, R.N. "The Role of Impurities in Refined ZnSe and Other II-VI Semiconductors." Journal of Crystal Growth, 59: 15-26 (September 1982).

11. Birman, J.L., H. Samelson, and A. Lempicki. "Reflection and Emission of Polarized Light in ZnS and CdS." GT&E Research and Development Journal, 1: 2-15 (January 1961).
12. Birman, J.L. "Theory of Luminescent Centers and Processes in ZnS Type II-VI Compounds." Proceedings of the International Conference on Luminescence 1966, 919-960. Budapest: Akademiai Kiado, 1968.
13. Bochkov, et al. "Photoluminescence of ZnS with Ion-Implanted Ne Impurity." Journal of Applied Spectroscopy, 30: 179-182 (February 1979).
14. Bogdankevitch, O.V. et al. "Recombination Radiation of ZnS Single Crystals Excited by a Beam of Fast Electrons." Soviet Physics-Solid State Physics, 8 2039-40 (March 1970).
15. Bonfiglioli, G. and A. Suardo. "Cu Reprecipitation and Electroluminescence in ZnS Single Crystals." Physics Letters, 13 no. 3: 197-8 (December 1964).
16. Bonfiglioli, G. and A. Suardo. "Cu Reprecipitation and Electroluminescence in ZnS Single Crystals." Contract # AF-EOAR-87-63. National Electrotechnical Inst Turin, Italy, October 1964, (AD-617 817).
17. Broser, et al. "Luminescence of an M Center in ZnS?" Journal of the Physics and Chemistry of Solids, 41: 101-107 (1980).
18. Brovetto, P. et al. "Electroluminescent Patterns and Crystal Defects in ZnS." Contract # EOOAR-68-0007. National Electrotechnical Inst Turin, Italy, January 1971. (AD-727 386).
19. Bryant, F.J. and S.A. Hamid. "Electron-Induced Traps in Zinc Sulfide Single Crystals." Physical Review Letters, 23 no. 6: 304-6 (August 1969).
20. ----- "Electron Irradiation and Trapping Centres in Zinc Sulfide Single Crystals." Physica Status Solidi (A), 2 no 3: 597-605 (1970).
21. ----- "Heat Treatment of Trapping Centres in Zinc Sulfide Single Crystals." Physica Status Solidi (A), 2 no 3: 607-18 (1970).
22. Bryant, F.J. and P.S. Manning. "The Effect of Zn Displacement on the Luminescence of ZnS." Solid State Communications, 10: 501-504 (1972).

23. Busca, G. et al. "Thermal Treatments and Electroluminescence Yield in Zinc Sulfide." Contract # EOOAR-70-0074, National Electrotechnical Inst Turin, Italy, June 1971. (AD-740 071).
24. Carter, D.B. "Zinc Sulfide." Report # EPIC-DS-135-(2-ED), Hughes Aircraft Co Culver City, California, Electronic Properties Information Center, November 1966, (AD-803 885).
25. Colman, D. and D.E. Mason. "The Suppression of the Yellow Emission of ZnS-In." Proceedings of the International Conference on Luminescence, 1966, 1169-76. Budapest: Akademiai Akaido, 1968.
26. Cusano, D.A. "Cell Storage Studies." Contract # DA-44-009-AMC-201(T), U.S. Army Engineer Research and Development Laboratories, Report by General Electric Research Laboratory, Schenectady, New York, August 1963. (AD-430462L).
27. Datta, S. et al. "The Shape of the Self-Activated Cathodoluminescence Band in ZnS:Cl Crystals." Journal of Luminescence, 21: 53-73 (December 1979).
28. Datta, S., B.G. Yacobi, and D.B. Holt. "Scanning Electron Microscope Studies of Local Variations in Cathodoluminescence in Striated ZnS Platelets." Journal of Materials Science, 12: 2411-20 (1977).
29. Dean, P.J., et al. "Ionization Energy of the Shallow Nitrogen Acceptor in ZnSe." Physical Review B, 27: 2419-2428 (February 1983).
30. ----- "Optical Properties of Undoped Organometallically Grown ZnSe and ZnS." Journal of Crystal Growth, 59: 301-306 (September 1982).
31. Dickman, Robert S. "Energy Band Model for Infrared Stimulated Emission in Zinc Sulfide Single Crystals." Unpublished MS Thesis. AFIT School of Engineering, Wright-Patterson AFB, Ohio, June 1968. (AD 836 464).
32. Egee, M. "Spectral Distribution of the Green Emission Band of ZnS:Cu in Dependence on the Localization Diversity of the Radiative Recombination Process." Physica Status Solidi (A), 35: 361-70 (May 1976).
33. Egorov, V.Yu. et al. "Luminescence and Raman Scattering in ZnS-Mn Crystals." Optical Spectroscopy, 44: 354-6 (March 1978).

34. Enomoto, et al. "Investigation on Trap Distribution and Photoelectronic Effect due to UV, IR, and Visible Light Excitation in Self-Activated ZnS Crystals." Journal of the Physics and Chemistry of Solids, 38: 247-253 (1977).
35. Farkas-Jahnke, M., J. Schanda, and P. Kovacs. "Luminescent Properties of Different ZnS Polytypes." Proceedings of the International Conference on Luminescence, 1966, 1093-7. Budapest: Akademiai Akaido, 1968.
36. Flesch, U., et al. "Exciton Luminescence of Cubic ZnS Crystals." Journal of Luminescence, 3: 137-142 (1970).
37. Fleurov, V.N. and K.A. Kikoin. "Amphoteric Exciton Trapping by 3d-Impurities in A2B6 Semiconductors." Solid State Communications, 42 no 5: 353-7 (1982).
38. Georgobiani, A.N., et al. "Investigation of Deep Centres of Chlorine-Doped Zinc Sulfide Crystals." Physica Status Solidi (A), 38: 77-83 (November 1976).
39. Gezci, S. and J. Woods. "Edge Emission in ZnS." Journal of Applied Physics, 51: 1866-1867 (1973).
40. Gobrecht, H. et al. "Phase Transformation and Polytypism in ZnS." Proceedings of the International Conference on Luminescence, 1966, 1086-92. Budapest: Akademiai Akaido, 1968.
41. ----- "Analysis of Trap Spectra." Proceedings of the International Conference on Luminescence, 1966, 1078-85. Budapest: Akademiai Akaido, 1968.
42. Grasser, R., A. Scharmann, and W. Schwedes. "Further Effects of High Temperature Annealing on the Photoluminescence of an Ultra High Pure ZnS Crystal." Zeitschrift Fur Physik B, 28: 247-53 (1977).
43. Gumlich, H.E., R. Moser, and E. Neumann. "On the Mn-Mn Interaction and the Structure of Optical Spectra of ZnS (Mn)." Physica Status Solidi, 24: K13 (1967).
44. James, J.R. et al. "Donor-Acceptor Nature of the Blue Self-Activated Emission in ZnS Crystals." Solid State Communications, 17: 969-72 (1975).
45. Jaszczyk-Kopiec, P. and B. Lambert. "Red Luminescence of ZnS:Fe Crystals." Journal of Luminescence, 10: 243-60 (1975).

46. Jaszczyzn-Kopec, P., H.D. Fair, and D.S. Downs. "The Boron Center: A New Luminescence Center in ZnS Crystals." Journal of Luminescence, 18-19: 837-840 (January 1979).
47. Jaszczyzn-Kopec, P., et al. "High Pressure Action on the SA and Mn Emission in the Cubic, Faulted and Hexagonal ZnS Crystals." Solid State Communications, 32: 473-477 (June 1979).
48. Johnson, S.L. "Cathodoluminescence of Ion Implanted ZnS." Unpublished MS Thesis. Wright-Patterson AFB, Ohio, Air Force Institute of Technology, June 1973. (AD-767 877).
49. Kalman, Z.H., I. Kiflawi, and I.T. Steinberger. "On the Inapplicability of the Layer-Transposition mechanism to Polytype Formation in ZnS." Journal of Applied Crystology, Short Communications, 6: 292-3 (1973).
50. Kawai, H. and T. Hoshina. Exciton Structure in Luminescence Excitation Spectra of ZnS Phosphors." Solid State Communications, 22: 391-4 (1977).
51. ----- "Cathodoluminescent Properties of ZnS:Ce,Li Phosphor." Japanese Journal of Applied Physics, 20 no 7: 1241-7 (July 1981).
52. Kiefer, E. and U. Schroder. "Influence of Electron-Phonon Coupling on the Energy of an Exciton Bound to a Donor-Acceptor Pair." Journal of Luminescence, 14: 235-42 (1976).
53. Klein, Miles V. Optics. New York: John Wiley and Sons, 1970.
54. Klein, W. "Excitonenemission von Hexagonalem ZnS Bei Anregung mit 50-keV-Elektronen." Journal of the Physics and Chemistry of Solids, 26: 1517-1521 (1965).
55. Kobayashi, H. et al. "Excitation Mechanism of Electroluminescent ZnS Thin Films Doped with Rare-Earth Ions." Japanese Journal of Applied Physics, 13 no 7: 1110-4 (July 1974).
56. Kuboniwa, S., H. Kawai, and T. Hoshina. "Cathodoluminescence Saturation and Decay Characteristics of ZnS:Cu,Al Phosphor." Japanese Journal of Applied Physics, 19 no 9: 1647-53 (September 1980).

57. Kukimoto, H., S. Oda, and T. Nakayama. "Preparation and Characterization of Low-Voltage Cathodoluminescent ZnS." Journal of Luminescence, 18/19: 365-8 (1979).
58. Lambert, B., T. Buch, and A. Geoffroy. "Optical Properties of Mn²⁺ in Pure and Faulted Cubic ZnS Single Crystals." Physical Review B, 8 no 2: 863-9 (July 1973).
59. Langer, D. "Pressure Effects on the Band Structure of II-VI Compounds with Zincblende Structure." Physics of Semiconductors: Proceedings of the 7 th International Conference, 241-244. New York: Academic Press, 1964.
60. Lendvay, E., and P. Kovacs. "Luminescence and Impurity Precipitation in ZnS Single Crystals with High Cu Concentrations." Proceedings of the International Conference on Luminescence, 1966, 1098-1101. Budapest: Akademiai Akaido, 1968.
61. Lendvay, E. "Revealing of Dislocations in ZnS by Chemical Etching." Journal of Crystal Growth, 59: 375-83 (1982).
62. Lorenz, M.R. "Crystal Growth of II-VI Compounds." II-VI Semiconducting Compounds: 1967 International Conference, 215-243. New York: W.A. Benjamin, Inc., 1967.
63. Maxia, V., C. Muntoni, and M. Murgia. "On the ZnS(Cu) Luminescent Centre." Lettere Al Nuovo Cimento, 6 no 16: 636-8 (April 1973).
64. McKelvey, John P. Solid State and Semiconductor Physics. New York: Harper & Row, 1966.
65. Miloslavskii, V.K., E.N. Naboikina, and T.S. Kiyani. "Effect of Structure Defects on the Optical Properties of Thin ZnS Films in the Fundamental Absorption Edge Region." Soviet Physics-Semiconductors, 1 no5: 527-32 (November 1967).
66. Mita, Y. and K. Sugibuchi. "Luminescence Centres in Zinc Sulfide Activated with Group IV Elements." Proceedings of the International Conference on Luminescence, 1966, 1158-63. Budapest: Akademiai Akaido, 1968.
67. Morozova, N. K., et al. "On the Nature of SAL Bands in the Emission of ZnS." Journal of Applied Spectroscopy, 23: 933-936 (July 1975).

68. Morozova, N.K., M.M. Malov, and O.I. Korolev. "Presence of Oxygen in ZnS Single Crystals." Inorganic Materials, 8: 199-201 (February 1972).
69. Nemchenko, A.M. "Emission Spectra of ZnS:Cu Single Crystals." Journal of Applied Spectroscopy, 19: 930-933 (July 1973).
70. Nolle, E.L., et al. "UV Luminescence of ZnS Under Electron Excitation." Optics and Spectroscopy, 23: 144-145 (August 1967).
71. Otomo, Y. and H. Kusumoto. "Donor-Acceptor Pair Luminescence in Self-Activated ZnS Phosphors." Proceedings of the International Conference on Luminescence, 1966, 1143-8. Budapest: Akademiai Akaido, 1968.
72. Ozawa, L., R. Huzimura, and Y. Ato. "Dependence of Luminescence in ZnS-Mn Phosphor on the Concentration of Mn²⁺ Determined by ESR." Proceedings of the International Conference on Luminescence, 1966, 1177-85. Budapest: Akademiai Akaido, 1968.
73. Patel, J.L., et al. "Copper-Associated Donor-Acceptor Recombination in ZnS in the Far Blue Region." Solid State Communications, 43: 385-389 (August 1982).
74. Ray, Brian. II-VI Compounds. New York: Pergamon Press, 1969.
75. Regan, M. "Switching Elements for use with Multielement Arrays." Standard Telecommunication Labs LTD Harlow, England, 1974, (AD-922 937L).
76. Riehl, N. "On the Investigation of Trap and Other Disorder Structures in ZnS Phosphors." Proceedings of the International Conference on Luminescence, 1966, 974-87. Budapest: Akademiai Akaido, 1968.
77. Rizakhanov, M.A., M.M. Khamidov, and I. Ya. Abramov. "Explanation of the Characteristics of the Green-Blue Luminescence of ZnS on the Basis of a new Model of Luminescence Centers." Soviet Physics-Semiconductors, 12: 1301-4 (1978).
78. Roberts, S.H. and J.W. Steeds. "High Resolution in Scanning Cathodoluminescence of ZnS Edge Emission." Journal of Crystal Growth, 59 312-6 (1982).

79. Rodine, E.T., et al. "Thermoluminescence and Related Experiments on Bromine-Implanted Zinc Sulfide Crystals." Contract # F33615-72-C-1099, Systems Research Inc., Dayton, Ohio, 1974 (AD-787 009).
80. ----- "Ion Implantation in Semiconductors and Semi-Insulators." Report # SRL-6739-12, Contract # F33615-C-1099, Systems Research Labs Inc. Dayton, Ohio, April 1974, (AD-781 193).
81. Rossler, U. and M. Lietz. "Band Structure of Cubic and Hexagonal ZnS (APW)." Physics Status Solidi, 17: 597-604 (1966).
82. Russell, G.J. et al. "Mechanically Induced Phase Transformations in CdS, CdSe, and ZnS." Journal of Materials Science Letters, 1: 176-8 (1982).
83. Ryskin, A.L., et al. "Excitons in ZnS Crystals with Stacking Faults." Physica Status Solidi (B), 49: 875-884 (1972).
84. Ryzhikov, D. and E.F. Chaikovskii. "Development of New AII-BVI Compound-Based Scintillator Materials with Isovalent Activator." Izvestiya Akademii Nauk SSSR, 43 no 6: 1150-4 (1979).
85. Samelson, H. and A. Lempicki. "Fluorescence of Cubic ZnS:Cl Crystals." Physical Review, 125: 901-909 (1962).
86. Satoh, Shiro and Kenzo Igaki. "Effect of Native Defect Concentration on Free Exciton Luminescence in ZnSe." Japanese Journal of Applied Physics, 19: 1953-1958 (October 1980).
87. ----- "Photoluminescent Properties of ZnS Grown from Te Solution." Japanese Journal of Applied Physics, 18: 705-706 (March 1979).
88. Scharmann, A., D. Schwabe, and D. Weyland. "Properties of the Pb-Luminescence Centre in ZnSe, ZnS and some ZnSe_{1-x}S_x Single Crystals." Journal of Luminescence, 18/19: 833-6 (1979).
89. Schwenkenbecher, K., et al. "Optical Transitions at Ag Centers in ZnS Crystals." Physica Status Solidi (B), 101: 215-220 (September 1980).

90. Shaffer, J. and F. Williams. "Energy Levels and Transition Probabilities for Donor-Acceptor Pairs." Physics of Semiconductors, Proceedings of the 7th International Conference, 811-818. New York: Academic Press, 1964.
91. Shalimova, K.V., et al. "Temperature Dependence of the UV Radiation of ZnS." Soviet Physics Journal, 15: 1598-1604 (November 1972).
92. Shalimova, K.V., N.K. Morozova, and I.A. Karetnikov. "Luminescence of ZnS Thin Films." Optics and Spectroscopy, 30: 573-576 (June 1971).
93. Shalimova, K.V. et al. "Edge Emission of Zinc Sulfide." Proceedings of the International Conference on Luminescence, 1966, 1196-1200. Budapest: Akademiai Akaido, 1968.
94. Shalimova, K.V., N.K. Morozova, and M.M. Malov. "UV Spectra of Donor-Doped Single Crystals of ZnS." Inorganic Materials, 11: 530-3 (April 1975).
95. Shionoya, Shigeo. "Optical Properties of Defects in II-VI Compounds." II-VI Semiconducting Compounds: 1967 International Conference, 1-39. New York: W.A. Benjamin, Inc., 1967.
96. -----. "Investigation on Luminescence of ZnS-Type Crystals." Proceedings of the International Conference on Luminescence, 1966, 962-73. Budapest: Akademiai Akaido, 1968.
97. -----. "Review of Luminescence in II-VI Compounds." Journal of Luminescence, 1, : 17-38 (1970).
98. Shionoya, S., K. Era, and Y. Washizawa. "Time Resolved Spectra of the Green-Copper Luminescence In ZnS." Proceedings of the International Conference on Luminescence, 1966, 1164-8. Budapest: Akademiai Akaido, 1968.
99. Shionoya, S., H.P. Kallmann, and B. Kramer. "Behavior of Excited Electrons and Holes in Zinc Sulfide Phosphors." Physical Review, 121 no 6: 1607-19 (March 1961).
100. Shionoya, S., et al. "Nature of the Red-Copper Luminescence Centre in ZnS Crystals AS Elucidated By Polarization Measurements." Journal of Physics-Chemistry Solids, 27:865-9 (1966).

101. Shono, Yoshihiko and Toshio Yoshida. "Photoluminescence Induced in ZnS by Electron Irradiation." Journal of the Physical Society of Japan, 34: 1109 (April 1973).
102. Smith, R.A. Wave Mechanics of Crystalline Solids (second edition). London: Chapman and Hall LTD, 1969.
103. Suslina, L.G. and E.B. Shadrin. "Excitation of Exciton States in ZnS Crystals Containing Stacking Faults." Soviet Physics-Solid State, 14 no 1: 243-4 (July 1972).
104. Swaminathan, V. and L.C. Greene. "Photoluminescence in Polycrystalline Zinc Selenide Laser Window Material." Technical Report AFWL-TR-79-4039 Laser & Optical Materials Branch, Electromagnetic Materials Division, Wright-Patterson AFB, April 1979. (AD-B038963).
105. Sweet, M.A.S. and D. Urquhart. "Shallow Traps in ZnS Single Crystals." Physica Status Solidi (A), 54: K81-4 (1979).
106. Sziget, G. "The Role of Lattice Defects Produced by Deformation in the Luminescence of Zinc Sulfides." Proceedings of the International Conference, 1966, 907-18. Budapest: Akademiai Akaido, 1968.
107. Taguchi, T. et al. "Luminescence Properties of Iodine Doped Cubic ZnS Crystals and The Effect of Ion Implantation of N, P, and Ag." Journal of Crystal Growth, 59: 317-22 (1982).
108. Takagi, K. "Blue Luminescence in Copper-Activated Zinc Sulfide Phosphor." Proceedings of the International Conference on Luminescence, 1265-70. Budapest: Akademiai Akaido, 1968.
109. Taylor, R.L. and M. Lefebvre. "Recent Progress in the Development of a Rain Erosion Resistant Water-Clear ZnS (Cleartran)." Unpublished Report. Contract # F33615-81-C-5076, Air Force Aeronautical System Division, Wright-Patterson Air Force Base, Ohio. May 1983.
110. Tews, H. and H. Venghaus. "Selective Pair Luminescence in Semiconductors." Solid State Communications, 30: 219-21 (1979).
111. Thomas, D.G. and J.J. Hopfield. "Optical Properties of Bound Excitation Complexes in Cadmium Sulfide." Physical Review, 128 no 5: 2135-48 (December 1962).

112. Tripathi, L.N., G.R. Chaubey, and C.P. Mishra. "Luminescence in ZnS:(Cu,Tb) and ZnS:(Ag,Tb) Phosphors." Physica Status Solidi (A), 60: 185-92 (1980).
113. Tunitskaya, V.F., et al. "The Temperature Properties of the Individual Blue Bands of Self-Activated ZnS and the Nature of the Common Radiative Center." Journal of Applied Spectroscopy, 14: 182-186 (February 1971).
114. Van Doorn, C.Z. "Recombination Mechanisms for the Edge Emission in Cadmium Sulfide." Proceedings of the International Conference on Luminescence, 1966, 1124-30. Budapest: Akademiai Akaido, 1968.
115. Varni, Jamie. "The Optical Properties of ZnSe and ZnS: Special Report." Unpublished report. PhD Student at AFIT, Wright-Patterson AFB, Ohio, March 1983.
116. Werkhoven, C., et al. "High-Purity ZnSe Grown by Liquid Phase Epitaxy." Applied Physics Letters, 38: 540-542 (April 1981).
117. Wheeler, R.G. and J.C. Miklosz. "Exciton Structure and Zeeman Effects in Zinc Sulfide." Physics of Semiconductors, Proceedings of the 7th International Conference, 873-881. New York: Academic Press, 1964.
118. Wolfe, James P. "Thermodynamics of Excitons in Semiconductors." Physics Today, 35: 46-54 (March 1982).
119. Zacks, E. and A. Halperin. "Dependence of the Peak Energy of the Pair Photoluminescence Band on Excitation Intensity." Physical Review B, 6 no 8: 3072-5 (October 1972).
120. Conversations with Don Evans at the Optics Branch, Materials Laboratory, Wright-Patterson AFB, Ohio. (Sep 1983).

VITA

David Blessinger was born on 26 November 1952 in Evansville, Indiana. After graduation from high school at Holland, Indiana in 1971 he entered the United States Air Force Academy. Upon graduation in 1975 he received a bachelor of science degree in Physics and a regular commission in the United States Air Force. After completion of undergraduate pilot training he was assigned to fly the B-52. While an aircrew member he received a master of science degree in Public Administration from Northern Michigan University. He entered the School of Engineering at the Air Force Institute of Technology in June, 1982. Upon graduation he is being assigned to the Materials Laboratory at Wright-Patterson AFB.

Permanent Address

Rural Route #1
Holland, Indiana 47541

UNCLASSIFIED

SECURITY CLASSIFICATION OF THIS PAGE

REPORT DOCUMENTATION PAGE

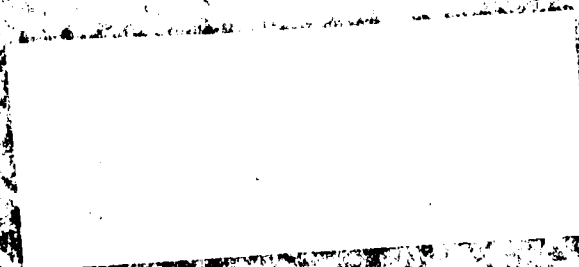
1a. REPORT SECURITY CLASSIFICATION UNCLASSIFIED		1b. RESTRICTIVE MARKINGS	
2a. SECURITY CLASSIFICATION AUTHORITY		3. DISTRIBUTION/AVAILABILITY OF REPORT Approved for public release; distribution unlimited.	
2b. DECLASSIFICATION/DOWNGRADING SCHEDULE			
4. PERFORMING ORGANIZATION REPORT NUMBER(S) AFIT/GEP/PH/83D-2		5. MONITORING ORGANIZATION REPORT NUMBER(S)	
6a. NAME OF PERFORMING ORGANIZATION School of Engineering	6b. OFFICE SYMBOL (If applicable)	7a. NAME OF MONITORING ORGANIZATION	
6c. ADDRESS (City, State and ZIP Code) Air Force Institute of Technology Wright-Patterson AFB, Ohio 45433		7b. ADDRESS (City, State and ZIP Code)	
8a. NAME OF FUNDING/SPONSORING ORGANIZATION	8b. OFFICE SYMBOL (If applicable)	9. PROCUREMENT INSTRUMENT IDENTIFICATION NUMBER	
8c. ADDRESS (City, State and ZIP Code)		10. SOURCE OF FUNDING NOS.	
11. TITLE (Include Security Classification) See Pox 19		PROGRAM ELEMENT NO.	TASK NO.
		PROJECT NO.	WORK UNIT NO.
12. PERSONAL AUTHOR(S) David Blessinger, B.S., M.A., Capt, USAF			
13a. TYPE OF REPORT MS Thesis	13b. TIME COVERED FROM _____ TO _____	14. DATE OF REPORT (Yr., Mo., Day) 1983 December	15. PAGE COUNT 131
16. SUPPLEMENTARY NOTATION			
17. COSATI CODES		18. SUBJECT TERMS (Continue on reverse if necessary and identify by block number)	
FIELD	GROUP	SUB. GR.	
2	2	SEE REVERSE	
2	12		
19. ABSTRACT (Continue on reverse if necessary and identify by block number)			
Title: HIGH RESOLUTION CATHODOLUMINESCENCE OF YELLOW AND WATERCLEAR CVD POLYCRYSTALLINE ZnS			
Thesis Chairman: Dr. Robert Hengehold			
20. DISTRIBUTION/AVAILABILITY OF ABSTRACT UNCLASSIFIED/UNLIMITED <input checked="" type="checkbox"/> SAME AS RPT. <input type="checkbox"/> DTIC USERS <input type="checkbox"/>		21. ABSTRACT SECURITY CLASSIFICATION UNCLASSIFIED	
22a. NAME OF RESPONSIBLE INDIVIDUAL Dr. Robert Hengehold	22b. TELEPHONE NUMBER (Include Area Code) 510-255-2012	22c. OFFICE SYMBOL AFIT/ENP	

Approved for public release: 1AW AFR 190-17.

[Signature]
WOLVER
 Dean for Research and Professional Development
 Air Force Institute of Technology (AFIT)
 Wright-Patterson AFB, OH 45433

END

FILMED



DTIC